Microscopic Analysis of *In Vitro* and *In Vivo* Effects of Functionalized Gold Nanoparticles on the liver, kidney, spleen, heart and pancreas of Male Wistar rats

By

Ekeoma F. Festus
(Student Number:3924595)

Thesis submitted in partial fulfilment of the requirements for the degree Master of Science in Medical Biosciences

Department of Medical Biosciences, University of the WesternCape, Bellville, South Africa.

Supervisor: Prof O. E. Ekpo

Co-supervisor: Prof A. M Madiehe

November 2022

Abstract

Nanotechnology represents a promising knowledge based platform that can solve human needs and ailments, especially in cases like cancers, diabetes, antibiotic drug resistances etc. Many metallic nanoparticles are being employed today to deliver drugs and other moieties to biological systems, however gold nanoparticles (AuNPs) is preferred because they are optically stable and easily manipulated to produce nanomaterials. However, AuNPs cytotoxicity have been reported in living systems, hence scientists are pushing boundaries to design more effective and biocompatible AuNPs. In this study, *in vitro* effects of 14 nm, citrate capped, chemically synthesized AuNPs (cAuNPs) on Caco-2 cells. The cAuNPs was functionalized with Adipose homing peptide AuNPs (AuNPs-AHP) or pro-apoptotic peptide KLA AuNPs (AuNPs-AHP-KLA). The particles were characterized with UV-Vis spectrometer (BMG LABTEC Germany), Malvern Zetas**izer** Nano ZS (England, UK) and TEM (TECNAI F20 HRTEM, Eind-hoven, Netherlands). Investigative methods included tissue culture of monolayer and multilayer Caco-2 cells to 80% confluence at 5% CO2 and 35ºC for 24 hrs. Caco-2 cells were furthe incubated with 14 nm AuNPs for 24 hours prior to WST- 1, DAPi, Trypan blue dye exclusions, APO% assays. DAPi stained cells were examined under florescent ((Leica DM 2500: LED, Germany) and Trypan blue under light microscope (Evos XL Core light microscope (Scientific, USA). Results revealed that AuNPs concentrations above 10 nM/ml altered cell nuclear and membrane morphologies, and induced apoptosis *in vitro*. *In vivo* studies investigated the microscopic effects of 16 nm phyto-AuNPs synthesized with *Carprobrotus edulis* (CeFe-AuNPs) on liver, spleen, kidney, pancreas and heart of diabetic, male Wistar rats. CeFe-AuNPs were characterized with instruments mentioned above plus FTIR (Scientific-US). The CeFe-AuNPs were incorporated into Jellies cubes at 100/200 mg/kg concentration and stored at 4 ºC until used. Male Wistars rats were obtained from SAMRC PUDAC and caged to acclimatized to 22-25 ºC temperature, 45-55% humidity under 12 hours light and dark circles. Water and food were provided *ad libitum*. Rats were injected with STZ (40 mg/kg in 0.1 M buffer, PH 4.5) solution to induce hyperglycaemia and diabetes. Animals were then fed daily with a single dose jelly containing 100 or 200 mg/kg CeFe-AuNPs for 21 days. Afterwards they were fasted 6-8 hours overnight before euthanized via inhalation. Their blood and organs were harvested and the organs were harvested fixed in buffered 10 % formalin solution for

Haematoxylin & Eosin (H&E) histology processing protocols. Tissue slides were examined under x10, x40 objectives (Evos XL Core light microscope (Scientific, USA). In vivo study results revealed that 16 nm CeFe-AuNPs exerted graded toxicity on all tissue. However, statistical analysis of the glomeruli distribution was insignificant ($P > 0.05$). This infer that AuNP's toxicity might not be readily obvious until a large portion of the tissues were damaged.

Keywords: Apoptosis, gold cytotoxicity, gold nanoparticles; gold fluoroscopy, gold nanoparticle uptake, gold nanoparticle distribution, gold nanoparticle clearance. CeFe-AuNPs. microscopy, effects of gold nanoparticles.

I declare that this thesis "Microscopic analysis of *in vitro* and *in vivo* effects of functionalized and non-functionalized gold nanoparticles on the liver, kidney, spleen, heart and pancreas of male Wistar rats is my work and has never been submitted for any degree or examination in this university or any other tertiary institution. All the sources used or quoted have been duly indicated and acknowledged in my references.

Ekeoma Festus Fidelia.

Signature

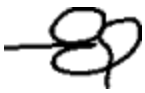

November 2022..

Acknowledgement

I am grateful to my maker for giving me the grace to complete this thesis that was like a mission impossible to accomplish. I am humbled by God's divine guidance in helping me contribute to the progress of nanotechnological studies in UWC with a heart-felt gratitude, I thank my brother, Akobundu, Godson Festus for facilitating my trip to South Africa and paying my tuition fees for this Masters' degree. I also appreciate other family members who have supported me in one way or the other in this journey. May I humbly thank my supervisors, Professor Abram Madiehe and Professor Okobi Ekpo for their guidance and assistance in this work. I also appreciate my laboratory supervisor, Dr. Nicole Sibuyi for her guidance in carrying out lab investigations, computing results and writing this thesis. I thank Ubong-Abasi Moses (Jr) for assisting me to arrange my preliminary pages. Other appreciated colleges are Fadaka, Jumoke, Lauren. I thank them for putting me through with lab protocols and equipment handling. Lastly, but importantly, I thank Keletso Modise for proving the histological slides used for this study. Her support and guidance to locate the tiny ingredients for this work are duly appreciated by me. To all and sundry friends who supported me in one way or the other, "may God be there for you too when men fail you."

Lists of abbreviations

FDA – Food and Drug Administration

AuNPs - Gold nanoparticles

RES – Reticuloendothelial system

CdTe/CdS – Cadmium Tellurite/Cadmium Selenide

γFe_2O_3 – gamma Iron II oxide

Fe_3O_4 – Iron IV oxide

NP/s – Nanoparticle/s

MRI/CT – Magnetic Resonance Image/Computerized tomography

CD133 – Central Domain 133

CRCSC – Colorectal Cancer Subtyping Consortium

MCF-7 – Code for human breast cancer cells

cAuNPs – Citrate capped gold nanoparticle

AuNPs-KLA-AHP – gold nanoparticle conjugated with proapoptotic peptide and Adipose

Homing Peptide

AuNPs-KLA – Gold nanoparticle conjugated to proapoptotic peptide

DAPi - 4′,6-diamidino-2-phenylindole

WST- 1 - water-soluble tetrazolium salt

CTAB: Cetrimonium bromide

PEG: Polyethylene glycol

Da – Deca, unit of atomic mass

FTIR- Fourier Transform Infrared Spectroscopy

HR-TEM- High Resolution Transmission Electron Microscopy

ANOVA - Analysis of Vaiance

SAMRC South African Medical Research Council

GSH-AuNPs - Glutathione bond gold nanoparticle

Human K562 - human lymphoblast cell

DNA-AuNPs, - Deoxynucleic acid bound gold nanoparticle

EDTA - Ethylenediaminetetraacetic acid

RSA - Republic of South Africa

KLA: D(KLAKLAK)2-DEVD-SH], - code

D(CKGGRAKDC)]. - code

AHP - Adipose homing Peptide and,,

PBS - phosphate buffered saline

PEG-OH - Hydroxylated Polyethylene glycol

DMSO - Dimethyl sulfoxide

cDMEM - complete Dulbecco's Modified Eagle Medium

DMEM - Dulbecco's Modified Eagle Medium

TEM - Transmission electron microscope

Av - Average

Aspr - highest Surface plasmon absorbance

A450 - Absorbance at 450 wavelengths

DOX - Doxorubicin

STZ Streptozotocin

AGE - Advance Glycated End products

DLS - Dynamic Light Scattering

PDI - Polydispersity index

AV - Atrial ventricle

MPS - Mononuclear phagocyte

PALS - periarteriolar lymphoid sheath

ECRA- Ethics Committee for Research on Animal

HSA- Human serum albumin

Lists of Tables

List of Figures

Chapter 1: Literature Review

1.1 Introduction

Nanomaterials are molecules or compounds that have at least one of their dimensions within 0- 100 nm nanoscale. They could be naturally occurring or fabricated. They could be used in arts/aesthetics, engineering, technology, construction, applied sciences, biomedicine, pharmaceutics, agriculture, biotechnology, cosmetics, food technology, etc (Barman *et al*, 2022; Glover *et al*. 2021; Khan *et al*, 2013; Balaguru *et al*, 2006; Weiss *et al*, 2006). The tendency to manipulate the surface properties of nanomaterials to achieve a desired physical or chemical outcome makes nanotechnology an interesting field for production and manufacturing companies (Adeola *et al*, 2019; Weiss *et al*, 2006; Papadopoulos *et al*, 2019). In the last decade, nanotechnology has consistently drawn attention from researchers all over the world because it provides a platform for solving problems for humanity and the biosphere. Our body and world are made of nanomolecules that we can only see with aided technologies. Hence the bid to understand ourselves, our world and how we interact with ultra-microscopic particles, sscientists are pushing to unravel more discoveries on ways to manoeuvre challenges face on earth. Presently nanomaterials can be used in consumables like coated electrodes combustion fuels, drugs, DNA primers, cosmetics etc. Notwithstanding, all these benefits, there have been concerns on environmental and health hazards associated with unregulated use of nanomaterials (Rajput *et al*, 2020; Pattan *et al*, 2014; Lanone *et al*, 2006). Scientists are concerned that unguided use of fabricated nano products could cause health and environmental hazards for humans and animals (Pattan *et al*, 2014; Kabir *et al*, 2018). Biomedical scientists are concerned about poor regulatory use of nanomaterials in medicine because humans constantly use drugs and cosmetics (Gubala *et al*, 2018), to that effect, monitoring bodies were constituted to regulate how nanoparticles are synthesized and used. These regulatory organizations are meant to enforce policies that ensure nanoparticles' synthesis follow credible meticulous and standardized protocols (Hasan *et al*, 2012; Dehhagh *et al*, 2019). The standardized protocols are guidelines that ensure that nanoparticles (NPs) production, uptake, distribution, and application pose little or no risks to health and the environment (MacPhai *et al*, 2013). Guidelines are provided by Drug Agency (FDA) in the United States (US) as researchers push to break grounds in the field (Ali, 2022, Nabil *et al*, 2019; Foulkes *et al*, 2020). The possibilities in nanotechnology achievements towards faster disease management and eradication of infectious disease is huge, however there have been reported cases of toxicity.

Hence regulatory bodies caution against premature claims on the safe use of nnanomaterials in biological systems without validatory investigations (Boisseau and Loubation, 2011; Justo-Hanani *et al*, 2015).

Before now, man-made nanoparticles were usually chemical synthesized. Chemically synthesized nanoparticles have been used for lots of ground-breaking discoveries and researches, however, their application in biomedical systems were limited due their cytotoxicity effects. Chemically synthesized nanoparticles are reported to adsorb toxic surface radical from there synthesizing milieu (Sengupta, Jayeeta, *et al*, 2012). Such toxic compound are responsible for the toxic effects in biological systems (Djurišić, *et al*, 2015). But presently, more attention is shifting towards green synthesized alternatives. Many researches are seeking ways to synthesize eco-friendlier and biocompartible nanomaterials for delivering drugs, gene, antibodies etc to biological systems (Konishi and Uruga, 2007; Vigneshwaran *et al*, 2007; Willner *et al*, 2006; Zhang and Shen, 2007; Shankar *et al*, 2004). However, in order to better understand the interactions between nanoparticles and biological systems, biomedical nano researchers and fabricators need to understand the nano scale sciences and how they impact nanotechnological applications (Lieber, 2003; Wang *et al*, 2012).

1.2 Nanoscience and nanotechnology

Nanoscience is the study of objects/particles within 1nm - 100nm on the nanometric scale. 1 nm is equivalent to 10-9 m. The planets, plants and animals are all built by particles; hence nanoparticles form part of life forms and cosmic particles. Figure 1.1 puts nanotechnology into perspective, relative to nature particles and matter. For instance, 10 atoms of hydrogen have a diameter of 10 nm, hence hydrogen molecules are nanoparticles (Bhushan, 2021; Donegá, 2014). Biologically occurring nanomaterials include the deoxynucleotide acids (DNA) nucleotides, proteins (2.5 nm), microorganisms: virus (10-6 nm), bacteria (30 nm – 10 µm). Natural nanomaterials include dust, haze, fumes, fog, dyes, cotton wool, silk. Crystals, nanospheres, nanoshells, nanowires etc. (Quan and Fang, 2010).

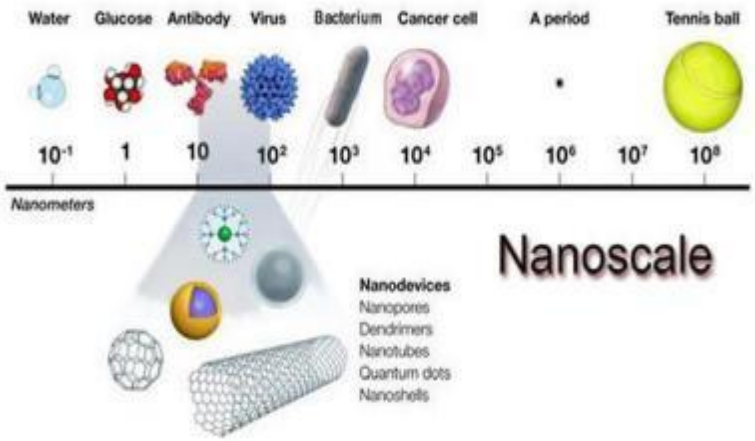

Figure 1. 1 Nanoparticle and non-nanoparticles on the nanoscale

Water molecules are the smallest sized (0.1 nm) molecules on the nanoscale in Figure 1.1 followed by glucose molecules, viruses, and antibodies respectively. These substances are naturally occurring biological nanoparticles that have all their dimensions within 0- 100 nm scale. The bacterium and cancer cells are microscopic organisms, but they are larger than 100 nm, hence will not be regarded as nanoparticles. The period and ball are macroscopic objects whose sizes are expressed in the nanoscale, but their sizes are far greater than bacteria or cancer cells - they can be seen with unaided eyes - hence they are not nanoparticles. Aggregates of nanoparticles form nanomaterials like graphene, nanotubes, nanopores, nanoshells etc (Glover *et al*, 2021; de Mello Donegá, 2014).

Organic and carbon-based nanoparticles are naturally occurring nanoparticles (Holder and Xu, 2008). Examples of organic nanoparticles include chitosan, dendrimers, liposomes, micelles.They have been reported to be biocompatible delivery systems for biomedical systems (Ealias and Saravanakumar, 2019). Inorganic nanoparticles include metallic, magnetic and quantum dots; there widely studied examples include nanoparticles made from noble metals like gold (Au), silver (Ag) and Copper (Cu), platinum (Pt); magnetic and superparamagnetic iron γFe_2O_3 and Fe_3O_4 and semiconductor nanocrystals (quantum dots made from Cadmium, Selenium Tellurite and Indium) (Krumeretal, 2013; Vander Stam, 2014). Nanoparticles differ in shapes, sizes and chemical properties differ from their bulk materials (Ito *et al*, 2005. Gubin *et al*, 2005); they could be zero dimensional - their length, breadth and height are at fixed point (e.g nano dots), or 1-dimensional - have only length (e,g graphene) or 2-dimensional - have only length and breadth (e.g nanotubes) or 3-dimensional - have length, breath and height (nanospheres). Organic and carbon-based nanoparticles are naturally occurring nanoparticles

(Holder and Xu, 2008). Examples of organic nanoparticles include chitosan, dendrimers, liposomes, micelles. They have been reported to be biocompatible delivery systems for biomedical systems (Ealias and Saravanakumar, 2019). They can be solid crystals, amorphous or loose aggregates or agglomerates. They can exist as spherical, cylindrical, starlike, rodlike, triangular, polygonal, tubular, irregular, etc, shapes of varying sizes (Donegá, 2014) and physiochemical properties are determined by their synthesis methods (Holder *et al*, 2008).

1.3 Nanoparticle synthesis

Different synthesis methods abound for nanoparticles, and researchers are constantly improving on them to enhance their ability to deliver desired goals. Basically, nanoparticles can be synthesized by physical, chemical and biological methods. These methods go through four major processes: gaseous phase, liquid phase - wet chemistry, solid phase - vapor deposits and grinding techniques (Sau and Murphy, 2004). Gas phase methods include the following procedures: evaporation, chemical vapour reaction, chemical vapour condensation and sputtering. The liquid phase method includes hydrolysis, precipitation, spray-solvent thermal process, oxidation-reduction process, emulsion-radiation-assisted chemical synthesis, solvent evaporation, pyrolysis and sol gel procedure. The solid phase methods involve solid state reactions like thermal decomposition, milling and stripping methods to produce agglomerated crystals and powders (Martinez *et al*, 2012; Bulychev, 2021).

1.3.1 Chemical synthesis

The wet chemistry is the most preferred method in AuNPs synthesis due to the various limitations associated with the other methods. Organic AuNPs nanoparticles are more biocompatible and biodegradable than inorganic ones (Mottaghitalab *et al*, 2019; Rabiee *et al*, 2020; Zhang *et al*, 2018). However, metallic or inorganic nanoparticles are versatile and easy to manipulate for a desired application (Chen *et al*, 2016; Lima-Tenorio *et al*, 2015). Synthesis of nanoparticles can be via Top-down or Bottom-up approaches as discussed below.

1.3.1.1 Top bottom synthesis

Top-bottom synthesis involves the breaking down of bulk materials into nanoparticles using various physical techniques. Examples of such techniques include laser ablation, sputtering,

thermal decomposition, mechanical milling, and nanolithography processes. Laser ablation involves synthesis in solution. It irradiates metal nanomaterial contained within a solvent. The irradiation causes excited atoms on the metal to react with the solvent to form nanoparticles (Amendola and Maneghetti, 2009, 2013). Thermal decomposition involves an endothermic reaction to introduce heat into a system to initialize chemical reactions between the precursors and the substrates. Metal nanoparticles are produced from thermal decomposition of a metal at specific temperatures where they combine with other molecules to yield their nanoparticle derivatives (Salavati-naisari *et al*, 2008).

1.3.1.2 Bottom -up synthesis

The Bottom-up approach involves the building up of nanoparticles from their atom clusters. It employs processes like Sol gel, Spin Disk Reactor (SDR), pyrolysis and Chemical Vapour Deposition (CVD). Sol gel is a wet chemical method which involves a precursor in the sol gel that can integrate with discrete nanoparticles in solution. Oxides of metals and chlorides are the common precursors used in sol gel (Ramesh, 2016). It involves a solid-liquid interphase which requires the precursor to be dispersed within the hosting liquid. The mixture is stirred or sonicated to attain even precursor dispersity. The nanoparticles are recovered by phase separation techniques such as centrifugation, sedimentation, filtration (Ramesh, 2016; Davis *et al*, 1997).

SDR involves an enclosed system without oxygen interference. The spinning chamber is filled with inert gas like nitrogen to avoid oxygen's oxidation. The temperature of the chamber is also controlled to avoid chemical reaction. As the rotor disc of the chamber is spinning, a precursor solution is fed into the chamber. The rotor disc speed bombard atoms and molecules against one another, causing them to cling together and precipitate out of solution. Factors that determine the characteristics of the synthesized nanoparticles include the disc surface, the rotation speed, the precursor flow rate, the precursor-liquid ratio and location of feed (Tai *et al*, 2006; Mohammadi *et al*, 2014). However, pyrolysis is the most used industrial process for nanoparticle production. It involves chemical combustion of precursors in flames - here the precursor liquid or vapor is fed into a temperature control furnace at high pressure. The gaseous by-product of the combustion process is passed through host liquid solid substrate to precipitate the corresponding nanoparticles (Madla *et al*, 2002).

CVD process involves a solid-gas phase reaction where chemical vapor reactants are deposited on the surface of substrate at controlled temperature. The process involves heating a substrate first, then introducing the vapor in an enclosed chamber. The vapor molecules react with the heated substrate to deposit a thin film coating which can be recovered. The downside of the procedure is that it requires specialized equipment; also, gaseous by-products are very toxic (Bhaviripudi *et al*, 2010; Adachi *et al*, 2003).

1.3.2 Biological (green) synthesis

This involves synthesizing nanoparticles from biological materials such as microorganisms (bacteria, virus, actinomycetes, fungi) and plants (Saratale *et al*, 2018; Kaviya *et al*, 2011; Glover *et al*, 2021; Salem and Fouda, 2021). It involves a bottom-up approach of harnessing biomolecules, followed by a chemical reduction of the metallic compound with biomolecules. It is unlike the chemical synthesis that uses physical and/or chemicals reagents alone. It is inexpensive and eco-friendly (Glover *et al*, 2021). Green synthesized nanoparticles in recent times are receiving more attention because scientists are looking for ways to make nano medications more compatible and less toxic to biological systems. Apart from being eco-friendly and biocompatible, biologically synthesized nanoparticles contain natural bioactive molecules that can be beneficial to health. This advantage is most exploited in biomedical applications (Prasad, 2008; Husen and Mohammed, 2019; Tangthong *et al*, 2021; Dhingra *et al*, 2010). However, the microbial synthesis method has been reported to be tedious and slower than plant extracts synthesis (Phyto-synthesis). Phyto-synthesis is reported to be more economical because plant materials are renewable (Kora *et al*, 2018), hence this study has paid attention to it.

1.3.3 Phyto-synthesis of nanoparticles

It is believed that phyto-synthesized nanoparticles make nano therapeutic more biogenic and less toxic to biological systems (Glover *et al*, 2021). Plants and plants products have been employed in the synthesis of metallic nanoparticles because the contain phytochemicals that can cap and stabilizes nanoparticles (Kuppusamy *et al*, 2016; Yasmin *et al*, 2014). Some identified plant phytochemicals include reducing sugars, proteins, polymers, flavonoids, organic acids, etc, (Ahmed et *al*, 2021). Phytochemicals like alkaloids, phenols, flavonoids and terpenoids give the nanoparticles their therapeutic properties (Akbar *et al*, 2020; Singh *et*

al, 2017; Vijayaraghavan and Ashokkumar, 2017; Agarwal *et al*, 2017). Several medicinal plants have been successfully used in nanophytosynthesis (Goodsell, 2004; Shankar *et al*, 2003; Shankar *et al*, 2004; Kasthuri *et al*. 2009a). The phytochemicals are employed as coatings and stabilizing agents using nanotechnological processes.

1.3.4 Nanotechnology

Nanotechnology involves developmental principles that measure and manipulate matter at the atomic, molecular and supramolecular levels. The measuring scale requires the nanomaterial to have at least one of it dimensions within approximately 1-100 nm (Glover *et al*, 2021). Atoms can be manipulated and molecules could be fabricated into nanostructures that reflect the properties desired by fabricator. Nanotechnology applied in various fields of sciences including in medicine (Seo and Song, 2006; Qiu *et al*, 2016). Nanotechnological application in health care includes Magnetic Resonance Image/Computerized tomography (MRI/CT) scan in imaging and diagnosis (Ding *et al*, 2013), dye fluoroscopy for living cell studies (Shin *et al*, 2017; Hong *et al*, 2014), antiseptics soaps, gels and creams for cosmetics (Katz *et al*, 2015; Mihranyan *et al*, 2012). Nanotechnology is also used for targeted drugs and gene delivery to cells (Peng *et al*, 2016; Daraee *et al*, 2016; Zhao *et al*, 2014; Oiu *et al*, 2022). AuNPs are widely used in biomedical applications, in respect to that, this study will dwell on AuNPs biomedical properties and applications.

1.3.5 Why gold?

Colloidal gold has been used as therapeutics since ancient times, long before the modern ages, as traditionally elixir for longevity and fertility. The history of bulk gold (Au) materials included being used as topical therapeutics for infectious conditions (Mahdihassan, 1984). In 1890, Robert Koch discovered that Au salts had anti-bactericidal effects on tuberculosis, and ever since then their usefulness in biomedical applications have increased (Balfourier et *al*, 2020; Saku *et al*, 2018). Some people had also used Au for neurological disorders and syphilis treatment before the 20th century (Sibuyi *et al*, 2021). Au has also been used for rheumatoid disease treatment (Wang *et al*, 2017). AuNPs are among the most researched and used metallic nanoparticle in biomedical and biotechnological applications because of their unique properties. Their optical and plasmon properties are importantly employed in their behaviour optimization and characterization during synthesis (Barabadi, 2014). AuNPs uniqueness leverages on the

stability of their bulk metal parent - which are considered bio-inert, safer, and less toxic (Zhang *et al*, 2022). Within a nanoparticle, the Au element is found at the core, surrounded by a corona of organic ligands which improve their biocompatibility by facilitating their uptake and distribution in biological systems (Kus-Liśkiewicz *et al*, 2021; Liu and Juewen, 2019). Different Au nanostructures (nanorods, nanospheres, nanocubes) are employed in various biomedical applications as carrier molecules because of surface area, flexibility and functionality.

1.3.6 Biomedical application of AuNPs

AuNPs can be easily ligated to desired drugs and moieties to target a specific cell/tissue receptors or enzyme (Negahdary, 2020; Zhang *et al*, 2018). This unique property makes them excellent delivery systems (Karthik *et al*, 2021; Wang *et al*, 2018; Qiu *et al*, 2016). Hence researches in Au nanotechnology are seeking ways to use them in drug delivery to cancers. Some studies reported that AuNPs can be used to successfully treat diseases like obesity (Sibuyi *et al*, 2018; Nijhawans *et al*, 2020), diabetes (Alomari *et al*, 2021; Dong *et al*, 2010), microbial infection (Vijayakumar, 2017; Khan *et al*, 2019), and cancer (Albarwary *et al*, 2021). Figure 1.2 represents AuNPs biomedical application overview.

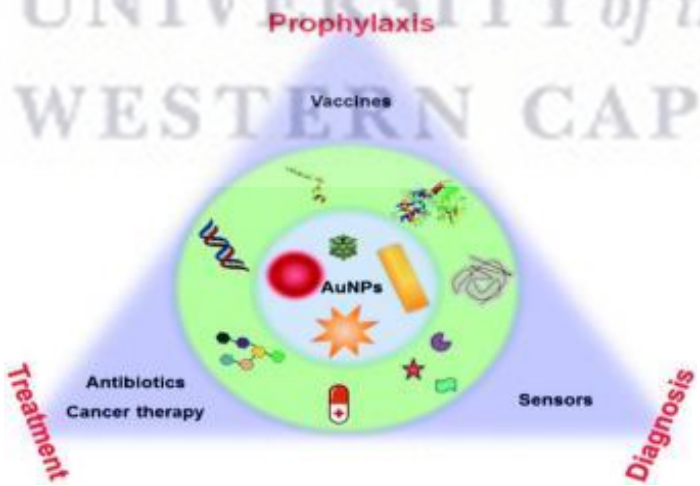

Figure 1. 2AuNPs surface chemistry and application in nanomedicine

The nanomaterials come in different designs as show in Figure 1.2 and can be ligated onto drugs, antibodies or nucleic acids, liposomes, phytochemicals, proteins etc for disease treatment. The latter group are important resources for vaccine synthesis and assay kit

biosensors (Abu-Dief *et al*, 2021). Different medicinal plants have been found to contain phytochemicals that improve disease like cancer and diabetes and nanotechnology applications complex AuNPs with phytochemicals that can be therapeutic to disease management. AuNPs have also been reported to reduce oxidative stresses and inflammatory cytokines by alleviating reactive Oxygen Species (ROS) generated in diabetes and cancerous conditions (Yu *et al*, 2021; Selim *et al*, 2015). It has been reported that the AuNPs anit-cancer mechanism involves the reduction of glutathione within cancer milieu to induces oxidative stress that destroys cancer cells (Kowsalva *et al*, 2021; Ramalingam *et al*, 2016). Hence the application of AuNPs in diabetes melitus would provide a two-way benefit that relieves oxidative stress as well as deliver anti-diabetic phytochemicals that willpromote insulin secretion and glucose uptake. Hence designing and synthesis phyto-nanomaterials for Type II diabetes management requires good understanding of glucose regulatory pathways and the defunct mechanisms that lead to the conditions. In this study, phyto-AuNPs was used for anti-diabetic studies as plausible therapeutics, hence the next literature review focuses on understanding diabetes and ways to employ green nanotechnology in its management.

1.3.6.1 Diabetes and health risks

Diabetes mellitus is a disease that affects the endocrine organs. It is characterized by sustained hyperglycaemia, with insulin resistance (Type II) or insulin deficiency (Type I) (Sirsikar *et al*, 2016). Insulin is secreted by beta cells of the pancreas. International diabetes foundation worries that over 450 million world population are battling the scourge of diabetes (Sutradhar *et al*, 2022) while 19.3 million cancers (Sung *et al*, 221. Shahid *et al*, (2021), reported that over 8-18% of cancer patients have diabetes as an underlying medical condition. Hence diabetes is one of the illnesses that requires urgent green nanotechnological interventions. Discussions from here gives examines diabetes and factors that lead to its debilitating effects.

1.3.6.2 Hyperglycaemia and role of glycation in diabetes

Hyperglycaemia means elevated glucose level in the blood. Usually, the hormone insulin helps the body cells take up glucose for energy production. However, there are metabolic conditions that prevents glucose from entering the cells, even in the presence of adequate insulin (insulin resistance) – a condition called Type I1 diabetes. Conversely, when insulin secretion is deficient (due to inefficient pancreatic beta cells activity), hyperglycaemia also results and is

called Type I diabetes (Morviducci *et al*, 2018). Conditions for diagnosing diabetes include fasting blood glucose level of ≥7.0 mmol/L (126 mg/dL) or 2 hours post prandial glucose level of ≥11.1 mmol/L (200 mg/dL) following oral glucose tolerance test (GTT), HbA1c value of ≥ 6.5% (48 mmol/mol) and a random blood sugar level of (200 mg/dL), (American Diabetes Association, 2021). Inability of cells to utilize glucose for metabolism will causes glucose build up in the blood. Glucose being a good reducing agent will complex with haemoglobin (HbA1c) and albumin in a non-enzymatic reaction called glycation– Haemoglobin is a key protein for cellular respiration, its glycation will affect the blood PH and homeostasis (Kaiafa *et al*, 2021). Early glycation form Schiff base (HbA1c) and Amadorin products while late glycation causes the formation of Advanced Glycated End products (AGE). AGEs could bind onto plasma proteins other than albumin to form toxic compounds (Mendes and Serrano, 2018; Kaiafa *et al*, 2021). which affects the metabolic enzymes and cause endocrine dysfunction.

1.3.6.3 Pathological markers of diabetes

Glycated haemoglobin, HbA1c: Protein glycation is a process that involves non-enzymatic addition of carbohydrate residues to their structure to form HbA1c, a Schiff base marker used in monitoring blood glycaemic index: It indicates the blood glucose state and the amount of circulating lipids in the blood over 2-3 months period (Sirsikar *et al*, 2016). It helps to ascertain how well diabetes Type II is being managed. It is an early marker for gestation diabetes too (Arab *et al*, 2019). It is been found associated with hyperlipidaemia which leads to arteriosclerosis in cardiovascular diseases (Sultan *et al*, 2011).

Blood sugars studies have reported that D-ribose sugar is implicated in HbA1c formation even though both D-glucose and D-ribose monosaccharides react with Hb to form glycated haemoglobin (Chen *et al*, 2017). D-ribose is reported to have more reducing effect on amino acids, proteins peptides, enzymes than D-glucose. (Chen *et al*, 2009; Wei *et al*, 2009). Sirsikar *et al*, (2016) reported that patients with HbA1c >7% have high lipid profiles compared to those with lower HbA1c value. High level of blood lipids is associated with impaired function of liver apolipoprotein. Liver apolipoprotein regulates the function of lipoprotein lipase and lipoprotein lipase controls the release of fatty acids from cholesterol and cholesteryl esters (Goldberg, 2009). However, HbA1c is considered a non-suitable glycaemic marker in liver cirrhosis, haemolytic anaemic and nephropathic conditions (Kaiafa *et al*, 2021; Jeffcoate, 2004). Studies argue that in these conditions, glycated albumin represents an accurate glycaemic

marker than HbA1c, because albumin glycation occurs more readily than haemoglobin glycation (Iberg and Flückiger; 1986).

Glycated albumin: Albumin, just like haemoglobin undergo glycation to form Schiff base in the early stage of hyperglycaemia and later stage Advanced Glycated End products (AGEs). Human Serum Albumin (HSA) is the most abundant plasma protein, hence, in early diabetes, glycation affects albumin primarily (Mendes and Serrano, 2018: Bhonsle *et al*, 2008). However, with prolonged hyperglycaemia, glycation will affect other proteins like ferritin, crystallin, collagen and apoproteins etc (Tomizawa *et al*, 1993; Guerin-Dubourg *et al*; 2017). Studies suggest HSA should be used as diabetes marker because it complexes with blood sugars 10 times more readily than Haemoglobin. Plasma albumin binds and transports a wide range of metabolites (drugs, metal ions, fatty acids, bilirubin). Early-stage albumin glycation alters the HSA structure and affects the efficiency of the binding sites and the specificity for metabolites and enzymes (Mendes and Serrano, 2018).

AGE products: AGE products are stabilized products of glycation that have undergone further irreversible oxidation (Chetyrkin *et al*, 2008). They have varying structures whose biological and chemical properties differ also. They can cross-link with proteins to form detergent insoluble aggregates that cause protein degeneration in metabolic disorders (Kepchia *et al*, 2003; Rosenberg *et al*, 2006) - as seen in diabetes mellitus. AGE products are considered markers for arteriosclerosis, nephropathy, and Alzheimer diseases. Howerver, they are increased in normal aged adults (Ulrich and Cerami, 2001). AGE is responsible for the aging process (Baynes, 2001; Moldogazieva *et al*, 2019).

1.3.7 Role of Diabetes mellitus in cancer and obesity onset

Diabetes mellitus is associated with various cancers like lung cancer, pancreatic cancer, liver cancer, gut cancer, breast cancer etc (Liu *et al*, 2020). The disease is associated with several risk factors that include, elevated insulin and insulin-like growth factors, hyperglycaemia, insulin resistance, inflammatory cytokines, dyslipidaemia, increased leptins and adiponectin etc., (Sunghwan and Kim, 2019; Chari *et al*, 2019). Obesity has also been reported to be an underlying factor for diabetes aetiology. Obesity is said to be a potent cytokine and lipogenic gene stimulator that promotes the release of endocrine hormones like oestrogen and growth

hormone to increase insulin secretion (Mendonca *et al*, 2015). End stage glycated products stimulate inflammatory cytokines which generates reactive oxygen species that counteracts glutathione protective effects on cells, predisposing them to oxidative damages (Arasteh *et al*, 2014). Oxidative damage orchestrates the stage for cancer aetiology (Sciacca *et al*, 2013). In the fight against diabetes, obesity, cancer and other debilitating diseases, biomedical scientists have continued to look for improved and better anti-dotes. Due is a growing need for therapeutics that lack widespread systemic cytotoxicity researchers are exploring green synthesized nanomaterials, especially phyto-synthesized for treatment of diabetes and cancers (Naeem *et al*, 2020; Yoo *et al*, 2019; Choi and Hands, 2018; Wicki *et al*, 2015).

1.4 Role of green nanotechnology in diabetes management

Phyto-nanotechnology for diabetes treatment could be the panacea and alternative to hormone replacement therapy and side effects due to prolonged dependence on prescription drugs. Nanomaterial can be designed to induce or knock out enzymes that are implicated in schiff base formation - HbA1c affects respiratory enzymes and energy dynamics negatively. (Kaiafa *et al*, 2021). Targeting enzyme that promote glucose uptake and schiff base formation requires extensive research to understand glucose uptake mechanism in hepatocyte. The liver and pancreas are key endocrine organs that are affected by insulin, hence they are more susceptible to diabetes induced cancers (Mattew *et al*, 2019; Hiller-Sturmhöfel 1999). The green success of synthesized nanoparticles for diabetes and cancer management will be dependent on successful enzyme modulations by biocompatible nanoparticles (Rodrigo *et al*, 2011; Lie *et al*, 2016). Hence targeting liver and pancreatic enzymes are plausible routes of approaching the problem because the organs play key endocrine roles in glucose metabolism (Chen *et al*, 2009; Wei *et al*, 2009). Sekar *et al* 2022 study reported that 36 nm AuNPs synthesized from *Physalis minima* extract were good anti-diabetic agents; they reduced free radicals and killed bacterial cells. Ayurrub *et al*, (2022) also reported that 20 nm -50 nm phyto- AuNPs lowered blood glucose levels in experimental animals. Several other studies have demonstrated the anti-diabetic activity of phyto-AuNPs (Oladipo *et al*, 2020; Guo *et al*, 2020).

1.4.1 Targeted delivery of phyto-AuNPs in biomedical application

Nanomaterials are engineered to carry anti-cancer drugs/agents to ensure that AuNPs-cargo remains intact in circulation until they reach their targeted sites. The conjugates will only target

the receptors on the cells and get internalized, then release their cargo to the target cells (Siddique and Chow, 2020; Naeem *et al*, 2020; Yoo *et al*, 2019; Sztandera *et al*, 2018). Targeted drug delivery is one way to circumvent the limitations of convectional cancer chemotherapy by improving drug specificity, prolonged circulation, controlled systemic release and drug resistance (Gu *et al*, 2012). This technology ensures that cancer/tumour cells had enough contact time with the drugs released by the nanoparticles within the cancer environment to elicit their anticancer effect before they are cleared from circulation (Mitra *et al*, 2015; Kalaydina *et al*, 2018; Rasha *et al*, 2021). Some researchers have been able to conjugate folic acid to AuNPs to carry Cisplatin to cancer cells (Feng *et al*, 2015). Others have functionalized gemcitabine adsorbed AuNPs with Cetuximab to target pancreatic cancer cells (Vijaya *et al*, 2013; Dhar *et al*, 2008; Petra *et al*, 2010). It has been reported that citrate capped AuNPs were successfully delivered to the human epithelial cervical adenocarcinoma cells (HeLa) (Barabadi *et al*, 2020); doxorubicin-AuNPs delivery complexes were used to target and kill cancer (Zhang et *al*, 2015); 5-fluorouracil (5-FU) functionalized AuNPs. successfully targeted CD133 receptors on colorectal cancer stem cells (CRCSC) (Mohd-Zahid *et a*l, 2020). There have equally been reports of successful use of green-AuNPs as anti-cancer therapeutics (Jain *et al*, 2012; Thakur *et al*, 2021; Al-Yasiri *et al*, 2017) even without additional targeting moieties (Khoobchandani *et al*, 2021). Ganeshkumar *et al*, (2013) reported that green synthesized AuNPs functionalized with folic acid exhibited anti-cancer effects on MCF-7 (breast cancer) cells and were not toxic to red blood cells at 1.6 µg/ml.

1.4.2 Limitations of AuNPs biomedical application and the future of green nanomaterials

Most reported nanotherapeutics are non-toxic at very low concentrations and the future speaks green nanotherapy because of biocompatibility. Green nanotherapeutics promises bio-compatibility, however there is still work to be done. Design is as important as compatibility because with nanomaterial can be made efficacious at low concentrations. Designing an efficient, targeting nanoparticle is the challenge of the modern-day scientists (Bourgine *et al*, 2011; Lea *et al*, 2015). In order to broaden the understanding of the effects of AuNPs in biological systems this study investigated the microscopic effects of AuNPs *in vitro* and *in vivo*.

Aim of the study

The aim of this study is to investigate the morphological effects of chemical synthesized AuNPs on monolayer and multilayer Caco-2 cells *in vitro*. In addition to that, investigate the morphological effects of green synthesized AuNPs on the liver, heart and kidney, spleen and pancreatic tissues of diabetic male Wistar rats.

Objectives

1. To synthesize citrate capped functionalized AuNPs with and without the targeting and therapeutic molecules

2. To characterize AuNPs using spectrometry and Dynamic Light Scattering (DLS)

3. To determine the cytotoxicity of the functionalized and unfunctionalized cAuNPs in monolayer and multilayer Caco-2 cells

4. To study the morphological effects of Carpobrotus edulis AuNPs (CeFe-AuNPs) in the heart, liver, kidney, spleen and liver tissues of diet-induced obese rats.

Chapter 2: Morphological effects of chemical synthesized AuNPs on monolayer and multilayer Caco-2 cells.

Abstract

Various AuNPs delivery systems have successfully targeted and destroyed cancer cells, thereby validating AuNPs' ability to penetrate the cell membrane to deliver targeted moieties to biological systems. However, studies have reported that Au residues accumulate in liver endosomes and in reticuloendothelial cells (RES) for a long-time post exposure. Hence this

study investigated the *in vitro* uptake and microscopic effects of 14 nm citrate capped AuNPs (cAuNPs), functionalized with AuNPs Adipose Homing Peptide (AuNPs-AHP) and targeting proapoptotic peptides KLA (AuNPs-AHP-KLA) on Caco-2 cells. Single layer Caco-2 cells were grown for 24 hours to 80% confluence while multilayer cells were grown for 15-21 days in culture flasks before being used for assays. Cells were incubated with 2.5 – 40 nM concentrations of AuNPs for 24 hours before cytotoxicity assays (WST-1 & APO percentage) or dye assays (Trypan blue DAPi) were carried out. Synthesized AuNPs were characterized with BMG LABTECH (POLArstar Omega. Germany) spectrometer, Transmission Electron Microscope (Eind-hoven, Philips CM200, Netherlands) and Malvern Zetasizer NanoZS (England UK). WST-1 colorimetric results revealed that the AuNPs species exerted dose dependent toxicity on Caco-2 cells. Concentration > 10 nM caused apoptosis, membrane disruptions and modified that shape of cells. Cytotoxicity effects on multilayer cells were more that those observed with monolayer cells. Result indicates that colorimetric assays may not account for membrane alterations in treated cells exposed to higher concentrations of AuNPs.

2.1 Introduction

There are several conflicting reports on AuNPs cytotoxicity that need careful considerations before justifying the safe use of AuNPs in therapeutic medicine (Olusola *et al*, 2019). Studies have reported that Au element is chemically inert and is non-toxic to biological systems since it had been used as therapeutics far back in history (Connor *et al*, 2005; Granitzer *et al*, 2013; Peng *et al*, 2009). However, some other studies have reported that AuNPs are toxic based on their surface modifications. Correard *et al*, (2014); Hwang *et al*, (2012); Hwang *et al*, (2012) reported that AuNPs behave differently compared to their bulk materials and as such, are reactive because of the increased surface to volume ratio. So, there have been discrepancies in AuNPs toxicity reports and the right size for biomedical application (Hwang *et al*, 2012; Balasubramanian *et al*, 2010; Cho *et al*, 2009). For example, Chen *et al*, (2013) reported that 8-37 nm sized AuNPs were more toxic to mice while Zhang *et al*, (2012), reported that AuNPs less than 20 nm can be used for *in vivo* therapeutics. Many other studies have supported that less than 20 nm AuNPs have wide distribution *in vivo* and are less likely to be trapped intracellularly for longer periods provided their surface chemistries were well engineered (Yang *et al*, 2017; Sengupta *et al*. 2013; Chen *et al*, 2013, Kim *et al*, 2013). An in vitro cytotoxicity study by Yu *et al*, (2007) on the different cell lines exposed to 1.2 nm - 1.4 nm

AuNPs stabilized with triphenylphosphine derivatives reported that they induced apoptosis, necrosis and cell death with 12 hrs (Gupta *et al*, 2017). In another study 50 - 100 micrometer of 10 nm, 20 nm and 50 nm AuNPs injected intraperitoneally into rats for 3 - 7 days duration altered the histology of hepatocytes, sinusoids and portal triads. The alterations included cloudy swelling, congested/collapsed central portal vein, hydropic degeneration, fatty degeneration, portal and lobular macrophage infiltration. The researchers reported that the least sizes caused the greatest cellular alterations (Abdelhalim and Jarrar 2012). Apart from size, shape is another property that affects AuNPs' behaviour. Studies have reported that AuNPs' shape influence show they interact with biological systems, and their subsequent uptake. Consequently, AuNPs are named according to their shapes (Sun *et al*, 2015; Schaeublin *et al*, 2012). Possible types are Au nanorods, nanospheres, nanotriangles, nano prisms, icosahedral, octahedral, tetrahedral, subhedral and decahedral, twined, etc. (Khan *et al*, 2014). Nanospheres and nanorods are reported to be the most researched AuNPs. Studies have found nanospheres more biocompatible compared to nanorods (Olusola *et al*, 2019; Chithrani *et al*, 2006). Toxicity and bioactivity of nanorods and nanoshells have been well reported in literature; O'neal *et al*, (2004) reported that nanoshells injected into mice caused tumour cells' ablation but had low toxicity on the animal's normal cells. The animals were reported to be healthy after 90 days post exposure to nanoshells. Lankyeld et *al*, (2011) reported that Cetyltrimethylammonium bromide (CTAB)-Au-nanorods injected into the tail vein of animal models were cleared from blood circulation within 15 minutes post injection; the group reported that PEG capping prolonged the blood circulation of the Au-nanorods (19 hrs half-life). Over the years, polyethylene glycol (PEG) has gained popularity as a capping agent for AuNPs because of its versatility, solubility and biocompatible. Zhang and co., (2015) reported that high molecular weight (5000Da) PEG is less toxic than low molecular weight PEG (2000Da). They also reported that AuNPs functionalized with double molecules of PEG are even more stable and less toxic with less aggregation tendencies. Recently, researchers are considering ligating PEG with glutathione (GSH) because the latter is less immunogenic and more biocompatible in living systems. Studies have found that >3 nm GSH-AuNPs resist opsonization by serum proteins, hence were efficiently cleared via the kidney (Ning *et al*, 2017; Simpson *et al*, 2013). AuNPs are coated, stabilized, functionalized with different ligands to enhance their stability and specificity in biological systems. Their surface moieties also determine their uptake and elimination routes. Hence inefficient surface design could impair effective AuNPs clearance and subsequent excretion - this would cause them to build-up within tissues and cause toxicity (Robson *et al.* 2018; Sani *et al*, 2021; Jia *et al*, 2017; Patel *et al*, 2010; Zhang *et al*, 2009, 2020).

Although toxicity is being measured by enzymatic response in assays like tetrazolium-based and lactate dehydrogenase (LDH) based colorimetric assays, demonstrable morphological changes are the only visible cytotoxicity evidence (Bácskay *et al*, 2018; Henkart, 1985; Prasad *et al*, 2020). In a study, Zeng *et al,* (2014) demonstrated the cytotoxicity of AuNPs in animal histologically tissues after exposure to AuNPs via inhalation. They reported that high AuNPs dosing reduced the number of alveoli and induced inflammatory response in the lungs of animals, regardless that physiochemical assays on the animal found no toxicity markers. Therefore, AuNPs toxicity studies require more extensive microscopic investigations in order to draw accurate conclusions on its cytotoxicity, to this regard, this study investigated the microscopic effects of 14 nm chemically synthesized AuNPs on Caco-2 using dye assay.

2.2 Materials and Methods

Table 2. 1: Lists of materials used in this study

Materials	Brand and country
T25 cm^2, T75 cm^2 flask, 12, 24 and 96 microwells	Biosmart, Romania
Cell proliferation reagent WST-1	Roche, Germany
Dulbecol's modified eagle's medium (DMEM)	Dulbecco, UK
Penicillin-streptomycin	Biochrom, Germany
Fetal bovine serum	Lonza, Germany
APOpercentage™	Bicolor, UK
PBS (Phosphate buffered saline:without calcium or magnesium PH 7.4), Trypan blue, Trypsin Versene (EDTA), 4% Formaldehyde solution, Dimethyl Sulfoxide (DMSO) DAPi	Sigma Aldrich, France

2.3 Chemical synthesis of AuNPs

Citrate-capped AuNPs (cAuNPs) of 14-nm diameter were prepared following the protocol described by Sosibo *et al*, (2015), where trisodium citrate was used to reduce and stabilize hydrogen tetrachlorocuprate ($HAuCl_4$; Sigma, MO, USA) to produce colloidal, spherical cAuNPs.

2.4 AuNPs Functionalization

Synthesized AuNPs were functionalized with two different peptides at Mintek (Advanced Materials Division, Randburg, RSA). The method involved N-fluorenyl-9-methoxycarbonyl (Fmoc) standard solid phase peptide synthesis with D-amino acids. Synthesized peptides included the proapoptotic peptide [KLA: D(KLAKLAK)2-DEVD-SH], and biotinylated PHB-targeting peptide [AHP:D (CKGGRAKDC)-biotin]. Their functionalization protocol is as described by Sibuyi *et al*, (2017).

2.5 Characterization of AuNPs and conjugates

The AuNPs were characterized by BMG LABTECH (POLARstar Omega, Germany) and Malvern Zetasizer Nano ZS (England, UK) as described by Sibuyi *et al*, (2017). For UV-vis, 1 in 49 dilutions of AuNPs were prepared with deionized water. 100 µl of the diluted AuNPs solutions were pipetted into 96 well plates and placed into a microplate spectrometric reader to estimate their surface resonance and absorbance. The UV-vis data was used to estimate the concentration of the cAuNPs and conjugates using the formula generated by Haiss *et al*, (2007) (Data as reported by Sibuyi *et al*, 2017). DLS data was used to estimate the AuNPs core sizes and polydispersity.

2.6 In vitro investigations on monolayer and multilayer Caco-cells

Caco-2 cells lines well sourced from the American Type Culture collection (USA) and subcultured into Dulbecco's Modified Eagle Medium (DMEM) (Dulbecco, UK) that was supplemented with 10% bovine serum and 1% penicillin (Lonza, Germany) in T75 cm2 flask. The Cells were incubated at 5% CO_2 humidified atmosphere at 37 °C. The cells were inspected daily for consistency. The growth

medium was changed every 2 to 3 days until they reached 80%. Then they were split and suspended in 10 ml 10% DMSO solution for stock making.

2.6.1 Cryopreservation

80% confluence cells in T75 cm2 flask were removed from the incubator and allowed 5- 10 minutes to equilibrate to room temperature before they were trypsinized (see trypsinization in the next paragraph), The cells were suspended in 10% DMSO medium (1 ml DMSO + 9 ml complete DMEM) at 1 x 10^5 cells/ml density. Using 10 ml sterile pipette, 1.5 ml aliquots of the cell suspension were placed into 2 ml cryovials. Each cryovial was capped tight and immediately placed on ice. The cryovials were stored at - 120 ºC. Each time a frozen cryovial stock was thawed and subcultured in complete DMEM (cDMEM), the cells were allowed to grow slowly to reach 80% confluence before they were split and subculture for the second time. After the second subculture, the cells were ready for assay investigations.

2.6.2 Trypsinization

The cells were aseptically washed twice with 5 ml PBS (Sigma-Aldrich, France). After second washing, the PBS solution was removed and replaced with 2 ml Trypsin-EDTA (Sigma-Aldrich, France). The flask was placed in the incubator for 1 - 2 minutes, after which the flask was placed under an inverted microscope to check for the rounded-up cells. Then, the flask was gently tapped to lift the cells. With a sterile 10 ml pipette, the cells were gently dispersed, aspirated, and placed into a sterile 15 ml centrifuge tube. 3 ml complete cDMEM was immediately added to the 15 ml tube to stop trypsin action. The tube was then centrifuged at 3000 g for 3 minutes. The supernatant was removed aseptically, and the pellet was gently re-dispersed in 1 ml of cDMEM. 20 ul was then pipette out for cell density estimation.

2.6.3 Trypan blue exclusion assay for cell counting

Cell viability was assessed using trypan blue exclusion assay (95% and above viability was acceptable pre-assay conditions). Briefly, 20 µl of cell suspension were aseptically withdrawn and diluted with an equal volume of 4% Trypan blue dye reagent. The mixture was added into the cell counter slide, then the slide was inserted into the Countess cell counter ((Introgen-

Korea) for cell density estimation. Afterwards, the required DMEM volume that will give 10^5 cells/ml was calculated and the cells are re-suspended in desired volume.

2.6.4 Monolayer Caco-2 cell culture

A cryovial of Caco-2 cells was retrieved from - 120 °C and rapidly thawed at room temperature. The contents of the vial were immediately aspirated with 10 ml sterile pipette and placed inside 15 ml centrifuge tube containing 10 ml cold complete DMEM (cDMEM - supplemented with 10% fetal bovine serum (Biochrom Germany) and 1% penicillin-streptomycin cocktail (Lonza, Germany). The tube and contents were centrifuged at 3000g for 3mins. Supernatant was aseptically removed, and pellets resuspended in 1 ml fresh cDMEM. The cell suspension was gently mixed, then 20 µl was pipetted for cell counting in Countess cell counters. to estimate cell concentration/ml. The required cell seeding volume needed to achieve $1x10^5$ cells/cm^2 density in fresh DMEM was then calculated. The required volume is added to the T25 cm^2 flask containing fresh 15 ml cDMEM. The flask was incubated in a 5% CO_2 humidified incubator at 37 °C. The morphology and growth rate of cells were inspected daily under a light microscope (Evos XL Core – USA) for consistency. The culture growth medium was aseptically changed with fresh one every 2-3 days until the monolayer cells reached 80% confluence, before the cells were split and subcultured again.

2.6.5 Multiplayer Caco-2 cell culture

Monolayer cells at the second subculture stage are allowed to reach 100 % confluence, overgrow and then differentiate to multilayer cells. The cells were allowed to grow in a T25 cm^2 flask for up to 14 to 21 days. They were inspected daily, and their growth medium was changed 2-3 days initially. However, as the cells reached 100% confluence within 5-7 days; the growth medium was changed every day until they were split and seeded into appropriate microwell plates. They were then grown for 24 hrs at 5% CO2, 37 °C in a humidified incubator prior to assay.

2.6.6 WST-1 investigation: effects of AuNPs on Caco-2 cells

Both multilayer and monolayer Caco-2 cells were seeded at 1 x 10^5 cells/ml into 96 well plates, 100 µl of suspended cells per well, except for the reagent blank. The microplates were incubated at 5% CO2 humidified atmosphere at 37°C for 24 hrs before treating. Prior to treating the AuNPs stock solutions were serial diluted with fresh cDMEM. The temperatures of all reagents were maintained at room prior to treatment. Then the cell culture flask was retrieved from the incubator and allowed 5- 10 minutes in the culture hood before treating; within this period, the microplates' outer covers were marked and labelled to represent negative, positive and AuNPs sections. The negative sections received no treated, the positive sections were treated with 100 µl of 15% DMSO while the AuNPs sections were treated with 100 µl of 2.5 40 nM/ml of cAuNPs, AuNPs-KLA or AuNPs-AHP-KLA. Cells were incubated with treatments at 5% CO^2 humidified atmosphere at 37 °C for 24 hrs. After incubation, growth media were removed from all wells and 50 µl of WST-1 solution was immediately added to all wells except the row for interference estimation. The microplates were wrapped with foil and incubated for 3 to 4 hrs. At the end of the incubation period, microplates were retrieved, and the UV-vis were read with BMG LABTECH (POLARstar Omega, Germany) spectrometer at 440 nm and 630 nm (all the absorbances were read at 440 nm, only the interference absorbance was read at 630 nm). The result was then exported to Microsoft (Ms) excel sheet for computation. The average values of triplicate microwell readings for each sample were calculated. The inference values were then subtracted from their corresponding average triplicate values to get the final values. The final sample values were then divided by the value of the negative control and multiplied by 100 to give their percentage cell viability.

% Cell viability = average absorbance of test samples ⁄ average absorbance of negative control x 100%

2.6.7 Cytology Investigations: AuNPs morphological effects on Caco-2 cells

The cellular morphological changes in monolayer and multilayer Caco-2 cells were assayed with Trypan blue, APO % and DAPI dyes and microscopically investigated with light (Evos

XL Core: Scientific, USA) and fluorescent (Leica DM 2500: LED fluorescent, Germany) microscope.

2.6.7.1 Trypan Blue Assay

Both multilayer and monolayer Caco-2 cells were seeded at 1 x 105 cells/ml into 96 well plates, 100 µl of cells per well. The microplates were incubated at 5% CO2 humidified atmosphere at 37°C for 24 hrs before treating. Prior to treating the AuNPs stock solutions were serial diluted with fresh cDMEM to have 2.5-40 nM/ml AuNPs concentrations. The temperatures of all reagents were maintained at room prior to treatment. The culture flask was then retrieved from the incubator and allowed 5-10 minutes in the hood before treating; within this period, the microplates' outer covers were marked and labelled accordingly. The negative sections received no treated, the positive sections were treated with 100 µl of 15% DMSO while the AuNPs sections were treated with 100 µl of 2.5 - 40 nM/ml of cAuNPs, AuNPs-KLA or AuNPsAHP-KLA. Cells were incubated with treatments at 5% CO_2 humidified atmosphere and 37°C for 24 hrs. Afterwards, treatments were aspirated with micro pipettes and the cells were washed with PBS before 50 µl of 4% Trypan blue reagent diluted with cDMEM (1:2 dilution) was added to each well and incubated for 30 minutes. The Trypan blue solution was removed quickly, and the cells were washed twice with 100 µl of PBS before viewing under an inverted microscope (Evos XL Core: Scientific, USA). Images were captured under x100, x400 magnifications and saved in pixels.

2.6.7.2 APO percentage assay assay of monolayer and multilayer Caco-2 cells

Cells (500 µl) in cDMEM were seeded into 24 microplates at 5 x 10^4 cells/500 ul culture medium and incubated in 5% CO2 humidified atmosphere at 37 °C for 24 hrs. Prior to the end of the incubation period, 40 nM/ml AuNPs (1000ml); 10 mM/ml hydrogen peroxide (1000 ml) (Sigma-Aldrich France) (apoptotic agents/reagent A) were prepared for test and positive treatment samples respectively. 500 µl of the apoptotic agents (reagents A) were used to prepare reagent B (500 µl apoptotic agent + 500 µl of 5% APO dye {10% DOX} for untreated control, 500 µl cDMEM + 500 ul of 10 % DOX). At 80% confluence, growth medium was removed from the culture wells and replaced with 500µl of apoptotic agents (AuNPs for test sample; hydrogen peroxide for positive control, no treatment for the negative control). The

plates were incubated in the same atmospheric conditions for 23 hrs 30 minutes. Then all the media are removed from cells and replaced with 500 µl reagent B (In all wells: for tests, untreated and positive control). The plates were returned to the incubator to complete the remaining 30 minutes incubation period. Afterwards the cells were washed twice with PBS (Sigma-Aldrich France). The last washing is retained as the cells were imaged under inverted light microscope (Evos XL Core: Scientific, USA) and viewed at x100 and x400 magnifications.

2.6.7.3 AuNPs Uptake and morphology and effects

Coverslips for this procedure were first cleaned and sterilised. Using sterile forceps, the coverslips were placed inside the wells of 12-microwell plates. Then 2.4 x 10^5 cells/ml of cells (500 µl/well) were seeded onto the 12 well plates and incubated at 5% CO2 humidity at 37 °C for 24 hrs. After 24 hrs, cells were treated with 20nM/ml AuNPs for 3 hrs. The treatment was aspirated, and the cells were washed twice with x1 PBS. Then the cells were fixed with 4% formaldehyde (Sigma-Aldrich France) solution. The cells were then washed with several changes of deionized water. 10 µl DAPI mounting medium was placed on a clean slide, the covers slips were carefully picked from the wells with the tweezers, excess fluid on the edges were blotted off on absorbent paper towel before they were placed face-down onto the DAPi mounting medium. The slides were allowed to air dry in the dark cupboard, before cell slides were imaged with fluorescent microscope (Leica DM 2500: LED fluorescent, Germany), pictures were taken and digitally analysed at x200, x400 magnifications.

2.6.7.3 AuNPs Uptake and morphology and effects

changes of deionized water. 10 µl DAPI mounting medium was placed on a clean slide, the covers slips were carefully picked from the wells with the tweezers, excess fluid on the edges were blotted off on absorbent paper towel before they were placed face-down onto the DAPi mounting medium. The slides were allowed to air dry in the dark cupboard, before cell slides were imaged with fluorescent microscope (Leica DM 2500: LED fluorescent, Germany), pictures were taken and digitally analysed.

2.7 Results

2.7.1 Synthesis and characterization of chemically synthesized AuNPs

The AuNPs were synthesized as previously described by our laboratory (Thovhogi *et al*, 2015; Sibuyi *et al*, 2017) following the citrate reduction method to produce 14 nm cAuNPs. They were functionalized by conjugating targeting peptide (AuNPs-AHP), non-targeting peptide and therapeutic agents (AuNPs-KLA-AHP). The physicochemical properties of the functionalized AuNPs were analysed by spectrometer BMG LABTECH (POLARstar Omega, Germany).

Figure 2.1 represents the absorbance spectrum for AuNPs used in this study. Their Surface Resonances (SPR) are within normal range for Au (517-575 nm), The graph shows that cAuNPs had the highest peak. The functionalized AuNPs has lesser peaks which correlates to the modifying effects exerted by their surface conjugates. cAuNPs had the highest peak at 520 nm, however, after functionalization with AHP its peak was at 526 nm and further shifted 528 nm after conjugation with non-targeting peptide KLA. The broader peak signifies increase in the spatial width of the AuNPs composite (surface conjugates, reduced absorbing energies in cAuNPs core making them more stable stabilized. It also reduces polydispersity index, PDI, which optimizes molecular interactions between different ligands.

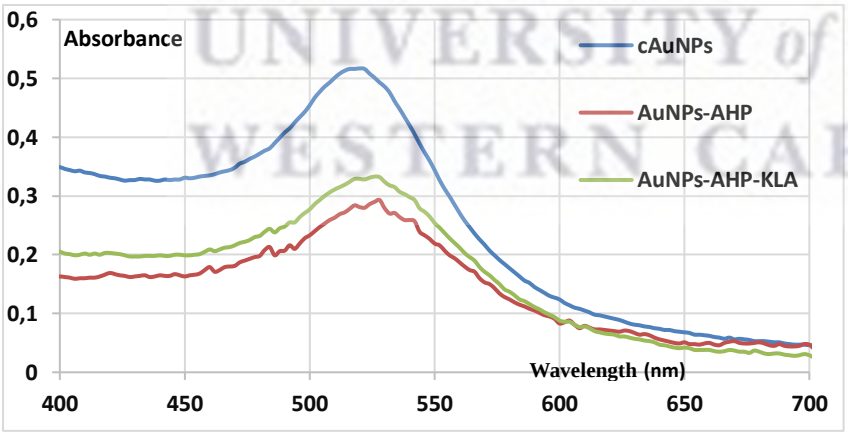

Figure 2. 1: Absorbance spectra of cAuNPs and conjugates

Table 2.2. describes the Dynamic Light Scattering potential of the synthesized cAuNPs and conjugates estimated with Malvern Zetasizer Nano ZS (England, UK). The functionalized

AuNPs have more homogenous polydispersity compared to the cAuNPs because of their surface modifications. The core size of the conjugated AuNPs is lower because of the nature of peptide bonds interaction with AuNPs. The C-N terminals of peptides are capable of several overlapping bonds that could shift its perceived centre.

Table 2. 2: Physiochemical properties of cAuNPs and conjugates

cAuNPs and conjugates	λ max (nm)	PDI	Core Size
cAuNPs	520	0.36	23.1 : 04
AuNPs-AHP	526	0.16	22.2 : 06
AuNPs-AHP-KLA	528	0.17	19:09

cAuNPs: Citrate capped AuNPs, AuNPs-AHP: Adipose homing peptide AuNPs, AuNP-AHP-KLA: Adipose homing peptide, proapoptotic AuNPs.

2.7.2 WST-1 Cell viability assay for monolayer and multilayer Caco-2 cells

Both monolayer and multilayer cells were grown to 80% confluence in 96 well plates. They were incubated with serial dilutions of 40 nM/ml AuNPs for 24 hours before WST- 1 cell viability estimation with spectrometer BMG LABTECH (POLARstar Omega, Germany).

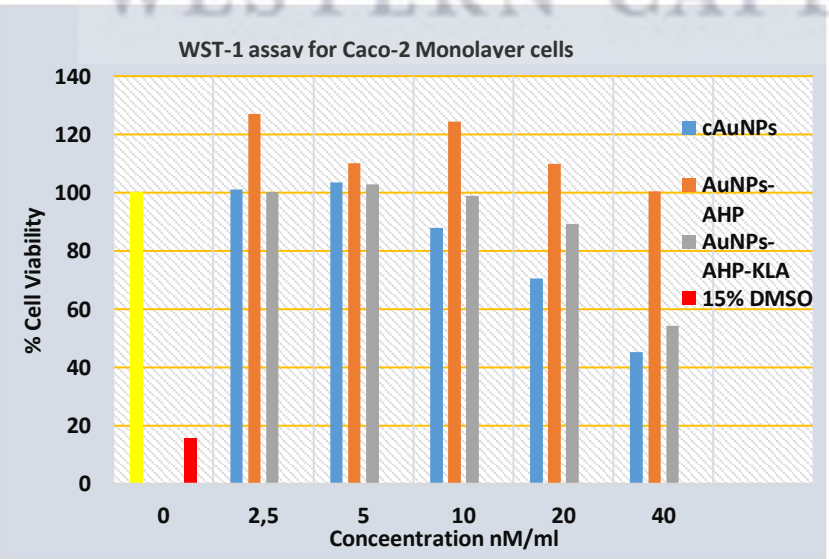

Figure 2. 2: WST-1 cell viability assay of monolayer Caco-2 cells

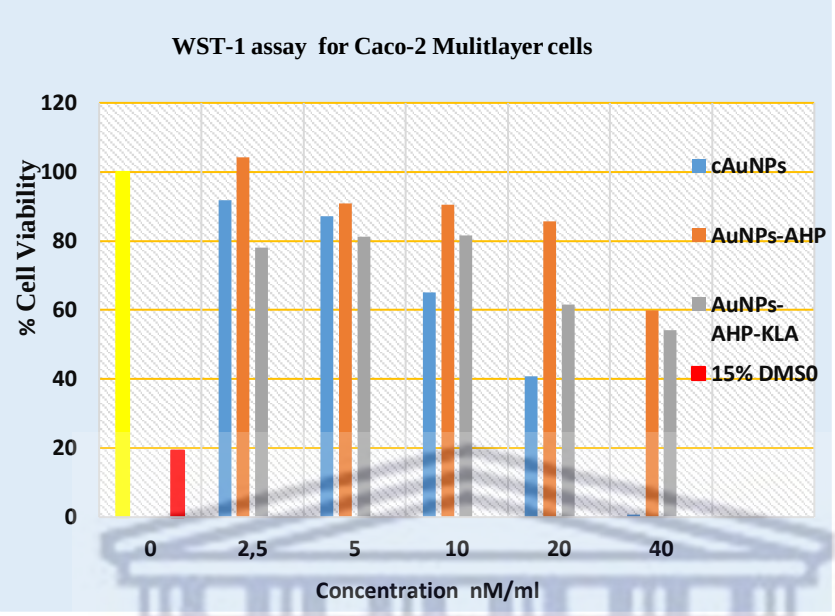

Figure 2. 3: WST-1 Cell viability assay of multilayer Caco-2 cells

Figures 2.2 and 2.3 describes WST-1 cell viabilities of monolayer and multilayer Caco-2 cells respectively in a bar chart. Cells treated with cAuNPs, AuNP-AHP and AuNPs-AHP-KLA showed high viabilities at 10 nM/ml and below. Above 10 nM/ml the viabilities decreased significantly, this supports similar results from previous studies done by Sibuyi *et al*, (2017). cAuNPs and AuNPs-AHP-KLA had lesser viabilities compared to AuNPs-AHP at higher concentrations. At 40 nM/ml, cells treated with cAuNPs had viability below 50% for monolayer cells and 0 for multilayer cells; showing that multilayer cells do not tolerate high concentrations of cAuNPs. This could be linked to the fact that citrate is a critical biological metabolite for biomolecule synthesis in the body. Excess citrate uptake could skew the normal metabolic pathways (Adedoja *et al*, 2022; Icard et *al*, 2012; Costello *et al*, 2016). Cells exposed to AuNP-AHP at lower concentrations (≤ 5 nM/ml) had viabilities above 100% and cells remained viable even at 40 nM/ml for monolayer cells. However, AuNPs-AHP viability fell below 60% for multilayer cells at 40 nM/ml inferring that AHP conjugate is the more tolerated AuNPs species.

2.8 In vitro cytologic effects of AuNPs conjugates on Caco-2 cell lines

The assays were conducted to investigate the morphology of Caco-2 cells after being exposed to chemically synthesized cAuNPs and its conjugates. The assays carried out included Trypan blue assay, APO percentage and DAPi staining and fluoroscope.

2.8.1 Trypan blue cytologic assay

Treated and untreated monolayer and multi-layer Caco-2 cells were incubated with 1:2 solutions of 0.4%Trypan Blue (Sigma, France) and cDMEM. Figures 2.3 and 2.4 represents viability states of treated cells compared with the untreated and positive controls after exposure to Trypan blue dye solution. Monolayer layer cells and multilayer differentiated cells were grown for 24 hrs in complete DMEM medium in 96 microwell plates to attain 60-80% confluence prior to assay.

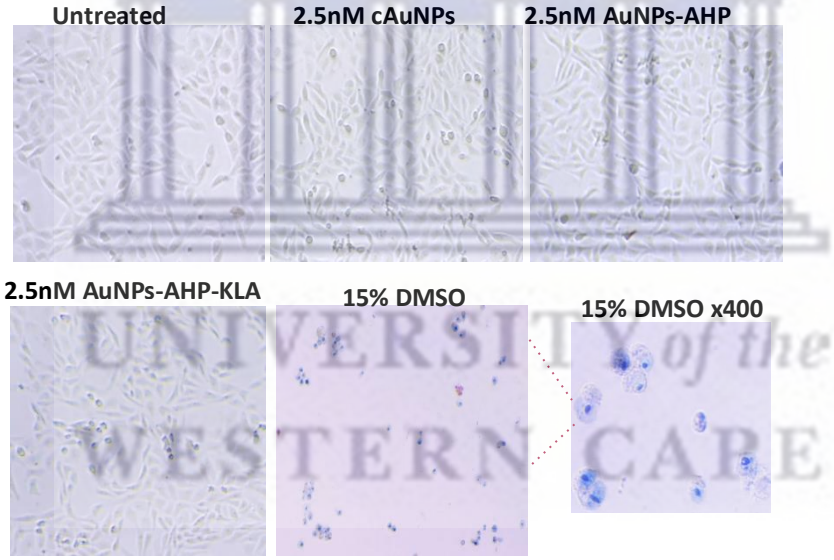

Figure 2. 4: Trypan blue assay for treated and untreated monolayer Caco-2 cell lines. Viewed @ x100 magnification (15% DMSO was viewed at x100 and x400)

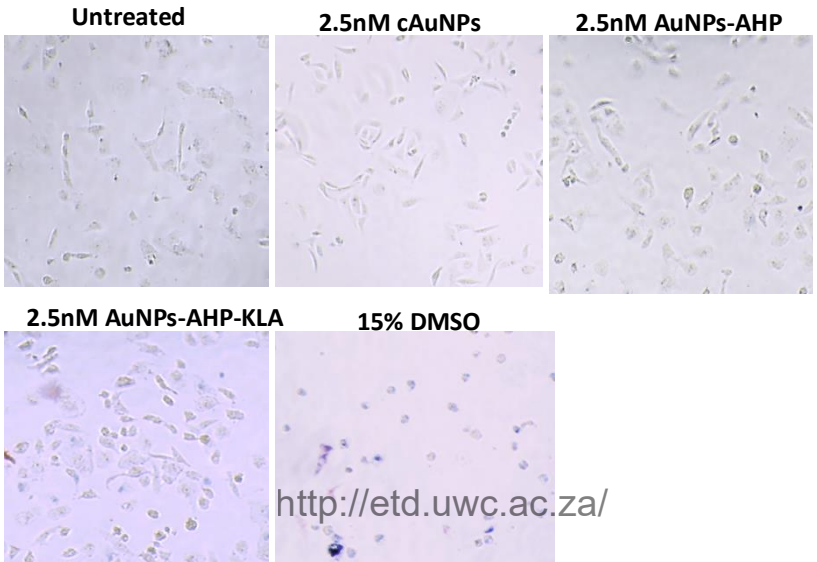

Figure 2. 5: Trypan blue assay for treated and untreated multilayer Caco-2 cell lines. Viewed @ x100 magnification**.**

Figures 2.4 and 2.5, represents monolayer and multilayer grown Caco-2 cells stained with 0.4% Trypan blue(sigma) respectively. Although the cell densities are reflected in the high viabilities of WST- 1 colorimetric results, morphological modifications are observed in treated cells. Monolayer cells treated with cAuNPs and AuNPs-AHP show areas of active cell division making them look more fusiform than the untreated control. The least membrane modifications can be seen in AuNPs-AHP treated cells, followed by cAuNPs treated. In Figure 2.4 Cells exposed to AuNPs-AHP-KLA, some of the cells absorbed the Trypan blue dye, and are apoptotic. However, Figure 2.2 show that AuNPs-AHP-KLA treated cells recorded high cell viability at 2.5 nM/ml with WST- 1 assay. The morphological changes and dye uptake indicated that their membrane have been compromised and they are dying. (Trypan blue dye is only taken up by dying or dead cells) (Kerschbaum *et al*, 2021). AuNPs-AHP-KLA effects on multilayer were more pronounced compared to the monolayer cells.

2.8.2 APO percentage assay of monolayer and multilayer Caco-2 cells

APO percentage assay used to investigate apoptotic effects of AuNPs on Caco-2 cells. The assay was carried out according to Bicolor protocol (www.bicolor-assay.com) The method included normal APO percentage protocol, however, the assay did not involve colorimetry investigation because this study is only interested in the cell microscopy. Figures 2.5 and 2.6 demonstrated the effects of AuNPs-AHP-KLA (therapeutic AuNPs).

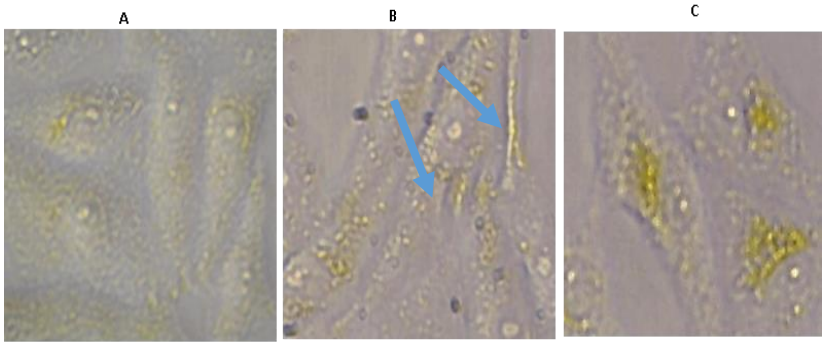

Figure 2. 6:APO percentage assay of monolayer Caco-2 cells
A represents cells treated with only APO dye in cDMEM solution, it is the negative control. B represents cells treated with 40 nM/ml AuNPs-AHP-KLA apoptotic agent and APO dye. C represents cells treated with hydrogen peroxide and APO dye. The dye agent used was 10% D0X. Microscopy @400 magnification- Blue arrow marks areas of membrane distruptions.

In Figure 2.6, nuclear condensation is visible at B, blue arrows point to area with disrupted membrane. 40 nM. AuNPs-AHP-KLA disrupted the membrane integrity allowing which will lead to loss of protoplasm.

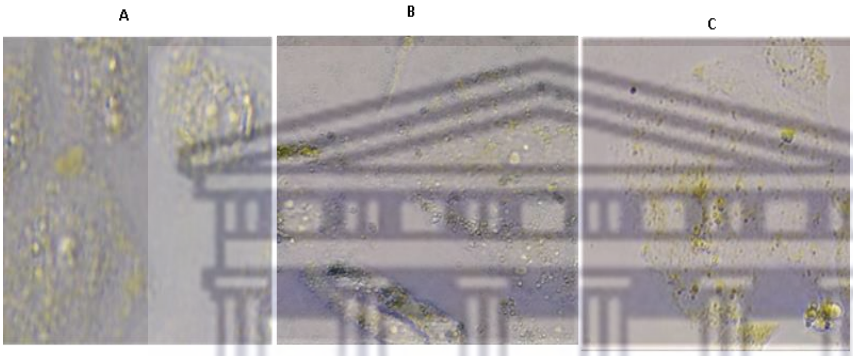

Figure 2. 7:APO percentage assay of multilayer Caco-2 cells
A represents cells treated with only APO dye in cDMEM solution, it is the negative control. B represents cells treated with 40 nM/ml AuNPs-AHP-KLA apoptotic agent and APO dye. C represents cells treated with hydrogen peroxide and APO dye. The dye agent used was 10% D0X. Microscopy @400 magnification.

Figures 2.7 shows that AuNPs-AHP-KLA induced apoptosis and necrosis of cells.

2.8.3 AuNPs Uptake and distribution

This assay was conducted to determine AuNPs uptake and visualize their effects on Caco-2 cells. Cover-slip seeded cells were treated with 20 nM concentrations of cAuNPs, AuNPs-AHP and AuNPs-AHP-KLA for 3 hrs in a 24 well plate. Cells were washed, fixed with DAPi mounting medium and placed face down on slides. Dried cell slides were imaged with a Fluorescent microscope (Leica DM 2500: LED fluorescent, Germany) @ x200 and x400. Cell images were taken at dark fields and fluorescent channels. Fluorescent images were overlaid on dark fields. Figure 2.7 and 2.8 describes AuNPs uptake and distribution in dark field, DAPi fluorescence and overlay.

2.8.3.1 Monolayer Caco-2 cells showing AuNPs uptake

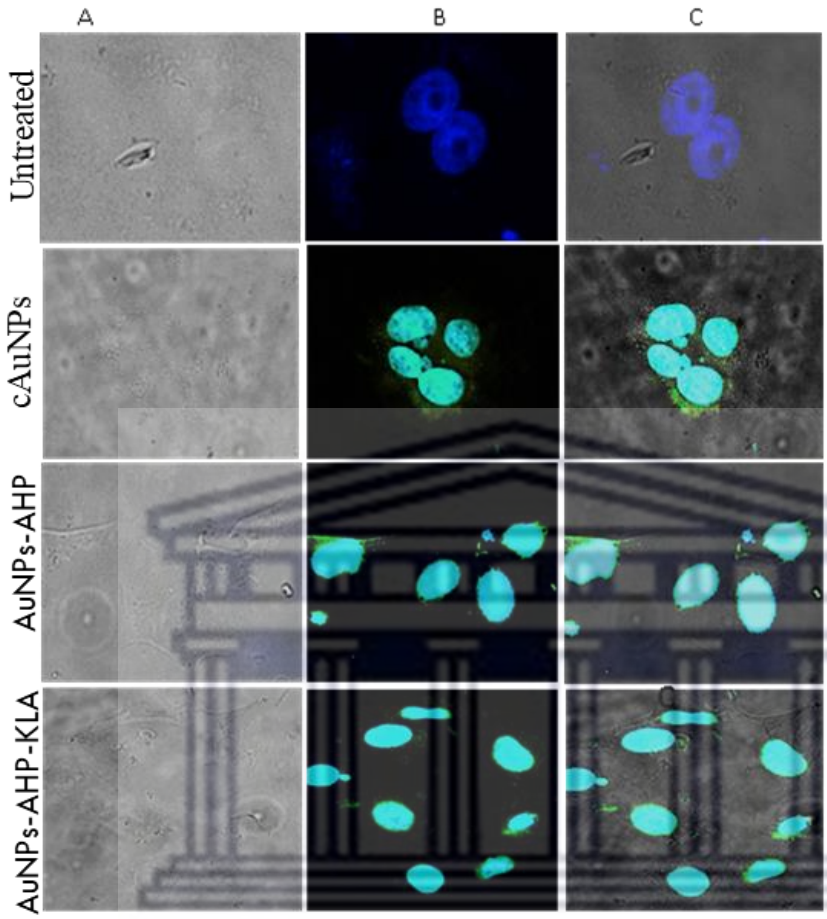

Figure 2. 8: DAPi fluoroscopy showing AuNPs uptake and distribution in monolayer Caco-2 cells.
Column A represents dark field, column B represents DAPi fluoroscopy channel and C overlay of B on A @ 400 magnifications. Each sample occupies a row.

2.8.3.2 Multilayer treated Caco-2 showing AuNPs uptake

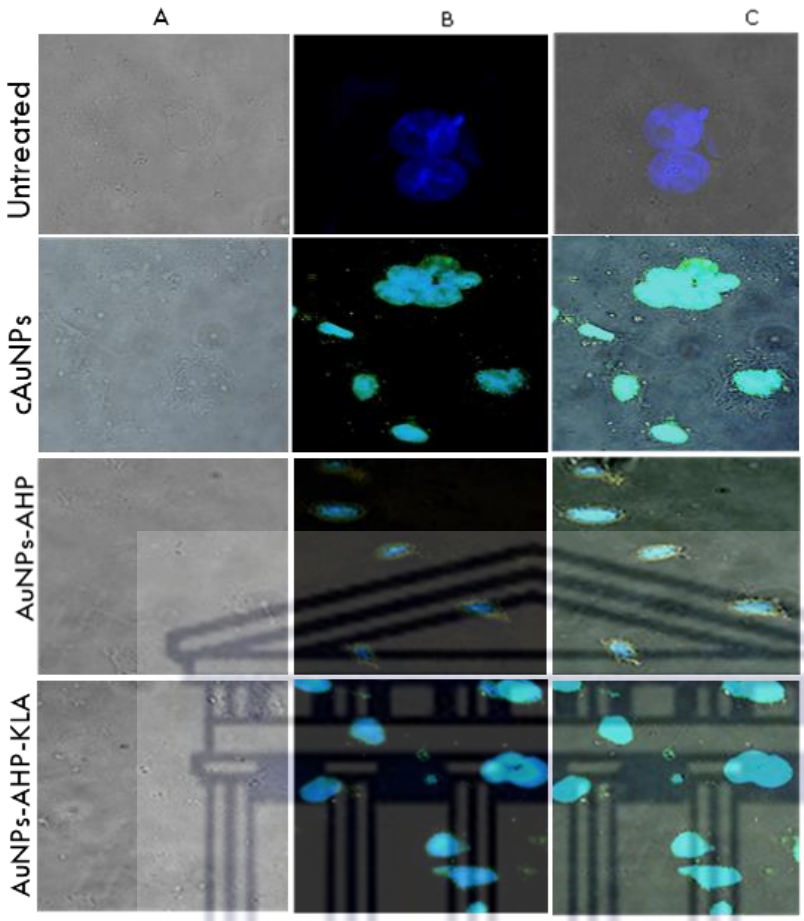

Figure 2. 9: DAPi flouroscopy, showing AuNPs uptake and distributiion in multilayer Caco-2cells.

Column A represents dark field, column B represents DAPi fluoroscopy channel and C overlay of B on A. Each sample occupies a row. Micrographs for the Control, AuNPs-AHP-KLA, cAuNPs treated where viewed @ x400 magnifications. AuNPs-AHP was viewed at x200.

Figure 2.9: AuNPs are seen as greenish-gold glow around different cell compartments of the cytoplasm and nuclei. Cells treated with cAuNPs show that cAuNPs are widely distributed across various compartments of the cell. cAuNPs had the highest uptake and distribution both in monolayer and multilayer cells because citrate is a normal biomolecule. The nuclei of monolayer cells treated with cAuNPs in Figure 2.8 were more regular than AuNPs-AHP and AuNPs-AHP-KLA. In figure 2.9 cAuNPs cells show similar nuclear consistency with the functionalized AuNPs - showing that effects of AuNPs on multilayer cells was more. Overall, cAuNPs treated cells have more regular nuclei. However, there were observable alterations in nuclear shapes on all treated cells. The nature of this alteration needs further studies. AuNP-AHPs accumulated more on the nuclear membranes. They demonstrated more specificity for the nuclei than the cytoplasmic organelles. because the treatment induced cell targeted apoptosis in treated cells. This agrees with reports that surface chemistry determines AuNPs effects on living systems. However, there were also modifications on the nuclei which required

further studies. AuNPs-AHP-KLA accumulated both within the cytoplasm and around the nuclei, however, the effects on the nuclei made them irregular and abnormally shaped. These effects are reflected in Trypan blue and APO percentage results as cytotoxicity. However, more studies are required to validate toxicity.

2.9 Discussion on in vitro results

It has been reported that different cytotoxicity assays produce varying results that may be contradictory, our findings in this study supports that notion. In our investigation, WST-1spectrometric assay readings infer high percentage cell viabilities for Caco-2 cells exposed to ≤10nM, 14 nm AuNPs species. However, this does not quite tally with the microscopic revelations. Microscopic investigations revealed that treated cells' structural integrity and functionality were modified or altered. The lowest AuNPs concentrations had the least cytotoxicity effects and corroborated with what had been already reported: that AuNPs cytotoxicity is dose dependent for both functionalized and unfunctionalized AuNPs. (Ganeshkumar *et al*, 2013, 2014; Sani *et al*, 2021).

2.9.1 Cytologic assays

Results in this study shows that high spectrometric viabilities do exclude microscopic membrane, nuclear and cytoplasmic modifications and/or alterations. Other researchers, Vetten *et al*, (2013) and Kroll et *al*, (2009) have also reported that assay contradictions correlate with interference between AuNPs and assay systems. Alkilany *et al*, (2010) inferred that AuNPs can adsorb indicator dyes in colorimetric analysing systems to quench their fluorescence. In this study we found that WST- 1 colorimetric assay was not sensitive to membrane disruptions/modifications, nuclear dysfunction or degenerative signals that could help in defining toxicity. DAPi fluoroscopy, APO percentage and Trypan blue.

microscopic analysis helped to elucidate AuNPs effects on cellular and nuclear components. The membrane extensions displayed by treated cells in images supports the report that receptor-based endocytosis is the major mechanism for AuNPs uptake (Shukla *et al*, 2005; Chithrani and Chan, 2007; Nativo *et al*, 2008). In Trypan blue and APO percentage assays, AuNPs modifications on Caco-2 were visualized. The numerous cellular membrane expressions and multinucleation expressed by AuNPs treated cells suggested increased

nuclear activity and gene activation as have been reported by other researchers. Falagan-Lotsch *et al*, (2016) reported that a single AuNPs dosage has a long-term effect on human cells. Another study by Ibrahim *et al*, (2018) reported that AuNPs induces acute inflammation and increased gene expressions. All the AuNPs species used in this study exerted greater toxic effects on multi-layer cells (differentiated cells) compared to their monolayer counterparts. It can be inferred that multilayer cell expresses greater number of receptors for AHP and citrate, hence they accumulated more of those AuNPs. This result agrees with reports by Thovhogi *et al*, (2015), that AHP increased AuNPs binding specificity and uptake. High AuNPs concentrations within multilayer caused toxicity and necrosis as seen in APO percentage microscopic assay. Other researchers have also reported that AuNPs' *in vitro* cytotoxicity affects the cell membrane, mitochondria or nucleus and could cause protein down regulation, DNA damage/mutagenesis, apoptosis, and cell death (Aillon *et al*, 2009; Alklany and Murphy, 2010; Jia *et al*. 2009).

In the present study, Caco-2 cells exposed to cAuNPs and AuNPs-AHP-KLA had high cell viabilities at ≤10nM/ml concentrations, however there were visible membrane and nuclear modifications on cells, even at 2.5 nM/ml concentration. This observation agrees with Adedoja *et al*, (2022) reports that although low concentrations of 14 nm cAuNPs were non-toxic to Caco-2 cells, they cause endoplasmic reticulum (ER) oxidative stress which activated cellular cytoprotective processes. Some other studies had reported that cAuNPs are non-toxic: Dobrovolskaia *et al*, (2013), reported that 30 nm – 50 nm cAuNPs were blood compatible because they induced no visible haemolysis, platelet aggregation, immune response, or reduced coagulation time *in vitro;* Villier *et al*, (2009), investigated the effects of 10 nm cAuNPs on immune dendritic cells and reported that they did not induce gene activation or cause phenotypic changes. However, result in this study show increased nuclear activities in AuNPs and AuNPs-AHP treated cells, increased nuclear activities equated to increase gene activation (see Figures 2.3, 2.7 and 2.8). Sani *et al*, (2021), reported that 13 nm cAuNPs had cell line dependent cytotoxicity: cAuNPs were toxic to human lung carcinoma cells but non-toxic to liver carcinoma cells. Enea *et al*, (2020) investigated the effects of 13 nm, 60 nm cAuNPs and 11-mercaptoundecanoic acid coated (MUA) AuNPs and found that 13 nm size had the most toxic effects because they increased cell glutathione and ATP levels and induced programmed cell death by activating the intrinsic and extrinsic pathways.

2.9.2 AuNPs Cellular uptake and their effects

DAPi staining demonstrated AuNPs distribution within the cellular compartment and the nucleus in this study. It is evident that cAuNPs were evenly distributed across various compartments of the cell compared to other species. AuNPs-AHP and AuNPs-AHP-KLA demonstrated more affinity for the nuclei than the cell membrane or cytosol. The results here agree with reported literature on the targeted delivery of functionalized AuNPs (Sibuyi *et al*, 2017; Thovhogi *et al*, 2015). The three AuNPs species used in this study modified CaCo-2 cells' membrane and nuclei. All the species of AuNPs exacted greater modifications on the multi-layer Caco-2 cells than they did on mono layer cells. Many researchers have established that AuNPs uptake and cellular internalization are different for varying cell lines. The variance was reportedly due to their charges, sizes, shapes, surface chemistry and functionalization. Hence uptake mechanisms could be passive or facilitated by phagocytosis, pinocytosis, receptor-mediated-endocytosis, and non-specific-receptor-independent endocytosis (Mao *et al*, 2013; Zhu *et al*,2014). However, other researchers reported that AuNPs uptake was size dependent (Yue *et al*, 2017; Chithrani *et al*, 2007; 2006; Chen *et al*, 2017; Choi *et al*, 2009b). The results in this study supported reports that AuNPs' uptake can be multifactorial.

2.9.3 Conclusion

Cytologic investigations revealed that high colorimetric cell viability estimations do not factor in cellular modifications that could prime cells for delayed autolysis, hence, biochemical assays should not be a stand-alone parameter for cytotoxicity investigations.

Chapter 3: Morphological effects of green synthesized AuNPs on RES tissues of diet-induced obese mice.

Abstract

Biomedical applications of Phyto-AuNPs is an alternative, eco-friendly approach to synthesizing AuNPs with enhanced biogenic effects against cancer, bacteria, free radicals, hyperglycaemia etc. This study investigated the microscopic effects of 16 nm AuNPs

synthesized from *Carprobrotus edulis* extract (CeFe-AuNPs) on liver, spleen, kidney, pancreas and heart of diabetic, male, Wistar rats. CeFe-AuNPs were characterized with TEM (TECNAI F20 HRTEM, Eind-hoven, Netherlands), UV-Vis spectrometer (BMG LABTEC, Germany), Malvern Zetasizer Nano ZS (England, UK) and FTIR spectrophotometer (Scientific, US). The CeFe-AuNPs were incorporated into Jellies cubes at 100/200 mg/kg concentrations and stored at 4 ^{o}C until used. Male Wistars rats were obtained from SAMRC PUDAC and caged under 22-25 ^{o}C temperature, 45-55% humidity and 12 hours light and dark circles. Water and food were provided *ad libitum*. After 2 weeks acclimatization period, the animals were grouped into 7 under same housing conditions prior to investigations. Group 1 received no treatment. Animals in other groups were intraperitoneally injected with STZ (40 mg/kg in 0.1 M buffer, PH 4.5) solution to induce hyperglycaemia and diabetes. Animals for CeFe-AuNPs studies were then fed a single dose of 100 or 200 mg/kg CeFe-AuNPs jellies daily for 21 days. Afterwards, animals were fasted 6-8 hours overnight before euthanized via inhalation and ensanguined via the vena cava. Their organs were harvested and fixed in 10 % buffer formalin solution. Tissues were processed and stained according to Haematoxylin & Eosin (H&E) protocols. Histology slides were examined under x10, x40 objectives (Evos XL Core light microscope (Scientific, USA). Results revealed 200 mg/kg of 16 nm CeFe-AuNPs induced blood vessel necrosis, tissue hydropism, vacoulation, and apoptosis in the liver and kidney; vein occlusion, necrosis and connective tissue disruptions in the spleen; membrane disruptions of myocytes and coronary vessels in the heart; membrane disruptions of Islets and acini in the pancreas. However, the damage severity was not the same across the organs, toxic effects were mild in the pancreas. Investigations of the kidneys' glumeruli distribution was statistically insignificant ($P>0.05$). The inference to draw is that CeFe-AuNPs toxicity might not be readily obvious until majority of tissues were damaged.

3.1 Introduction

Green nanotechnology is an unveiling field in biomedical sciences with great potential and resources that could alleviate varying human debilitating diseases. Several studies that synthesized metallic nanoparticles from medicinal plants and found they possesses antimicrobial, anti-inflammatory, and anticancer, anti-diabetic properties (Geetha *et al,* 2013; Shaneza *et al,* 2018). As green nanotechnology continues to advance, the use of gold nanoparticles (AuNPs) is taking centre stage in biomedical applications because of their unique

properties. Studies have demonstrated phyto-AuNPs' potency on cancer cells, diabetic conditions and bacterial infections (Hosny *et al,* 2021; Castillo-Henríquez *et al*, 2020; Satpathy *et al*, 2020; Arunachalam *et al*, 2003). Wang *et al*, (2019) studied the anti-cancer effects of AuNPs synthesised from aqueous root extracts of Scutellaria barbata and reported that the AuNPs were potent against colorectal cancer, breast cancer, hepatocarcinoma, skin cancer, lung cancer and ovarian cancer. In another study, Chen *et al*, (2021) investigated the anti-ovarian cancer in vitro and reported that 8 – 25 nm sized AuNPs were synthesized with aqueous extracts from *Curcumae Kwangsiensis folium* leaves. When PA-1, SW-626, and SK-OV-3 cells were incubated with the phyto-AuNPs, they exhibited size dependent toxicity on the cancer cells without apparent cytotoxicity to normal cells. In a similar study, Pechyen *et al*, (2022), reported that AuNPs synthesized from Spondias dulcis (SPE) extract were potent against breast cancer (MCF-7) cells in a dose and time dependent manner. They claimed that the SPE-AuNPs were non-toxic to Vero normal cells.

Green synthesized AuNPs apart from having anticancer, anti-diabetic abilities have been found to exert other bioactive effects that are beneficial in medicine. Bakur *et al*, (2019) investigated the effects of microbial glycolipid, mannosylerythritol lipid (MEL) synthesized gold nanoparticle (MEL-AuNPs) and reported that they exhibited antimicrobial activity against gram negative bacteria and had anti-oxidative effects on free radicals. They also exerted a dose-dependent cytotoxicity on liver cancer cells. Sekar *et al*, 2022 in a more recent study reported that 36 nm AuNPs synthesized from *Physalis minima* extract were good anti-diabetic agents; they reduced free radicals and killed bacterial cells. Ayurrub *et al*, (2022) also reported that 20 nm -50 nm phyto-AuNPs lowered blood glucose levels in experimental animals. several other studies have demonstrated the anti-diabetic activity of phyto-AuNPs (Oladipo *et al*, 2020; Guo *et al*, 2020).

Although biomedical applications of phyto-AuNPs have been successful in some areas, however, there have been reports that AuNPs exerted toxic effects on normal cells at elevated concentrations (Ganeshkumar *et al*, 2023; 2014; Peng *et al*, 2013; Chen *et al*, 2021). Ritz *et al*, (2015), Boulos *et al*, (2013) reported that proteins adsorb unto the surfaces of AuNPs to form a protein corona within biological systems, but more studies are required to elucidate the resultant effects of such interactions, both long term and short-term. Lankveld *et al*, (2011) reported on AuNPs bio-distributions blood clearance mechanisms, however mechanisms for Au residue exocytosis from endosomes have not been well elucidated in literature. Green

nanotechnology is believed to be a safer ground for synthesis of nanomaterials, hence there is hope that efficient green nanomaterial engineering will enhance their biocompatibility and efficacy within systemic circulation (Seku *et al*, 2018; Gubala *et al*. 2018). It will also ensure that nanomaterials are safely excreted from biological system after their delivery activities. As a result, nanotechnologist/scientists are saddled with the responsibility of improving on the efficiency of green synthesized nanotherapeutics. One way of improving efficiency in targeted delivery. Conversely, untargeted AuNPs delivery might mean unguided systemic exposure to AuNPs effects. This could have more adverse effect than targeted phyto-AuNPs delivery. As such, the challenge to green nanotechnology revolve around understanding the chemical interactions between AuNPs and biomolecules *in vivo*. Other challenging factors include accurate evaluation and determination of safe dosing thresholds for normal cells; fabricating degradable nanomaterials that can be easily excreted from biological systems without damage to vital organs (Ahmad *et al*, 2021). No doubt, comprehensive investigations on the effects of phyto-nanotherapeutics on healthy cells are crucial to advancing biomedical nanotechnology. Hence this work investigated the histologic effects of AuNPs synthesized from *Carpobrotus edulis* on the heart, pancreas, spleen, liver and heart on Wistar rats.

3.2 Materials and methods

Methodology: Haematoxylin Eosin histological protocol as below. (https://etd.uwc.ac.za/handle/11394/8319).

3.2.1 CeFe-AuNPs synthesis and characterization

16 nm CeFe-AuNPs were synthesized and characterized as described by Modise, (2021) (https://etd.uwc.ac.za/handle/11394/8319). CeFe gold nanoparticle (CeFe-AuNPs) analysis included spectrometry by BMG LABTECH (POLARstar Omega, Germany), Malvern Nano-ZS90, HRTEM, and FTIR. BMG LABTECH measured their UV-Vis; SPR was recorded at

532 nm. Malvern Zetasizer Nano-ZS90 at 25 °C was used to estimate the Dynamic light scattering (DLS) of the CeFe-AuNPs and its hydrodynamic size. The PDI and Zeta potential describes poly-dispersity potential (0.435) of CeFe-AuNPs in solution. Their polydispersity suggested complex surface modifications that restricted optimal polydispersity. When particles are well dispersed, they are primed for optimal interaction with surrounding molecules. CeFe-AuNPs core sizes (16 nm) were analysed with Transmission Electron Microscopy (HRTEM): FTIR analysis was used to characterize the organic bioactive phytochemical moieties, Modise, 2021, Madiehe *et al*, 2022. *In vitro* stability of CeFe-AuNPs in physiologic media like PBS, Serum Bovine Albumin, deionized distilled were determined with UV-Vis spectrophotometry as described by Modise, (2021).

3.2.2 *Carpobrotus edulis* fruit extract preparation

100 g dried *Carpobrotus edulis* (CeFe) fruits were bought from Bellville market and taken to lab for extract preparation. The fruits were hand-picked and cleaned off stalks before they were washed in distilled, deionized water. Afterwards, they were placed inside a clean container of 400 ml fresh distilled, deionized water and left to soak over-night to rehydrate. After rehydration, they were placed in a blender (Torrington Conn, USA) and homogenized for 10 minutes. The well blended homogenate was allowed to equilibrate to room temperature before filtering with a glass wool. The filtrate was centrifuged at 9000 rpm for 10 mins at 25 ºC. The supernatant was then filtered through Whatman No.1 filter paper to obtain CeFe extract. The extract was constituted in 400 ml of distilled deionized water to obtain 0.25g/ml extract concentration. Extract was stored at 80 ºC until used.

3.2.3 Jelly cubes preparation

75 ml of distilled, deionized water was heated to 80 ºC before 2 ml of red food addictive was added and mixed. 47g of gelatine power (unflavoured) was then added and thoroughly mixed, then 75 ml of distilled, deionized water at room temperature was added to the mixture and homogenized. The mixture was transferred into silicon moulds. They were allowed 1 hour (at least) to cool and solidify in the fridge. Afterwards, they were stored at 4ºC until used. Jellies without treatment were fed to the animals during acclimatization phase. For the treatment, the gelatine was allowed to cool to 20 ºC before 100/200 mg/kg CeFe-AuNPs or 200/400 mg/kg

CeFe extract were added to the Jellies and mixed. Then the gelatine-treatment mixtures were left to set, afterwards they were stored at 4 ^{o}C until used.

3.3 Animal housing and care

Animal investigations were performed in accordance with the guidelines and approval of the South African Medical Research Council (SAMRC) Ethics Committee for Research on Animals (ECRA 08/19) and the University of the Western Cape Animal Research Committee (AR 20/1/1).

Animals were housed under 22-25 ^{o}C, 45-55 % humidity, and 24 hours light and dark cycles in the laboratory. 20 female and 40 male Wistar rats were sourced from SAMRC PUDAC and water and food were provided *ad libitum*. The female rats were used for lethal dose toxicity studies while the male once was used for anti-diabetic investigations (please Modise's report on toxicity investigations via the link (https://etd.uwc.ac.za/handle/11394/8319. 40 Wistar male rats used for anti-diabetic studies were grouped and treated as described in Table 3.1. For this purpose of this study, focus is on CeFe-AuNPs effects on tissue slides from Group 1, V and VII.

Table 3. 1: Animal groups for anti-diabetic studies

Groups	Animal conditions	Treatment
1	Non-diabetic	Untreated
II	Diabetic	Untreated
III	Diabetic	metformin treated

IV	Diabetic	200 mg/kg CeFe extract
V	Diabetic	400 mg/kg CeFe extract
VI	Diabetic	100 mg/kg CeFe-AuNPs
VII	Diabetic	200 mg/kg CeFe-AuNPs

3.3.1 CeFe-AuNPs anti-diabetes investigations

42 male Wistar rats were obtained from the SAMRC PUDAC and allowed to a week to acclimatized to their environment. They were randomly grouped into 7 groups (n=7) for several diabetic studies. Group I – non-diabetic control. Group VI and Group VII were treated with (100 mg/kg or 200 mg/kg) CeFe-AuNPs. Animal subjects were left to fast for 6 – 8 hours prior to STZ injection animals were placed on 10% sucrose water *ad libitum* for 3 days in order to prevent death due to sudden, induced hypoglycaemia. Freshly prepared STZ (40 mg/kg in 0.1 citrate buffer PH 4.5) was administered intraperitoneally into groups II – VI; Group I was injected with 0,1M citrate buffer, PH 4.5. Post injection, animals were placed on 10 % sucrose water for 3 days before they were allowed to drink regular water. After diabetic induction, animals that recorded less than 250 mg/dl blood glucose were removed from the group. Subsequently, single dose treatments were administered daily for 21 days. The animals were observed closely for toxicity signs during the entire process. Their body weights were recorded weekly. A day prior to necropsy, the rats were left to fast for 12 hours, afterwards, they were weighed, and their blood glucose measured. They were anesthetized with isoflurane via inhalation before being ensanguined and euthanized. Their vena cava blood was collected for analysis. Organs of interest were harvested and weighed before being fixed in 10% formalin

for histological studies. For this study, organs of interest included the heart, liver, spleen, kidney and pancreas.

3.3.2 Histology investigations

The organs were examined to spot and remove unhealthy tissue from the control group. Thereafter all organs are fixed in 10 % neutral buffered formalin. Tissues were cut and placed in tissue caskets, processed and stained with H & E at the National Health Laboratory Services, Department of pathology, University of Cape Town. The process involved organ orientation, sizing, dehydration and wax perfusion. The last two processes were automatically done in tissue processor: Afterwards the tissues were placed in cassettes moulds and embedded in molten paraffin wax to form tissues blocks. The blocks are effaced, before 2 µm tissue slices are cut with a microtome. Cut tissue slices were floated on a clean, distilled water bath at 40-45 ^{o}C until the paraffin creases were evenly spread out. (Precaution was taken against over hydrating cells on water.). The tissues were then picked up with well labelled charged slides and placed on ranks to air dry overnight. Dried tissue slides were dewaxed at 55 ^{o}C, before they were gradually re-hydrated in graded alcohol solutions. Then they were stained with H&E, washed, and blued. Afterwards they were dehydrated in graded alcohol solutions until they attain absolute dehydration. Then they were cleared in xylene, and cover-slipped with mounting medium. Cover slipped slides were stored in a well labeled box at room temperature until viewed. The slides were viewed under light microscope with x4, x10 and x40 objectives and image saved in pixels. Images were investigated under light microscopy and interpreted.

3.4 Statistical analysis

ImageJ, Excel sheet and SPSS software were used to analyze data. Data sampling was done with ImageJ. Measurements were uploaded to SPSS for two tail T--test and One-way ANOVA analysis. Excel was used for bar chart data representation.

3.4.1 Sampling method

The tissue slides of each rat subject were prepared in triplicates (3 rats in each group: VII, V and I) were investigated meaning 3 slides for 5 organs for just one group. This means triplicate slides for the five organs multiply by n(3x15) =45; the total number of investigated slides.

Three rat groups were investigated in this study and they are: the untreated control group, the CeFe-AnNPs treated and the CeFe extract groups (Group 1, V and VII). The slides were screen for artefacts. After screening the best 15 slides were selected from n (15)

3.4.2 Measurements

Micrographs (saved in pixels) under x100 were used for this investigation. The images were uploaded to ImageJ software for visual sampling within five sections of each renal tissue. Firstly, image dimensions in pixels were set to read micrometre by calibrating the analytic scale of the ImageJ software using a known control measurement (1 pixel =264 µm). For the kidney, five fields were viewed (north, east, west and south and central of the tissue slide), one field view from tissue section. Every glomerulus seen within field were measured and the software simultaneously recorded the distribution per field. Data from five fields for each slide was summed-up and the average estimated and recorded. The same procedure was done for the triplicate slide for each animal tissue n=3. For 3 groups, a total of nine slides were investigated. At the end of measurement, the average distributions for each group is estimation with SPSS. For the Islets, all viewable islets seen on the entire slide were counted as they were measure because their numbers were few. ImageJ lines selection tools were used to visually draw transverse line across each glomerulus/Islet and the system automatically estimated and recorded the dimension in micrometres. Similarly, a free hand selection tool was used to trace the circumference around each organelle and the software automatically estimated and recorded perimeter in micrometres.

3.5 Results

3.5.1 Introduction

The current study only investigated the microscopic effects of CeFe-AuNPs on the tissues diabetic rats to evaluate the effects of biocompatible, phyto-AuNPs (CeFe-AuNPs) on in vivo. This is an extension of an anti-diabetic studies by Modise, 2021. Hence microscopy of histology tissues and their effect is the focus. The characterization of synthesized CeFe-AuNPs is as described by Modise (https://etd.uwc.ac.za/handle/11394/8319), however, Table 3.1 represents data on their physiochemical properties of CeFe-AuNPs.

3.5.2 Glomeruli and Islets indirect size estimations

Classic glomerular size studies have used diameter profile accounting to randomly estimate the size and efficiency of the glomerulus (Moore *et al*, 1993; Bilous *et al*, 1987; Miller and Meyer, 1990; Newbold *et al*, 1990). In this study the diameters and perimeters of the glomeruli were measured with ImageJ software analyser because the perimeter highlights the surface area for filtration while the diameter highlights volume capacities for both for the kidney and pancreas.

3.5.2.1 Glomerular measurements

Kidney tissue micrographs in pixel were uploaded to ImageJ app and the dimensions where converted to micrometres by the software. The kidneys micrograph was divided into north, east, west, south and central section/fields with the help of software gridlines. The glomeruli diameters in one field were estimated with selection tools which simultaneously measure and counts the numbers per field. Glomerular measurements and distributions for the five fields were summed-up and data recorded. This was done for each triplicate slide of same organ. At the end of analysis, the average value was taken. Same measurements were done for the 3 groups studied ImageJ was used to analyse distributions, standard deviations and averages. SPSS was used for One-way ANOVA and Two-tail Test while Spread sheet was used for bar chart representation.

3.5.2.2 Islets measurements and estimations

Pancreatic tissue micrographs received the same conversion and measuring process above, however the sampling method differ slightly. There was no field sectioning done with the pancreatic tissue slide because the viewable Islets are few. The entire slide view was sampled and measured as a single data entry. Averages were only found for the triplicate slides that represent data animal from one group. Data was analysed as described in 3.5.2.1.

Table 3. 2: Physicochemical properties of CeFe-AuNPs

Treating agent	**λ max (nm)**	**PDI**	**Core Size**
CeFe-AuNPs	532	0.435	16 ± 0.31 nm

CeFe-AuNPs estimated surface plasmon resonance (SPR) 532 nm is normal. The Uv-vis value for gold is usually between 517 - 575 nm (Azzazy *et al*, 2012). The PDI value is at the upper range of normal values (5) and is due to complexity in their surface moieties. For detailed physiochemical properties see, Modise, 2021, Madiehe *et al*, 2022. (https://etd.uwc.ac.za/handle/11394/8319). In this study, the estimated surface resonance for the synthesized AuNPs is 532 nm. The value is normal for Au, usually the surface resonance for unconjugated AuNPs is higher than the conjugated composite due to the lowered energy of the latter. CeFe-AuNPs is not conjugated but capped and stabilized by phytochemicals. Elevated PDI suggest the CeFe-AuNPs has higher energies than conjugated AuNPs, hence they will be more reactive.

Table 3. 3: describes glomeruli and Islets measurements and distribution

Glomeruli/ Islet distributions and measurements			
Glomeruli	Av.No.. counted	Av. Diameter (µm)	Av. Perimeter (µm)
Negative control	82	32.40 ± 0.09	135.40 ± 0.29
CeFe-AuNPs	80	33.20 ± 0.06	136.80 ± 0.69
CeFe extract	81	30.20 ± 0.12	140.0 ± 0.21
Islets	Av. No.counted	Av. Diameter (µm)	Av. Perimeter (µm)
Negative control	13	18.04 ± 0.12	78.90 ± 0.47
CeFe-AuNPs	20	18.03 ± 0.06	83.20 ± 0.49
CeFe Extract	12	17.42 ± 0.16	111.62± 0.60
Av, no. represents average number of count and Av, average diameter or perimeter.			

The average number of glomeruli represents the filtration capacities of the nephrons of investigated animals (the control untreated group, the CeFe-AuNPs and CeFe extract treated groups). The average diameters and perimeters are morphometric properties that indicated the sizes of the organs. The diameter of an organ depends on the type of straight line measured. For this study, horizontal straight line was drawn from one side of the organelles to another (not from the macula densa pole). Figure 3.1 represents the bar chart for glomerular and Islet distributions while Figure 3.2 represents bar chart for size (diameter perimeter) measurements.

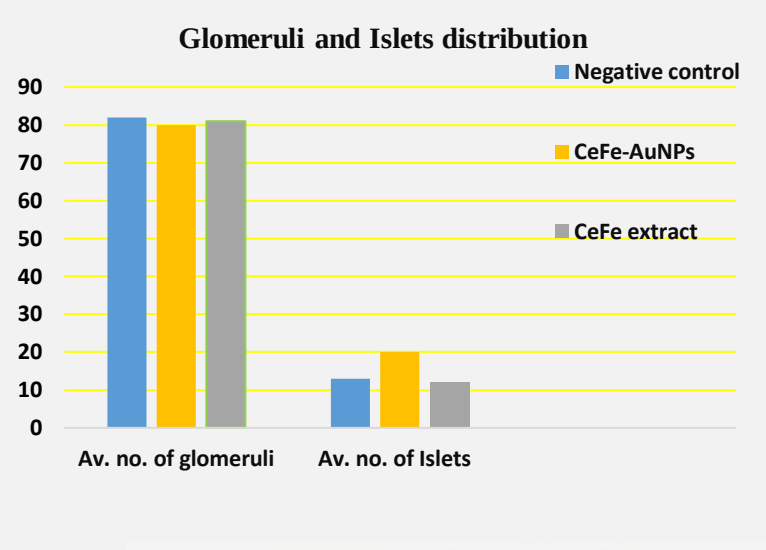

Figure 3. 1: describes the glomerulii and Islets distributions

In Figure 3.1 the average glomeruli seen on investigated tissue slides show that CeFe-AuNPs treated group had an average of 80 glomeruli per 5 sampled fields while the control and CeFe extract had a little more than 80. Also, the figure show that CeFe-AuNPs had an average of 20 viewable Islets per slide while the control and CeFe extract groups' Islets counts were above 10 but below 15. Statistical comparison of the glomeruli distribution of CeFe-AuNPs and CeFe extract with the control group returned $P>0.05$ for both treated groups. Meaning Kidneys are design to maintain glomerular distribution irrespective of functionality. Similarly, statistical comparing of Islet distribution was significant ($P< 0.05$) for CeFe-AuNPs treated groups and $P>0.05$ for CeFe extract. This indicates that CeFe-AuNPs extract enhanced the pancreatic endocrine function more than CeFe extract.

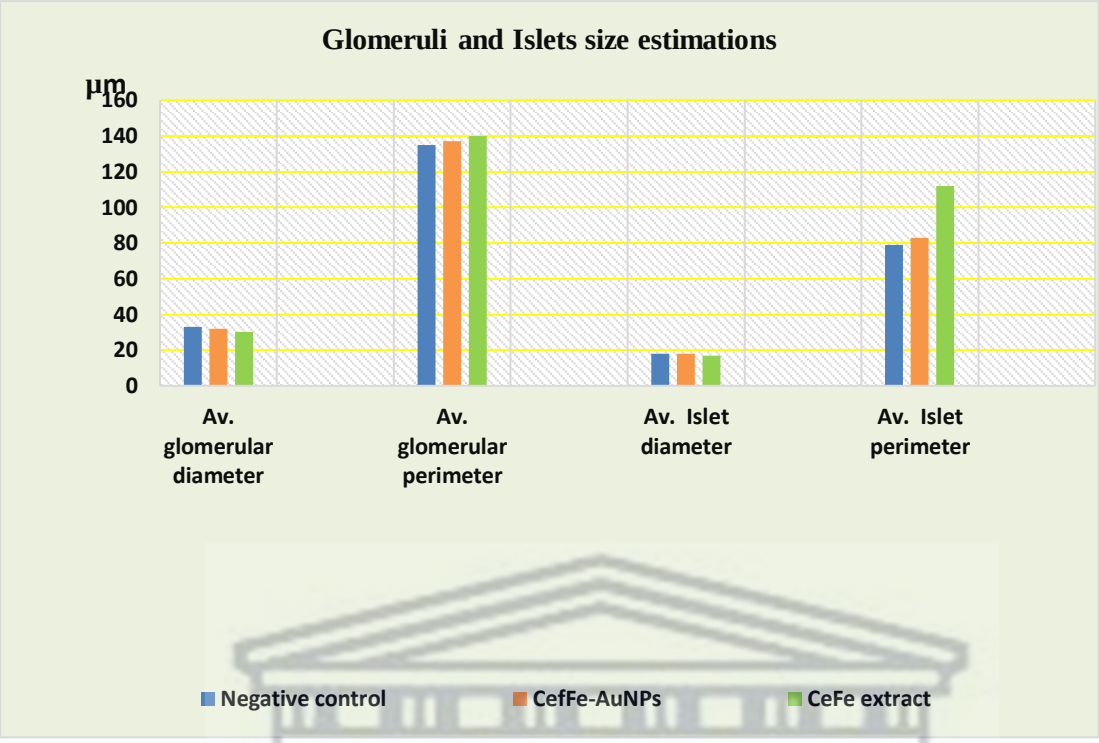

Figure 3. 2:describes the glomeruli and Islets sizes using their diameter and perimeter

Figure 3.2 shows that average glomerular diameter and perimeters of treated and control are relative and statistical comparison insignificant ($P>0.05$). This means that was no abnormal change in size of the organs in the control and treated groups. However, comparing Islets perimeter of CeFe extract with the control was significant ($P<0.05$) and it infers the Islets of CeFe treated group was larger or irregular or both.

3.5.3 Examination of histology micrographs

Triplicate tissue slides for the treated and untreated were examined under x4, x10 and x40 objectives with Evos XL Core light microscope (Scientific, USA). The slides with the best histological presentation (less artefacts) were chosen to represent the group morphological features. Figures 3.3 -3.13 represented the micrographs of histologic tissues for the control, and treated groups.

3.5.3.1 CeFe-AuNPs effects on the kidney

Kidney cortex

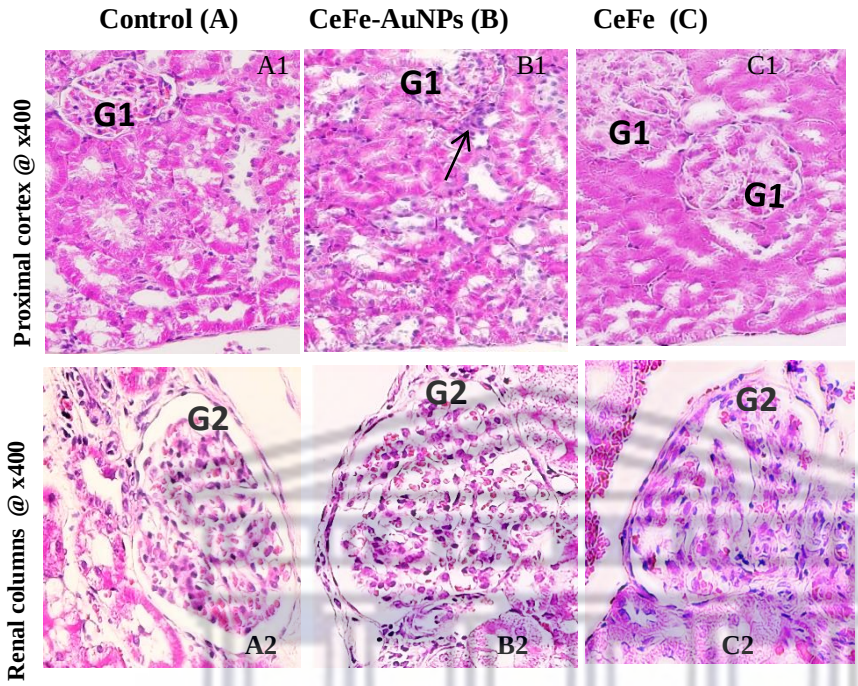

Figure 3. 3:kidney cortex showing glumerulus at proximal cortex and cortical columns

Figure 3.3 Compares untreated and treated kidney cortex @400 magnification. Column A represents untreated tissues. Column B represents the micrograh of the control. Column B represents micrographs of tissues that were treated with 200 mg/kg CeFe-AuNPs while Column C represents 400mg/kg CeFe treated tissues. A1, B1 and C1 structures seen at the proximal tubules while A2 B2 and C2 represents structures seen at the upper renal column of the cortex. G1 and G2 represents glomeruli seen at the proximal cortex and on the columns, between lobular pyramids. The thick arrow points inflammatory cell milieu close to the degenerative glomerulus.

The figure above shows the state of the proximal tubules, the ducts, and Bowman's capsule. Column B1 shows the presence of degenerating glomeruli at B (G1) and also inflammatory cells as pointed out by the thin arrows. The size of the glomerulus in B1 is larger than the control A1 and this agrees with greater perimeter estimations in Figure 3.2. The capsular space in B1 is reduced because the glomerular epithelium attached to ducts and tubules, this thus reduced the space between the bowman's capsule and the glomerulus.

Kidney the medulla

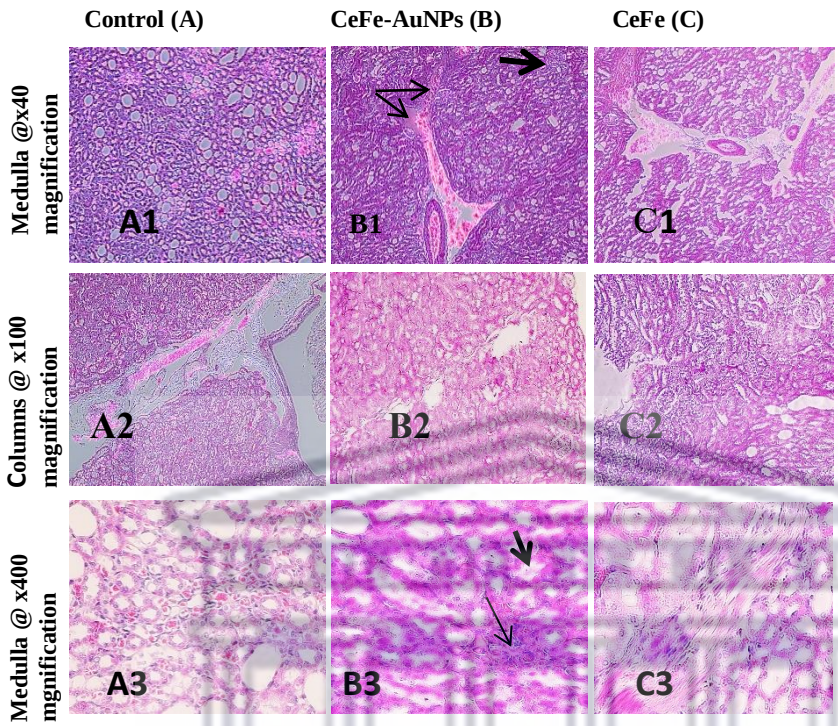

Figure 3. 4: kidney Medulla - comparing untreated and treated rat tissues in the medulla

The kidney tissue micrograph, Figure 3.4, compares the medulla of the treated with untreated control. Column A is the control, Column B is treated with 200 mg/kg CeFe-AuNPs, Column C is treated with 400 mg/kg of CeFe extract. Rows 1,2,3 were viewed under x40, x100 and x400 respectively. At B1 the thin arrows points tissue necrosis, the thick arrow seen in B1 points to glomeruli in the medulla. Thin arrow at B2 shows degenerating blood vessel. Thick arrow in B3 shows hydropic, inflammed tubules. The thin arrow points to inflamed, occluded arterioles and venules. The alphabets A1--3, B1-3, C1-3 represents tissues at Column A, B and C.

The above micrograph describes the state of kidney's distal tubules, medulla and apex. The CeFe-AuNPs treated tissue micrograph at B1 shows necrosing interlobular blood vein (thin arrows point at the locations). The thick arrow points to a glomerulus within the medulla which signify alteration of normal kidney architecture. Similar observation is seen at C1 too. B2 show blood vessel and connective tissues generation. B3 show an inflamed, hydropic medulla with occluded venules and arterioles.

3.5.3.2 CeFe-AuNPs effects on the liver

Hepatocyte showing Kupffer cell and phagocytes in the liver

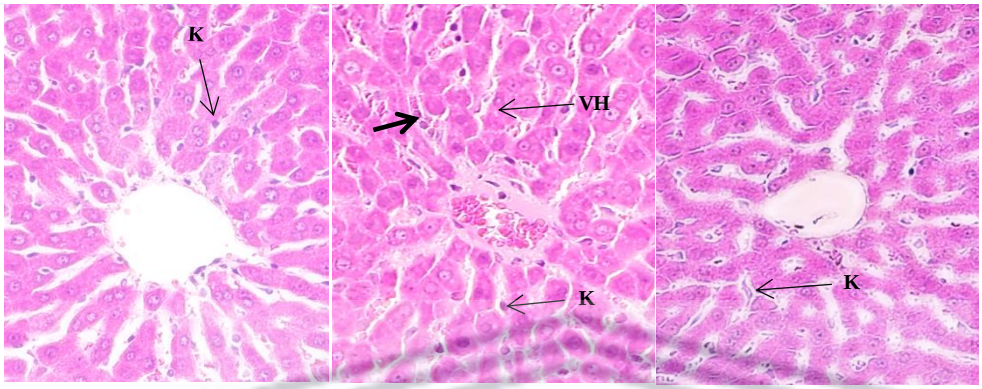

Figure 3. 5**: Liver - comparing hepatocytes, Kupffer cells in the liver of untreated and treated rat tissues.**

The liver tissue micrograph, Figure 3.5, compares the treated with untreated control. Column A is the control, Column B is treated with 200 mg/kg CeFe-AuNPs, Column C is treated with 400 mg/kg of CeFe extract viewed under x400 magnification. At B, VH represents vacoulated and apoptotic hepatocytes, thick arrow points to necrosing hepatocytes within sinusoids, K represents Kupffer cells.

In the above micrograph, CeFe-AuNPs treated liver tissues in B show vacuolated and apoptotic hepatocytes. The liver tissue was hydropic. The central vein was occluded with fluid and red cells. There necrosing tissues are seen within the sinusoids. Inflammatory cells and Kupffer cells were reduced compared to the control (chronic inflammatory state).

Overview of the liver tissue

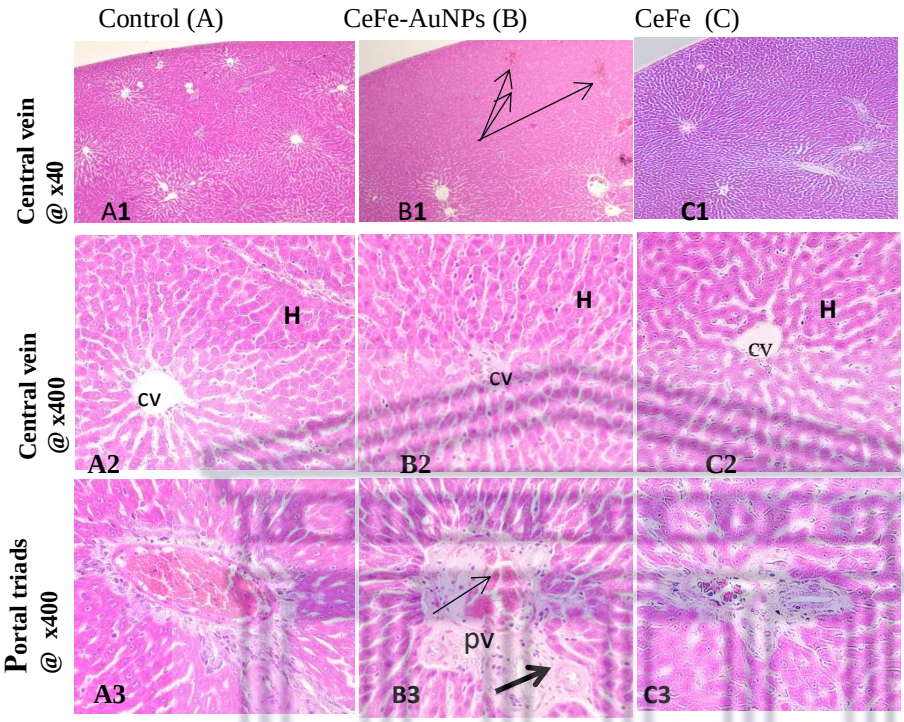

Figure 3. 6: Liver - comparing portal triads, portal and central veins in the liver of untreated and treated rats.

The liver tissue micrograph, Figure 3.6, compares different parts of the liver tissue at once. Column A is the control, Column B is treated with 200 mg/kg CeFe-AuNPs, Column C is treated with 400 mg/kg of CeFe extract. Row 1, 2 and 3 represent micrographs viewed under x40, x100 and x400 magnifications respectively. At B1, the thin arrows point to necrosing central veins. H represents hepatocytes while cv represents central veins and pv portal vein. Row 3 shows the portal triads (the portal vein, artery and lymphatics). In B3, thin arrow points to hydropic portal vein; thick arrow points lymphatic duct. The alphabets A1--2, B1-2, C1-2 represents tissues at Column A, B and C.

In Figue 3.5 CeFe-AuNPs treated liver tissues at B1 show necrosis of central veins, B2 show hydropic occluded central vein while B3 show hydropic portal vein (pv) (thin arrow) and lymphatic ducts with wider lumen. The lymphatics are trying to accommodate more fluid in response to venous hydropism.

3.5.3.3 CeFe-AuNPs effects on the spleen tissue

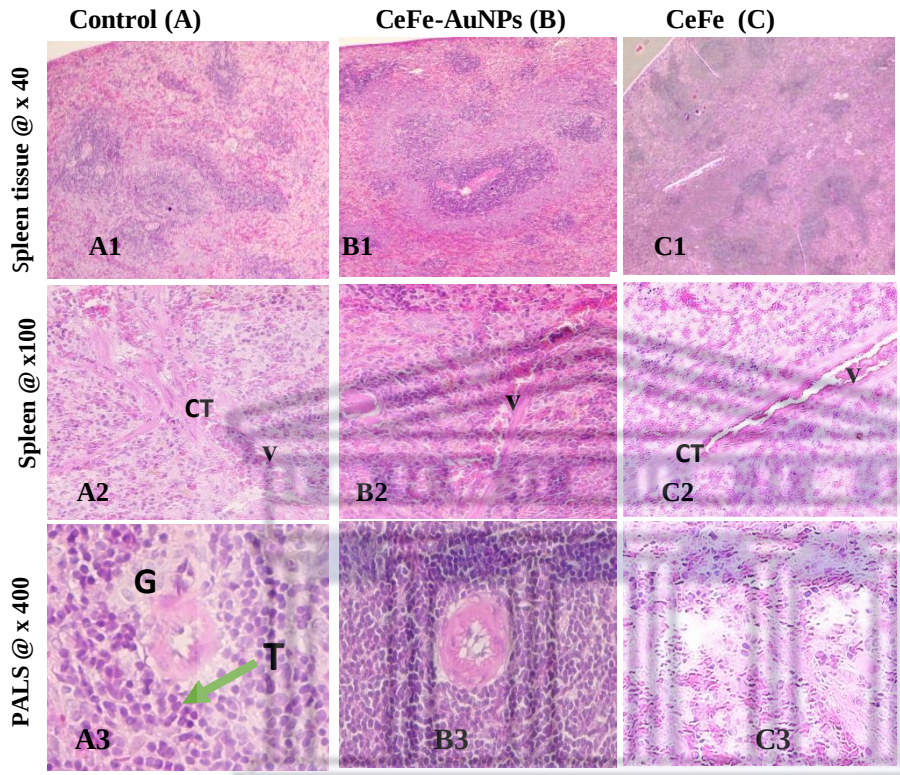

Figure 3. 7: Spleen tissue - comparing PALS, White and Red pulp and blood vessels in the spleen of untreated and treated rat tissues.

The spleen tissue micrograph, Figure 3.7, compares different parts of the spleen tissue at once. Column A is the untreated control, Column B is treated with 200 mg/kg CeFe-AuNPs, Column C is treated with 400 mg/kg of CeFe extract. Row 1, 2 and 3 represent micrographs viewed under x40, x100 and x400 magnifications respectively. CT represent connective tissue trabeculae. V represent vein, G represent germinal centre and T represents T-lymphocyte. The alphabets A1--3, B1-3, C1-3 represents tissues at Column A, B and C.

Figure 3.7 B1 shows the presence of increased blood sequestration in the red pup due to clearance of dysfunctional red blood cells (rbc). Presence of occluded vein within the trabeculae at V. Presence of T-lymphocytes hyperplasia within the PALS. Connective tissue disruptions are seen within the white and red pulp.

3.5.3.4 CeFE-AuNPs effects on the pancreas

Effects on the Islet

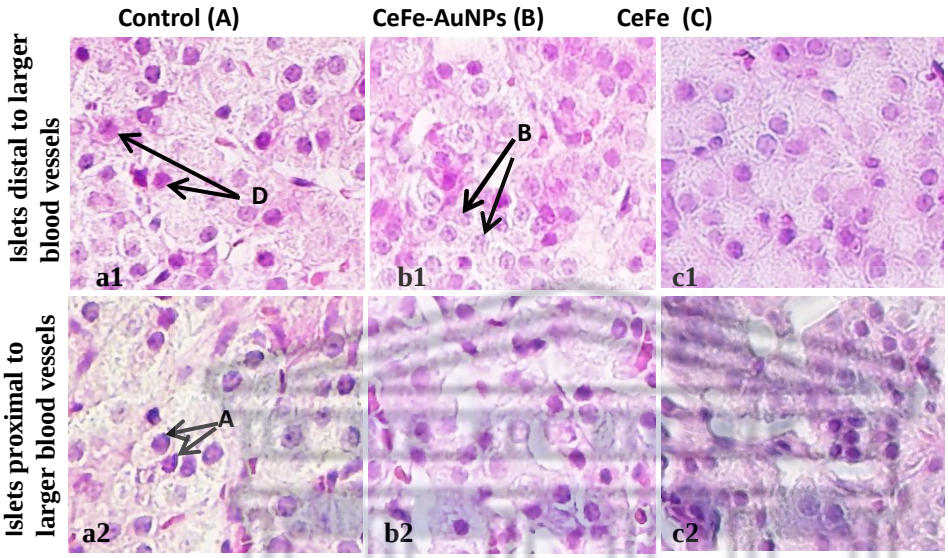

Figure 3. 8: Pancreas Islets - comparing secretory cells, membrane and connective tissue in Islets of untreated and treated rat tissues

Figure 3.8 islet tissue micrograph compares Islets closer to the major blood supply (row 2) and the one farther from (row 1). Column A represent the untreated control, Column B is treated with 200 mg/kg CeFeAuNPs, Column C is treated with 400 mg/kg of CeFe extract. Micrographs were viewed at x400 magnification. The secretory cells: alpha cells - A, beta cels - B and delta cells - D. a1-2, a1-2, c1-2 represents tissues at different parts of Column A, B and C.

The above micrograph of the Islets at B2 (the Islets closer to the major blood supply) show membrane disruptions.

Effects of CeFe-AuNPs on pancreatic tissue

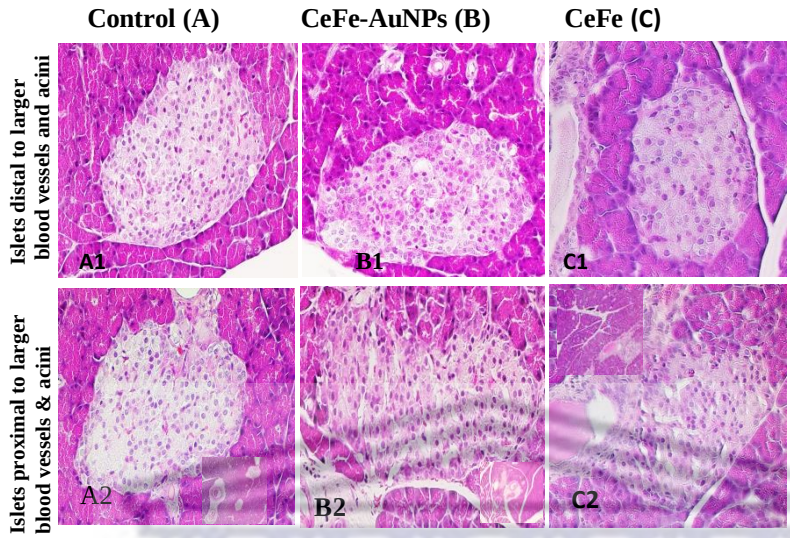

Figure 3. 9: Pancreas Islets - comparing secretory cells, membrane and connective tissue in Islets of untreated and treated rat tissues

The pancreatic tissue micrograph, figure 3.9, compares pancreatic structures at x400 magnification. Column A is control, Column B treated with 200 mg/kg CeFe-AuNPs, Column C is treated with 400 mg/kg of CeFe extract. The alphabets A1-2, B1-2, C1-2 represents tissues at Column A, B and C.

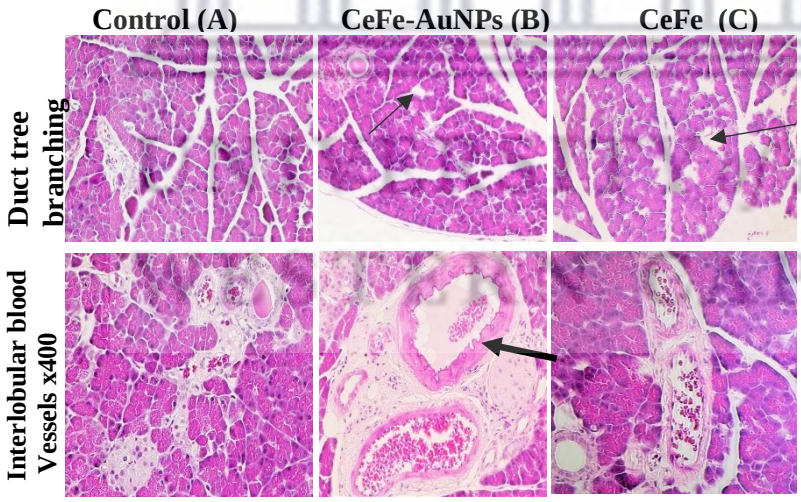

Figure 3. 10: Pancreatic tissue - comparing acini tree, acini and blood vessels in the pancreas.

The pancreatic tissue micrograph, Figure 3.10, compares structures at x400 magnification. Column A is control, Column B is treated with 200 mg/kg CeFe-AuNPs, Column C is treated with 400 mg/kg of CeFe extract. Micrographs were viewed at x400 magnification. The thin arrows at B1 and C1 points to sites of tissue ablation. Thick arrow at B2 points to arterial endothelial membrane disruption.

3.5.3.5 CeFe-AuNPs effects on the heart

Heart endocardium

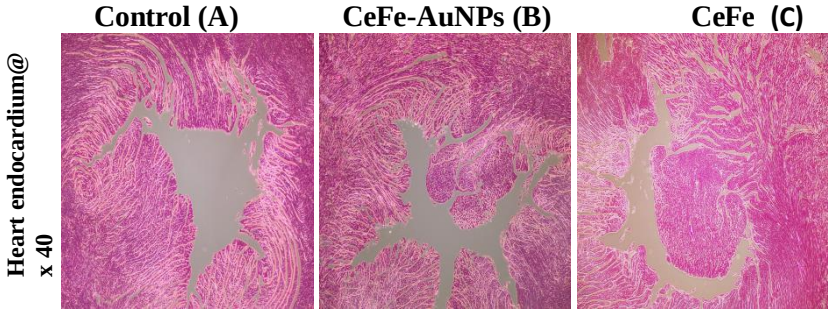

Figure 3. 11: Compared untreated and treated heart endocardium
@ x400 magnification. Column A represents untreated tissues, Column B represents tissue exposed to 200 mg/kg CeFe-AuNPs while column C represents tissues treated with 400 mg/kg CeFe extract. X represents fused membrane modifications on the endocardium.

The heart tissue in Figure 3.11 The atrial lumen of CeFe-AuNPs at B is narrower than the control.

Myocardium

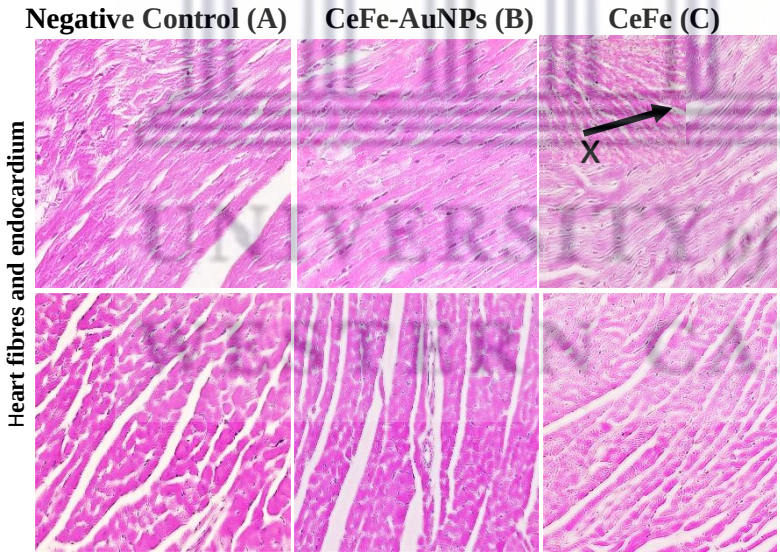

Figure 3. 12: Heart - comparing myocardial tissues and fibres in the heart of treated and untreated rats

The heart micrograph, Figure 3.12 compares untreated and treated heart endocardium @ x400 magnification. Column A represents untreated control tissues, Column B represents tissues treated with 200 mg/kg CeFe-AuNPs, Column represents tissue exposed while column C represents tissues treated with 400 mg/kg CeFe extract. X marks myocardial infiltration fat infiltration.

The heart micrograph in Figure 3.12 show increased presence of inflammatory cells at B (CeFe-AuNPs treated).

Overview of the heart tissues

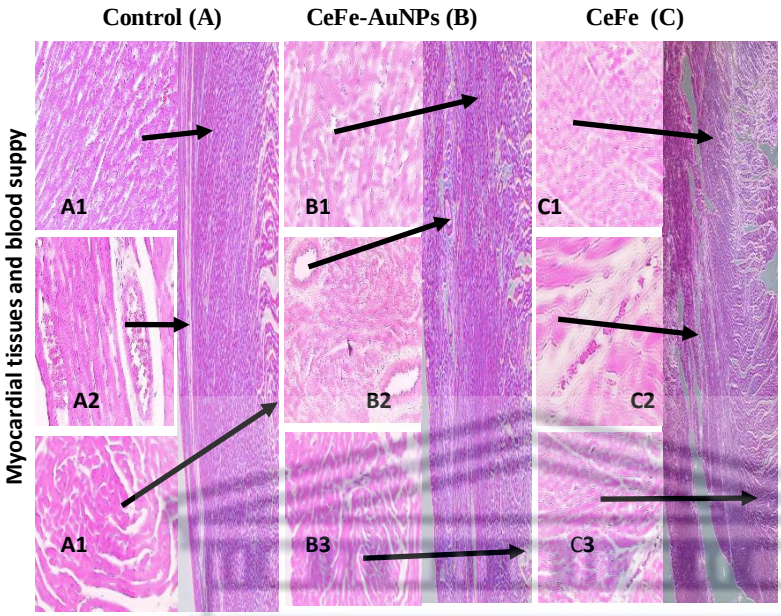

Figure 3. 13: Heart - comparing epicardium, endocardium and blood vessels in the heart of treated and untreated rats

The heart micrograph, Figure 3.13 compares untreated and treated heart epicardium and endocardium @ x400 magnification. Column A represents untreated control tissues. Column B represents tissue exposed to 200 mg/kg CeFe-AuNPs while column C represents tissues treated with 400 mg/kg CeFe extract. The alphabets A1-3, B1-3 and C1-3 represents tissues at Column A, B, C.

The heart tissue micrograph, Figure 3.13 show the tissue in B1 are effaced and have disruptive membrane. There was shape alterations too - signifies structural proteins were affected. The walls of blood vessels in B2 were thickened, their lumen narrowed and the intima epithelium disrupted.

Chapter 4: Discussion and Conclusion

AuNPs therapeutics for ailments like cancers, diabetes, infections are receiving great interest in biomedical applications, however, researhers are calling for more extensive cytotoxicity validation because AuNPs' exponential surface to volume ratio increases their reactivity when compared to their bulk material. This enhances their tendency to complex with biomolecules (proteins, nucleic acids, and lipids). Studies have reported that proteins adsorb onto the surfaces of nanoparticles to form a nanoparticle-protein corona (NP-PC). There is the fear that such occurrences could irreversibly damage the functionality of biomolecules (Shemetov *et al*, 2012; Peng *et al*, 2019, Ritz *et al*, 2015, Boulos *et al*, 2013). Most studies on the effects of AuNPs usually investigate the RES organs and kidneys. Investigations on heart, reproductive organs and brain are less common. For the purpose of the study, the microscopic effects of phyto-synthesize AuNPs on 5 vital organs (heart, liver, kidney, pancreas and spleen) were investigated in other to have a better understanding of the the holistic effects of AuNPs.

4.1 The state of kidney post CeFe-AuNPs treatment

The liver and kidney are two organs that play important roles during chemical detoxification and toxin excretion, Hence the kidney glomerular distribution and average size were necessary for this study (size was estimated indirectly by measuring glomerular diameter and perimeter). The endocrine function of the pancreas was also ascertained by estimating the Islets distributions. Evaluations from statistical data for the glomerular distribution was insignificant ($P>0.05$) (Figure 3.1 and Figure 3.2). and suggests that irrespective of the presence of tissue damage seen in Fig 3.3 and 3.4, the kidney maintained its glomerular distribution even though their functinal capacity is altered. It could also be inferred that the presence of glomeruli in the kidney medulla (Figure 3.4) was a compensatory mechanism to the necrosing glomerular tissues in the cortex. Observations obtained in this study are similar with some toxicity studies on the effects of AuNPs. Abdelhalim *et al*, (2011) reported that AuNPs induced cytoplamic degeneration in the kidney. Figure 3.4(B) show degeneration of glomeruli in the cortex and tubules in the medulla. Enea *et al*, (2020), Chen *et al*, (2013) reported that AuNPs induced oxidative stress and apoptosis in the human kidneys. Yamen *et al*, (2014) studied the effects of AuNPs in rats over two months of exposure and reported that the kidney was one of the organs that accumulated the highest amount of AuNPs. The inflammatory response seen in the medulla tissue micrograph Figure 3.4 (B3) study supports that AuNPs induced oxidative stress in the kidney to cause tissue damage. Balasubramanian *et al*, (2009) reported that AuNPs.

accumulated in more than 25 organs 24 hrs after a single dose of 0.2 ml intravenous injection. One-week post injection, the kidney maintained insignificant value. However, after two months post injection, the kidney recorded significant AuNPs accumulations. Figure 3.3 and 3.4 revealed the kidney is in a sub-acute inflammatory response after 21 days of AuNPs exposure when the liver in Figure 3.5 is showing chronic inflammatory state. This supports report that the kidney's inflammatory response to AuNPs toxicity delayed (depending on the size of the nanoparticle).

4.2 The State of the pancreas post CeFe-AuNPs treatment

The pancreas, like the liver, is an important endocrine organ that mediates glucose uptake and metabolism. With the advent of green nanotechnology, phyto-AuNPs have been synthesized from plant and plant products successfully (Ahmed *et al*, 2021). There have been several reports that phyto-AuNPs induced glucose uptake both *in vitro* and *in vivo*: BarathManiKanth *et al*, (2010) reported that AuNPs helped to reactivate glycolytic enzymes that were suppressed by hyperglycaemia. Ayyoub *et al*, (2022), reported that 20 nm-50 nm AuNPs synthesized from D. viscosa extract lowered the blood glucose levels in experiment animals by activating gene expression of hepatic PEPCK. The result in this study show enhance beta cells expression by Islets in Figure 3.8(B1) and the evaluation of Islets distribution was significant ($P<0.05$) - meaning there was increased insulin secretion and glucose uptake in CeFe-AuNPs treated animals. Tissue micrographs of CeFe-AuNPs treated tissue slide did not show fat cell deposits as the CeFe extract treated did, and this corroborates with data on increased islets distribution in figure (3.1). CeFe-AuNPs effects on Islets in this study also supports that AuNPs have radical scavenging property (anti-oxidative activity) (BarathManiKant *et al*, 2010; Abdelhalim *et al*, 2013). Figure 3.8 membrane disruptions on Islets that were closer to major blood vessels had membrane disruptions compared to those that are farther. It could be that mainstream blood supply high in oxygen species reduced CeFe-AuNPs anti-oxidant activities and exposed the membranes to disruptions seen in Figure 3.9(B2). It is plausible that reduction in ROS species enhanced the anti-diabetic effects of CeFe-AuNPs as has been reported by Ayyoub *et al*, (2022) and Hosny *et al*, (2021). Hence AuNPs would play a dual role in diabetes management. One will be to reduce oxidative stress that inhibits glycolytic enzyme activities, the other will be to delivery phytochemicals that will enhance transcriptions of pro-insulin release genes. As CeFe-AuNPs improved islets distribution, in this study, if could also improve management of Type I diabetes. However, this hypothesis needs further studies and validations.

4.3 The state of the liver post CeFe-AuNPs treatment

The liver is a major endocrine organ of metabolism (Mattew *et al*, 2019) and is widely researched in cytoxocity studies. The effects of CeFe-AuNPs in this study revealed the presence of hydropic, occluded central and portal veins, central vein ablation, vacoulated hepatocytes and sinusoids filled with necrosing hepatocytes Figures 3.5B and 3.6B. Other studies have reported similar outcomes: Abdelhalim *et al*, (2011) reported that AuNPs induced central vein intima disruptions, fatty change and caused Kupffer cell hyperplasia, however, it varied with this study on the hyperplasia. Figures 3.5B and 3.6B show Kupffer cells were not as many as the control as is expected in a chronic inflammation stage. This finding supports the report that AuNPs alleviated oxidative stress by reducing inflammatory cytokines ((Yu *et al*, 2021; Selim *et al*, 2015). Similarly, Sengupta *et al*, (2013) reported that 2 mg/kg 50 nm AuNPs exposed to rats induced both acute and chronic cytotoxic modifications. The reduction of phagocytes and presence of vacoulated hepatocytes buttressed the livers detoxification capacity. It also agrees with reports that AuNPs are trapped and degraded in the liver and spleen. Zhang *et al*, (2020); Pan *et al*, (2012); Alkilany *et al*, (2010); Sadauskas *et al*, (2009) have reported that the RES traps the non-degradable portion of the AuNPs and could retain them for a long time, even a lifetime.

4.4 The State of the spleen post CeFe-AuNPs treatment

The spleen is an organ for blood cell production and storage. The red pulp cleans the blood of old and dysfunction cells by sequestering and phagocytosing the cell debris. White pulp produces white blood cell. The spleen is one of the RES organs that have been reported to have the capacity of accumulation AuNPs to elicit inflammatory response (Alkilany *et al*, 2010; Sadauskas *et al*, 2009). Ibrahim *et al*, (2018) reported that AuNPs intraperitoneal injections in rats stimulated giant macrophages after 7 days exposure to 20-50 AuNPs. Result in this study revealed that CeFe-AuNPs induced T-lymphocyte hyperplasia, but no giant macrophage presence - this could be due to difference in expose routes. Zhang *et al*, (2010) reported that AuNPs caused reduced red cell volume, indicated by low hematocrit, findings in this study revealed increased red cell sequestration and vein occlusion in the red pulp (Figure 3.9) - This agrees with Zang that AuNPs reduce hematocrit index. This also agree with reports that proteins

form corrona around AuNPs. The red haemoglobin is a protein (Kumar *et al*, 2011; Ritz *et al*, 2015).

4.5 The State of the heart post CeFe-AuNPs treatment

The heart's function in the body distribution is very vital and as such it needed to be investigated for cytotoxicity because it is always in direct contact with all bioactive chemicals just like the blood vessels. Li *et al*, (2018) investigated the biodistribution of small and large size AuNPs and reported that small sized AuNPs accumulated in the heart. The result of this study show that 16 nm CeFe-AuNPs was toxic to the heart tissues and blood vessels (Figures 3.11, 3.12 and 3.13).

4.6 AuNPs Clearance

It has been reported that AuNPs exocytosis and excretion could be enhanced by fine-tuning the surface chemistries of conjugating ligands to facilitate exocytosis (Ding *et al*, 2018). Oh, and Park, (2014) reported that surface chemistry and opsonizing proteins play a crucial role in AuNPs exocytosis by macrophages. They suggested that Cationic AuNP residues are retained in macrophage longer than necessary while PEGylated residues are quickly exorcised. They suggested that intracellular cationic Au residue aggregation delayed their quicker exocytosis. Conversely PEGylated residues migrated as individual particles in the cytoplasm, hence, were promptly excreted. Studies have reported that AuNPs are cleared by mononuclear phagocytes (MPS) yet none had reported complete clearance within a reasonable time. Reported clearance rate is around 50% in 2 months period for polyethylene glycol (PEG)ylated residue, 10% clearance rate in six months for anionic Au residue (Zhang *et al*, 2016; Pan *et al*, 2012; Alkilany *et al*, 2010; Sadauskas *et al*, 2009). The damage to the liver, spleen and kidneys of treated tissues in this study support previous studies that RES organs are involved in CeFe-AuNPs clearance.

4.7 Conclusion

The recent enthusiasm on green and eco-friendly AuNPs sythesis if a welcomed development for cancer and diabetes management and requires more work to improve on findings. Investigations in this study found that 200 mg/kg of 16 nm CeFe-AuNPs orally administered to diabetic rats exerted graded toxicity on investigated organs. Microscopic effects identified incuded membrane disruptions in the pancreatic islets and heart tissues; hydropism,, necrosis, apoptosis in the kidney, spleen and liver tissues. However, CeFe-AuNPs increased the pancreatic Islets distribution and indicates increased beta cell expression and insulin secretion. CeFe-AuNPs treated animals did not accumulate fat like the CeFe extract treated did. More studies are required on the anti-diabetic properties of CeFe-AuNPs.

References

MacPhail, Robert C., Eric A. Grulke, and Robert A. Yokel. "Assessing nanoparticle risk poses prodigious challenges." *Wiley Interdisciplinary Reviews: Nanomedicine and Nanobiotechnology* 5.4 (2013): 374-387.

Justo-Hanani, Ronit, and Tamar Dayan. "European risk governance of nanotechnology: Explaining the emerging regulatory policy." *Research Policy* 44.8 (2015): 1527-1536.

Rachel Foulkes, Ernest Man, Jasmine Thind, Suet Yeung et al, "The regulation of nanomaterials and nanomedicines for clinical application: current and future perspectives." *Biomaterial sciences* 8 (2020): 4653-4664.

Jain, Ruchi et al. "Substrate specificity and mutational analysis of Kluyveromyces lactis gamma-toxin, a eukaryal tRNA anticodon nuclease." *RNA (New Y [kork, N.Y.)* vol.17,7 (2011): 1336-43. doi:10.1261/rna.2722711.

Yasuhiro Konishi, Kaori Ohno, Norizoh Saitoh, Toshiyuki Nomura, Shinsuke Nagamine, Hajime Hishida, Yoshio Takahashi, Tomoya Uruga, "Bioreductive deposition of platinum nanoparticles on the bacterium Shewanella algae." *Journal of Biotechnology* 128.3 (2007): 648-653. doi.org/10.1016/j.jbiotec.2006.11.014.

Boisseau, Patrick, and Bertrand Loubaton, 'Nanomedicine, Nanotechnology in Medicine Nanomédecine et Nanotechnologies Pour La Médecine.' *Comptes Rendus Physique* 12.7 (2011): 620–36 https://doi.org/10.1016/j.crhy.2011.06.001.

Vigneshwaran, N., Ashtaputre, N.M., Varadarajan, P.V., Nachane, R.P., Paraliker, K.M. and Balasubramanya, R.H., "Biological Synthesis of Silver Nanoparticles Using the Fungus Aspergillus flavus." Mater. Lett 61 (2007): 1413-1418.

Shraddha Chauhan, Anita Tirkey, Lata Sheo Bachan Upadhyay, Nanomaterials in biomedicine: Synthesis and applications, Advances in Nanotechnology-Based Drug Delivery Systems, 10.1016/B978-0-323-88450-1.00023-5, (585-604), (2022).

Willna 1, Baron R, Willna B, "Growing Metal Nanoparticles by Enzymes." *Advance Material* 18.9 (2006): 1109-1120. https://doi.org/10.1002/adma.200501865.

Zhang Yongfang and Shen Jaquan, “Enhancement effect of gold nanoparticles on biohydrogen production from artificial wastewater.” *International Journal of Hydrogen Energy* 32.1 (2007): 17-23. https://doi.org/10.1016/j.ijhydene.2006.06.004.

Abdelhalim Mohamed Anwar K and Sherif A. Abdelmottaleb Moussa., “The gold nanoparticle size and exposure duration effect on the liver and kidney function of rats: In vivo.” *Saudi Journal of Biological Sciences* 20.2 (2013): 177-181. https://doi.org/10.1016/j.sjbs.2013.01.007.

Abdelhalim, M.A.K., Jarrar, B.M., “Gold nanoparticles administration induced prominent inflammatory, central vein intima disruption, fatty change and Kupffer cells hyperplasia,” *Lipids in Health and Disease* 10 (2011): 133.

Abdelhalim, Mohamed Anwar K., and Bashir M. Jarrar. "Gold nanoparticles induced cloudy swelling to hydropic degeneration, cytoplasmic hyaline vacuolation, polymorphism, binucleation, karyopyknosis, karyolysis, karyorrhexis and necrosis in the liver." *Lipids in Health and Disease* 10.1 (2011): 1-6.

Abdelhalim, Mohamed Anwar K., and Bashir M. Jarrar. "The appearance of renal cells cytoplasmic degeneration and nuclear destruction might be an indication of GNPs toxicity." *Lipids in Health and Disease* 10.1 (2011): 1-6.

Abdelhalim, M. A. K. "Exposure to gold nanoparticles produces pneumonia, fibrosis, chronic inflammatory cell infiltrates, congested and dilated blood vessels, and hemosiderin granule and emphysema foci." *J Cancer Sci Ther*. 2012a 4.3 (2012): 046-050.

Abdelhalim, Mohamed Anwar K. "Gold nanoparticles administration induces disarray of heart muscle, hemorrhagic, chronic inflammatory cells infiltrated by small lymphocytes, cytoplasmic vacuolization and congested and dilated blood vessels." *Lipids in health and disease* 10.1 (2011): 1-9.

Abdelhalim, M. A. K. "Optimizing a novel method for synthesizing gold nanoparticles: biophysical studies." J Cancer Sci Ther 4 (2012): 140-143.

Deng Gui-Fang, Lin Xi, Xu Xiang-Rong, Gao Li-Li, Xie Jie-Feng, Li Hua-Bin, “Antioxidant capacities and total phenolic contents of 56 vegetables.” *Journal of Functional Foods* 5.2 (2012): 260-266. https://doi.org/10.1016/j.jff.2012.10.015.

Bhushan, Bharat. "Introduction to nanotechnology." *Springer handbook of nanotechnology*. Springer, Berlin, Heidelberg, 2017. 1-19.

Binns, Chris. *Introduction to nanoscience and nanotechnology*. John Wiley & Sons, 2021.

de Mello Donegá, Celso, ed. *Nanoparticles: Workhorses of nanoscience*. Springer, 2014.

Quan, Sewee, and Jaye Fang. "Superlattices with non-spherical building blocks." *Nano Today* 5.5 (2010): 390-411.

Zhang, H., C. Song, R. Yan, H. Cai, Y. Zhou, and X. Ke, 'High-Fat Diet Accelerate Hepatic Fatty Acids Synthesis in Offspring Male Rats Induced by Perinatal Exposure to Nonylphenol', *BMC Pharmacology and Toxicology*, 22 (2021), 22 https://doi.org/10.1186/s40360-021-00492-z

Holder, N., and Xu, Q., "The zebrafish: an overview of its early development." *Methods in molecular biology* (Clifton, N.J.) (2008): 461: 483-491.

Mary Ealias, Anu, and M. P. Saravanakumar. "A critical review on ultrasonic-assisted dye adsorption: Mass transfer, half-life and half-capacity concentration approach with future industrial perspectives." *Critical Reviews in Environmental Science and Technology* 49.21 (2019): 1959-2015.

Krumer, Zachar, et al. "Tackling self-absorption in luminescent solar concentrators with type-II colloidal quantum dots." *Solar energy materials and solar cells* 111 (2013): 57- 65.

Van der Stam, Ward, et al. "Self-assembly of colloidal hexagonal bipyramid-and bifrustum-shaped ZnS nanocrystals into two-dimensional superstructures." *Nano letters* 14.2 (2014): 1032-1037.

Ito, Akira, et al. "Medical application of functionalized magnetic nanoparticles." *Journal of bioscience and bioengineering* 100.1 (2005): 1-11.

Gubin, Sergei P., et al. "Magnetic nanoparticles: preparation, structure and properties." *Russian Chemical Reviews* 74.6 (2005): 489.

Holder, Elisabeth, Nir Tessler, and Andrey L. Rogach. "Hybrid nanocomposite materials with organic and inorganic components for opto-electronic devices." *Journal of Materials Chemistry* 18.10 (2008): 1064-1078.

Sau, Tapan K., and Catherine J. Murphy. "Room temperature, high-yield synthesis of multiple shapes of gold nanoparticles in aqueous solution." *Journal of the American Chemical Society* 126.28 (2004): 8648-8649.

Martínez, G., et al. "Use of a polyol liquid collection medium to obtain ultrasmall magnetic nanoparticles by laser pyrolysis." *Nanotechnology* 23.42 (2012): 425605.

Bulychev, N. A. "Obtaining of gaseous hydrogen and solid carbon nanoparticles by pyrolysis of liquid-phase media in low-temperature plasma." *International Journal of Hydrogen Energy* 46.76 (2021): 37768-37773.

Mottaghitalab, Fatemeh, et al. "New insights into designing hybrid nanoparticles for lung cancer: Diagnosis and treatment." *Journal of controlled release* 295 (2019): 250-267.

Ahmadi, Sepideh, et al. "Stimulus-responsive sequential release systems for drug and gene delivery." *Nano today* 34 (2020): 100914.

Rabiee, Navid, et al. "Nanotechnology-assisted microfluidic systems: from bench to bedside." *Nanomedicine* 16.3 (2020): 237-258.

Zhang, Kaitao, et al. "Facile synthesis of palladium and gold nanoparticles by using dialdehyde nanocellulose as template and reducing agent." *Carbohydrate polymers* 186 (2018): 132-139.

Cremosnik, Gregor S., Jie Liu, and Herbert Waldmann. "Guided by evolution: from biology-oriented synthesis to pseudo natural products." Natural Product Reports 37.11 (2020): 1497-1510.

Chen, Yiping, et al. "Click chemistry-mediated nanosensors for biochemical assays." *Theranostics* 6.7 (2016): 969.

Lima-Tenório, Michele K., et al. "Water transport properties through starch-based hydrogel nanocomposites responding to both pH and a remote magnetic field." *Chemical Engineering Journal* 259 (2015): 620-629.

Amendola, Vincenzo, and Moreno Meneghetti. "Laser ablation synthesis in solution and size manipulation of noble metal nanoparticles." *Physical chemistry chemical physics* 11.20 (2009): 3805-3821.

Amendola, Vincenzo, et al. "Coexistence of plasmonic and magnetic properties in Au 89 Fe 11 nanoalloys." *Nanoscale* 5.12 (2013): 5611-5619.

Salavati-Niasari, Masoud, Fatemeh Davar, and Noshin Mir. "Synthesis and characterization of metallic copper nanoparticles via thermal decomposition." *Polyhedron* 27.17 (2008): 3514-3518.

Ramesh, Suhas, et al. "Peptides conjugated to silver nanoparticles in biomedicine–a "value-added" phenomenon." *Biomaterials science* 4.12 (2016): 1713-1725.

Ramesh, S., et al. "Sol–gel synthesis, structural, optical and magnetic characterization of Ag 3 (2+ x) Pr x Nb 4− x O 11+ δ (0.0≤ x≤ 1.0) nanoparticles." *RSC Advances* 6.8 (2016): 6336-6341.

Kaviya, S., J. Santhanalakshmi, and B. Viswanathan. "Green synthesis of silver nanoparticles using Polyalthia longifolia leaf extract along with D-sorbitol: study of antibacterial activity." *Journal of nanotechnology* 2011 (2011).

Davis, Sean A., et al. "Bacterial templating of ordered macrostructures in silica and silica-surfactant mesophases." *Nature* 385.6615 (1997): 420-423.

Tai, Clifford Y., and Hwai-shen Liu. "Synthesis of submicron barium carbonate using a high-gravity technique." *Chemical engineering science* 61.22 (2006): 7479-7486.

Mohammadi, Yousef, et al. "Monte Carlo simulation of free radical polymerization of styrene in a spinning disc reactor." *Chemical Engineering Journa*l 247 (2014): 231-240.

Bhaviripudi, Sreekar, et al. "Role of kinetic factors in chemical vapor deposition synthesis of uniform large area graphene using copper catalyst." *Nano letters* 10.10 (2010): 4128-4133.

Adachi, Motonari, et al. "Formation of titania nanotubes and applications for dye-sensitized solar cells." *Journal of the Electrochemical Society* 150.8 (2003): G488.

Saratale, Rijuta Ganesh, et al. "New insights on the green synthesis of metallic nanoparticles using plant and waste biomaterials: current knowledge, their agricultural and environmental applications." *Environmental Science and Pollution Research* 25.11 (2018): 10164-10183.

Glover, Richard LK, et al., eds. *Green Synthesis in Nanomedicine and Human Health*. CRC Press, 2021.

Salem, Salem S., and Amr Fouda. "Green synthesis of metallic nanoparticles and their prospective biotechnological applications: an overview." *Biological Trace Element Research* 199.1 (2021): 344-370.

Husen, Azamal, and Muhammad Iqbal. "Nanomaterials and plant potential: an overview." *Nanomaterials and plant potential* (2019): 3-29.

Tangthong, Theeranan, et al. "Water-soluble chitosan conjugated DOTA-Bombesin peptide capped gold nanoparticles as a targeted therapeutic agent for prostate cancer." *Nanotechnology, science and applications* 14 (2021): 69.

Akbar, Sadia, et al. "An overview of the plant-mediated synthesis of zinc oxide nanoparticles and their antimicrobial potential." *Inorganic and Nano-Metal Chemistry* 50.4 (2020): 257-271.

Vijayaraghavan, K., and T. Ashokkumar. "Plant-mediated biosynthesis of metallic nanoparticles: a review of literature, factors affecting synthesis, characterization techniques and applications." *Journal of environmental chemical engineering* 5.5 (2017): 4866-4883.

Singh, Ajey, et al. "Effect of biologically synthesized copper oxide nanoparticles on metabolism and antioxidant activity to the crop plants Solanum lycopersicum and Brassica oleracea var. botrytis." *Journal of biotechnology* 262 (2017): 11-27.

Agarwal, Happy, S. Venkat Kumar, and S. Rajeshkumar. "A review on green synthesis of zinc oxide nanoparticles–An eco-friendly approach." *Resource-Efficient Technologies 3.4* (2017): 406-413.

Goodsell, David S. Bionanotechnology: lessons from nature. John Wiley & Sons, 2004.

Shankar, S. Shiv, Absar Ahmad, and Murali Sastry. "Geranium leaf assisted biosynthesis of silver nanoparticles." *Biotechnology progress* 19.6 (2003): 1627-1631.

Shankar, S. Shiv, et al. "Biological synthesis of triangular gold nanoprisms." *Nature materials* 3.7 (2004): 482-488.

Shankar, S. Shiv, et al. "Rapid synthesis of Au, Ag, and bimetallic Au core–Ag shell nanoparticles using Neem (Azadirachta indica) leaf broth." *Journal of colloid and interface science* 275.2 (2004): 496-502.

Kasthuri, J., K. Kathiravan, and N. Rajendiran. "Phyllanthin-assisted biosynthesis of silver and gold nanoparticles: a novel biological approach." *Journal of Nanoparticle Research* 11.5 (2009): 1075-1085.

Ding, Hong, Fang Wu, and Madhavan P. Nair. "Image-guided drug delivery to the brain using nanotechnology." *Drug discovery today* 18.21-22 (2013): 1074-1080.

Lim, Dong Chan, et al. "Towards fabrication of high-performing organic photovoltaics: new donor-polymer, atomic layer deposited thin buffer layer and plasmonic effects." *Energy & Environmental Science* 5.12 (2012): 9803-9807.

Qiu, Xiaofeng, et al. "Lead-free mesoscopic Cs2SnI6 perovskite solar cells using different nanostructured ZnO nanorods as electron transport layers." *physica status solidi (RRL)–Rapid Research Letters* 10.8 (2016): 587-591.

Qiu, Liqing, et al. "Shelf-life extension of aquatic products by applying nanotechnology: a review." *Critical Reviews in Food Science and Nutrition* 62.6 (2022): 1521-1535.

Peng, Zhili, et al. "Carbon dots: biomacromolecule interaction, bioimaging and nanomedicine." *Coordination Chemistry Reviews* 343 (2017): 256-277.

Daraee, Hadis, et al. "Application of liposomes in medicine and drug delivery." *Artificial cells, nanomedicine, and biotechnology* 44.1 (2016): 381-391.

Zhou, Xiang, et al. "Nanostructured energetic composites: synthesis, ignition/combustion modeling, and applications." *ACS applied materials & interfaces* 6.5 (2014): 3058-3074.

Lukianova-Hleb, Ekaterina Y., et al. "Cell-specific transmembrane injection of molecular cargo with gold nanoparticle-generated transient plasmonic nanobubbles." *Biomaterials* 33.21 (2012): 5441-5450.

Richards, Douglas G., et al. "Gold and its relationship to neurological/glandular conditions." *International journal of neuroscience* 112.1 (2002): 31-53.

Mahdihassan, S. "Tan, cinnabar, as drug of longevity prior to alchemy." *The American Journal of Chinese Medicine* 12.01n04 (1984): 50-54.

Mahdihassan, S. "History of cinnabar as drug, the natural substance and the synthetic product." *Indian journal of history of science* 22.1 (1987): 63-70.

Dykman, Lev, and Nikolai Khlebtsov. "Gold nanoparticles in biomedical applications: recent advances and perspectives." *Chemical Society Reviews* 41.6 (2012): 2256-2282.

Sasidharan, Abhilash, Parwathy Chandran, and Nancy A. Monteiro-Riviere. "Biocorona bound gold nanoparticles augment their hematocompatibility irrespective of size or surface charge." *ACS Biomaterials Science & Engineering* 2.9 (2016): 1608-1618.

Fricker, Simon P. "Medicinal chemistry and pharmacology of gold compounds." *Transition Metal Chemistry* 21.4 (1996): 377-383.

Shaw III, C. Frank. "The protein chemistry of antiarthritic gold (I) thiolates and related complexes." *Comments on Inorganic Chemistry* 8.6 (1989): 233-267.

Naeem, Ghassan Adnan, et al. "Punica granatum L. mesocarp-assisted rapid fabrication of gold nanoparticles and characterization of nano-crystals." *Environmental Nanotechnology, Monitoring & Management* 14 (2020): 100390.

Yoo, Jihye, et al. "Active targeting strategies using biological ligands for nanoparticle drug delivery systems." *Cancers* 11.5 (2019): 640.

Choi, Jane Ru, et al. "Black phosphorus and its biomedical applications." *Theranostics* 8.4 (2018): 1005.

Sztandera, Krzysztof, Michał Gorzkiewicz, and Barbara Klajnert-Maculewicz. "Gold nanoparticles in cancer treatment." *Molecular pharmaceutics* 16.1 (2018): 1-23.

Wicki, Andreas, et al. "Nanomedicine in cancer therapy: challenges, opportunities, and clinical applications." *Journal of controlled release* 200 (2015): 138-157.

Siddique, Sarkar, and James CL Chow. "Gold nanoparticles for drug delivery and cancer therapy." *Applied Sciences* 10.11 (2020): 3824.

Mitra, Ashim K., et al. "Novel delivery approaches for cancer therapeutics." *Journal of controlled release* 219 (2015): 248-268.

Kalaydina, Regina-Veronicka, et al. "Recent advances in "smart" delivery systems for extended drug release in cancer therapy." *International journal of nanomedicine* 13 (2018): 4727.

Rasha, Fahmida, Monica Sharma, and Kevin Pruitt. "Mechanisms of endocrine therapy resistance in breast cancer." *Molecular and Cellular Endocrinology* 532 (2021): 111322.

Vijaya Krishna, K., Nidhi Gour, and Sandeep Verma. "Peptide-Based Soft Spherical Structures." *Peptide Materials: From Nanostructures to Applications* (2013): 191-216.

Parveen, Asra, and Srinath Rao. "Cytotoxicity and genotoxicity of biosynthesized gold and silver nanoparticles on human cancer cell lines." *Journal of Cluster Science 26.3 (2015): 775-788.*

Mohd-Zahid, Manali Haniti, et al. "Colorectal cancer stem cells: A review of targeted drug delivery by gold nanoparticles." *RSC Advances* 10.2 (2020): 973-985.

Thakur, Piyush Kumar, and Varsha Verma. "A Review on green synthesis, characterization and anticancer application of metallic nanoparticles." *Applied Biochemistry and Biotechnology* 193.7 (2021): 2357-2378.

Khoobchandani, Menka, et al. "Green nanotechnology of MGF-AuNPs for immunomodulatory intervention in prostate cancer therapy." Scientific reports 11.1 (2021): 1-30.

Ganeshkumar, Moorthy, et al. "Spontaneous ultra-fast synthesis of gold nanoparticles using Punica granatum for cancer targeted drug delivery." *Colloids and Surfaces B: Biointerfaces* 106 (2013): 208-216.

Ganeshkumar, Moorthy, et al. "Green synthesis of pullulan stabilized gold nanoparticles for cancer targeted drug delivery." *Spectrochimica Acta Part A: Molecular and Biomolecular Spectroscopy* 130 (2014): 64-71.

Lea, Tor. "Caco-2 cell line." The impact of food bioactives on health (2015): 103-111.

Shemetov, Anton A., Igor Nabiev, and Alyona Sukhanova. "Molecular interaction of proteins and peptides with nanoparticles." *ACS nano* 6.6 (2012): 4585-4602.

Bourgine J, Billaut-Laden I et al. "Gene expression profiling of systems involved in the metabolism and the disposition of xenobiotics: comparison between human intestinal biopsy samples and colon cell lines.". *Drug Metab Dispos* 40(4): (2012): 694–705.

Adewale, Olusola B, Hajierah Davids, Lynn Cairncross, and Saartjie Roux, 'Toxicological Behavior of Gold Nanoparticles on Various Models: Influence of Physicochemical Properties and Other Factors', *International Journal of Toxicology*, 38(5) (2019), 357–84 https://doi.org/10.1177/1091581819863130

Connor, Ellen E., et al. "Gold nanoparticles are taken up by human cells but do not cause acute cytotoxicity." *Small* 1.3 (2005): 325-327.

Granitzer, Petra, et al. "Fe3O4-nanoparticles within porous silicon: magnetic and cytotoxicity characterization." *Applied Physics Letters* 102.19 (2013): 193110.

Peng, Shu-Fen, et al. "Effects of incorporation of poly (γ-glutamic acid) in chitosan/DNA complex nanoparticles on cellular uptake and transfection efficiency." *Biomaterials* 30.9 (2009): 1797-1808.

Correard, Florian, et al. "Gold nanoparticles prepared by laser ablation in aqueous biocompatible solutions: assessment of safety and biological identity for nanomedicine applications." *International journal of nanomedicine* 9 (2014): 5415.

Hwang, Tsong-Long, et al. "Cationic additives in nanosystems activate cytotoxicity and inflammatory response of human neutrophils: lipid nanoparticles versus polymeric nanoparticles." *International journal of nanomedicine* 10 (2015): 371.

Dong, Xuemeng, et al. "The size-dependent cytotoxicity of amorphous silica nanoparticles: a systematic review of in vitro studies." *International Journal of Nanomedicine* 15 (2020): 9089.

Sun, Ya-Nan, et al. "Shape dependence of gold nanoparticles on in vivo acute toxicological effects and biodistribution." *Journal of nanoscience and nanotechnology* 11.2 (2011): 1210-1216.

Schaeublin, Nicole M., et al. "Does shape matter? Bioeffects of gold nanomaterials in a human skin cell model." *Langmuir* 28.6 (2012): 3248-3258.

Khan, A. K., et al. "Gold nanoparticles: synthesis and applications in drug delivery." *Tropical journal of pharmaceutical research* 13.7 (2014): 1169-1177.

Chithrani, B. Devika, Arezou A. Ghazani, and Warren CW Chan. "Determining the size and shape dependence of gold nanoparticle uptake into mammalian cells." *Nano letters* 6.4 (2006): 662-668.

O'Neal, D. Patrick, et al. "Photo-thermal tumor ablation in mice using near infrared-absorbing nanoparticles." *Cancer letters* 209.2 (2004): 171-176.

Patel, Pinal C., et al. "Scavenger receptors mediate cellular uptake of polyvalent oligonucleotide-functionalized gold nanoparticles." *Bioconjugate chemistry* 21.12 (2010): 2250-2256.

Jia, Pengpeng, et al. "Recent advances and future development of metal complexes as anticancer agents." *Journal of Coordination Chemistry* 70.13 (2017): 2175-2201.

Zhang, Xian, et al. "Binding of PFOS to serum albumin and DNA: insight into the molecular toxicity of perfluorochemicals." *BMC molecular biology* 10.1 (2009): 1-12.

Kim, Ki-Tae, et al. "Gold nanoparticles disrupt zebrafish eye development and pigmentation." *toxicological sciences* 133.2 (2013): 275-288.

Goodman, Ann B. "Retinoid receptors, transporters, and metabolizers as therapeutic targets in late onset Alzheimer disease." *Journal of cellular physiology* 209.3 (2006): 598- 603.

Rai, Alex J., and Frank Vitzthum. "Effects of preanalytical variables on peptide and protein measurements in human serum and plasma: implications for clinical proteomics." *Expert review of proteomics* 3.4 (2006): 409-426.

Zou, X., et al. "The effects of L-carnitine on the combination of, inhalation anesthetic-induced developmental, neuronal apoptosis in the rat frontal cortex." *Neuroscience* 151.4 (2008): 1053-1065.

Zhang, Chunlei, et al. "Gold nanoclusters-based nanoprobes for simultaneous fluorescence imaging and targeted photodynamic therapy with superior penetration and retention behavior in tumors." *Advanced Functional Materials* 25.8 (2015): 1314-1325.

Ning, Limin, Benwei Zhu, and Tao Gao. "Gold nanoparticles: promising agent to improve the diagnosis and therapy of cancer." *Current drug metabolism* 18.11 (2017): 1055-1067.

Simpson, Carrie A., et al. "In vivo toxicity, biodistribution, and clearance of glutathione-coated gold nanoparticles." Nanomedicine: Nanotechnology, Biology *and Medicine* 9.2 (2013): 257-263.

Chen, Hui, et al. "In vivo study of spherical gold nanoparticles: inflammatory effects and distribution in mice." *PloS one* 8.2 (2013): e5820.

Hwang, Jung Hwan, et al. "Susceptibility to gold nanoparticle-induced hepatotoxicity is enhanced in a mouse model of non-alcoholic steatohepatitis." *Toxicology* 294.1 (2012): 27-35.

Balasubramanian, Suresh K., et al. "Characterization, purification, and stability of gold nanoparticles." *Biomaterials* 31.34 (2010): 9023-9030.

Cho, Wan-Seob, et al. "Acute toxicity and pharmacokinetics of 13 nm-sized PEG-coated gold nanoparticles." *Toxicology and applied pharmacology* 236.1 (2009): 16-24.

Zhang, Xiao-Dong, et al. "In vivo renal clearance, biodistribution, toxicity of gold nanoclusters." *Biomaterials* 33.18 (2012): 4628-4638.

Yang, Lin, et al. "Comparisons of the biodistribution and toxicological examinations after repeated intravenous administration of silver and gold nanoparticles in mice." *Scientific reports* 7.1 (2017): 1-12.

Sengupta, Jayeeta, et al. "In vivo interaction of gold nanoparticles after acute and chronic exposures in experimental animal models." *Journal of Nanoscience and Nanotechnology* 13.3 (2013): 1660-1670.

Chen, Hui, et al. "In vivo study of spherical gold nanoparticles: inflammatory effects and distribution in mice." *PloS one* 8.2 (2013): e58208.

Kim, Jinhwan, et al. "Transfection and intracellular trafficking properties of carbon dot-gold nanoparticle molecular assembly conjugated with PEI-pDNA." *Biomaterials* 34.29 (2013): 7168-7180.

Yu, Chenxu, Harikrishna Nakshatri, and Joseph Irudayaraj. "Identity profiling of cell surface markers by multiplex gold nanorod probes." Nano letters 7.8 (2007): 2300-2306.

Gupta, Indarchand, et al. "Bio-distribution and Toxicity of Noble Metal Nanoparticles in Humans." *Metal Nanoparticles in Pharma. Springer, Cham*, 2017. 469-482.

Zeng, Qinghui, et al. "Inhibitation of cellular toxicity of gold nanoparticles by surface encapsulation of silica shell for hepatocarcinoma cell application." *ACS applied materials & interfaces* 6.21 (2014): 19327-19335.

Sosibo, Ndabenhle M., et al. "Facile attachment of TAT peptide on gold monolayer protected clusters: Synthesis and characterization." *Nanomaterials* 5.3 (2015): 1211-1222.

Sibuyi, Nicole Remaliah, et al. "Peptide-functionalized nanoparticles for the selective induction of apoptosis in target cells." *Nanomedicine* 12.14 (2017): 1631-1645.

Bohren, Craig F., and Timothy J. Nevitt. "Absorption by a sphere: a simple approximation." *Applied Optics* 22.6 (1983): 774-775.

Parween, Shaheena, Ashraf Ali, and Virender S. Chauhan. "Non-natural amino acids containing peptide-capped gold nanoparticles for drug delivery application." *ACS applied materials & interfaces* 5.14 (2013): 6484-6493.

Alkilany, Alaaldin M., and Catherine J. Murphy. "Toxicity and cellular uptake of gold nanoparticles: what we have learned so far?" *Journal of nanoparticle research* 12.7 (2010): 2313-2333.

Shukla, Ravi, et al. "Biocompatibility of gold nanoparticles and their endocytotic fate inside the cellular compartment: a microscopic overview." *Langmuir* 21.23 (2005): 10644-10654.

Chithrani, Devika B. "Intracellular uptake, transport, and processing of gold nanostructures." *Molecular membrane biology* 27.7 (2010): 299-311.

Nativo, Paola, Ian A. Prior, and Mathias Brust. "Uptake and intracellular fate of surface-modified gold nanoparticles." *ACS nano* 2.8 (2008): 1639-1644.

Falagan-Lotsch, Priscila, Elissa M. Grzincic, and Catherine J. Murphy. "One low-dose exposure of gold nanoparticles induces long-term changes in human cells." *Proceedings of the National Academy of Sciences* 113.47 (2016): 13318-13323.

Ibrahim, Khalid Elfaki, et al. "Histopathology of the liver, kidney, and spleen of mice exposed to gold nanoparticles." *Molecules* 23.8 (2018): 1848.

Aillon, Kristin L., et al. "Effects of nanomaterial physicochemical properties on in vivo toxicity." *Advanced drug delivery reviews* 61.6 (2009): 457-466.

Dobrovolskaia, Marina A., and Scott E. McNeil, eds. Handbook of immunological properties of engineered nanomaterials. Vol. 1. *World Scientific*, 2013.

Villiers, Christian, et al. "From secretome analysis to immunology: chitosan induces major alterations in the activation of dendritic cells via a TLR4-dependent mechanism." *Molecular & cellular proteomics* 8.6 (2009): 1252-1264.

Sani, A., C. Cao, and D. Cui. "Toxicity of gold nanoparticles (AuNPs): A review." *Biochemistry and biophysics report* 26 (2021): 100991.

Enea, Maria, et al. "Gold nanoparticles induce oxidative stress and apoptosis in human kidney cells." *Nanomaterials* 10.5 (2020): 995.

Chen, Xinyi, and Changyou Gao. "Influences of size and surface coating of gold nanoparticles on inflammatory activation of macrophages." *Colloids and Surfaces B: Biointerfaces* 160 (2017): 372-380.

Choi, Soonmo, Anuj Tripathi, and Deepti Singh. "Smart nanomaterials for biomedics." *Journal of Biomedical Nanotechnology* 10.10 (2014): 3162-3188.

Cho, Wan-Seob, et al. "Acute toxicity and pharmacokinetics of 13 nm-sized PEG-coated gold nanoparticles." *Toxicology and applied pharmacology* 236.1 (2009): 16-24.

Mao, Yan, et al. "Stromal cells in tumor microenvironment and breast cancer." *Cancer and Metastasis Reviews* 32.1 (2013): 303-315.

Peng, Chen, et al. "Targeted tumor CT imaging using folic acid-modified PEGylated dendrimer-entrapped gold nanoparticles." *Polymer Chemistry* 4.16 (2013): 4412- 4424.

Zhu, Jingyi, et al. "Targeted cancer theranostics using alpha-tocopheryl succinate-conjugated multifunctional dendrimer-entrapped gold nanoparticles." *Biomaterials* 35.26 (2014): 7635-7646.

Yue, Jun, et al. "Gold nanoparticle size and shape effects on cellular uptake and intracellular distribution of siRNA nanoconstructs." *Bioconjugate chemistry* 28.6 (2017): 1791-1800.

Chen, Jingqin, et al. "Green synthesis, characterization, cytotoxicity, antioxidant, and anti-human ovarian cancer activities of Curcumae anagenesis leaf aqueous extract green-synthesized gold nanoparticles." Arabian Journal of Chemistry 14.3 (2021): 103000.

Geetha, N., et al. "A comparison of microwave assisted medicinal plant extractions for detection of their phytocompounds through qualitative phytochemical and FTIR analyses." *Iranian Journal of Science and Technology, Transactions A: Science* 43.2 (2019): 397-407.

Shaneza, A. "Herbal treatment for the ovarian cancer." *SGVU J Pharm Res Educ* 3.2 (2018): 325-329.

Hosny, Mohamed, et al. "Comparative study on the potentialities of two halophytic species in the green synthesis of gold nanoparticles and their anticancer, antioxidant and catalytic efficiencies." *Advanced Powder Technology* 32.9 (2021): 3220-3233.

Castillo-Henríquez, Luis, et al. "Green synthesis of gold and silver nanoparticles from plant extracts and their possible applications as antimicrobial agents in the agricultural area." *Nanomaterials* 10.9 (2020): 1763.

Satpathy, Swaha, et al. "Process optimization for green synthesis of gold nanoparticles mediated by extract of Hygrophila spinosa T. Anders and their biological applications." *Physica E: Low-dimensional Systems and Nanostructures* 121 (2020): 113830.

Arunachalam, Kantha D., Sathesh Kumar Annamalai, and Shanmugasundaram Hari. "One-step green synthesis and characterization of leaf extract-mediated biocompatible silver and

gold nanoparticles from Memecylon umbellatum." *International journal of nanomedicine* 8 (2013): 1307.

Wang, Lei, et al. "Green synthesis of gold nanoparticles from Scutellaria barbata and its anticancer activity in pancreatic cancer cell (PANC-1)." *Artificial cells, nanomedicine, and biotechnology* 47.1 (2019): 1617-1627.

Dreaden, Erik C., and Mostafa A. El-Sayed. "Detecting and destroying cancer cells in more than one way with noble metals and different confinement properties on the nanoscale." *Accounts of chemical research* 45.11 (2012): 1854-1865.

Pechyen, Chiravoot, et al. "Biogenic synthesis of gold nanoparticles mediated by Spondias dulcis (Anacardiaceae) peel extract and its cytotoxic activity in human breast cancer cell." *Toxicology Reports* 9 (2022): 1092-1098.

Pesce, Carlo. "Glomerular number and size: facts and artefacts." *The Anatomical Record: An Official Publication of the American Association of Anatomists* 251.1 (1998): 66-71.

Bilous, Rudolf W., et al. "Estimation of mean glomerular volume in patients with insulindependent diabetes mellitus." *Kidney international* 32.6 (1987): 930-932.

Madiehe, Abram M., et al. "Catalytic reduction of 4-nitrophenol and methylene blue by biogenic gold nanoparticles synthesized using Carpobrotus edulis fruit (sour fig) extract." *Nanomaterials and Nanotechnology* 12 (2022): 18479804221108254.

Moore, Lynette, Ruth Williams, and Alan Staples. "Glomerular dimensions in children under 16 years of age." *The Journal of pathology* 171.2 (1993): 145-150.

Meyer, Thomas J., et al. "Development and validation of the penn state worry questionnaire." *Behaviour research and therapy* 28.6 (1990): 487-495.

Newbold, K. M., et al. "Assessment of glomerular size in renal biopsies including minimal change nephropathy and single kidneys." The Journal of Pathology 160.3 (1990): 255-258.65.

Shemetov, Anton A., Igor Nabiev, and Alyona Sukhanova. "Molecular interaction of proteins and peptides with nanoparticles." *ACS nano* 6.6 (2012): 4585-4602.

Peng, Jingwen, and Xiaoqiu Liang. "Progress in research on gold nanoparticles in cancer management." *Medicine* 98.18 (2019).

Ritz, Sandra, et al. "Protein corona of nanoparticles: distinct proteins regulate the cellular uptake." *Biomacromolecules* 16.4 (2015): 1311-1321.

Boulos, Stefano P., et al. "Nanoparticle–protein interactions: a thermodynamic and kinetic study of the adsorption of bovine serum albumin to gold nanoparticle surfaces." *Langmuir* 29.48 (2013): 14984-14996.

Ayyoub, Sanaa, et al. "Biosynthesis of gold nanoparticles using leaf extract of Dittrichia viscosa and in vivo assessment of its anti-diabetic efficacy." *Drug Delivery and Translational Research* (2022): 1-7.

BarathManiKanth, Selvaraj, et al. "Anti-oxidant effect of gold nanoparticles restrains hyperglycemic conditions in diabetic mice." *Journal of nanobiotechnology* 8.1 (2010): 1-15.

Zhang, Jiangjiang, Lei Mou, and Xingyu Jiang. "Surface chemistry of gold nanoparticles for health-related applications." *Chemical Science* 11.4 (2020): 923-936.

Pan, Yu, Matthias Bartneck, and Willi Jahnen-Dechent. "Cytotoxicity of gold nanoparticles." Methods in enzymology. Vol. 509. *Academic Press*, 2012. 225-242.

Sadauskas, Evaldas, et al. "Protracted elimination of gold nanoparticles from mouse liver." *Nanomedicine: Nanotechnology, Biology and Medicine* 5.2 (2009): 162-169.

Oh, Nuri, and Ji-Ho Park. "Surface chemistry of gold nanoparticles mediates their exocytosis in macrophages." *ACS nano* 8.6 (2014): 6232-6241.

Shin, Kwangsoo, et al. "Multifunctional nanoparticles as a tissue adhesive and an injectable marker for image-guided procedures." *Nature communications* 8.1 (2017): 1-12.

Hong, Ye, et al. "Synthesis and radiolabeling of 111In-core-cross linked polymeric micelleoctreotide for near-infrared fluoroscopy and single photon emission computed tomography imaging." *Bioorganic & Medicinal Chemistry Letters* 24.12 (2014): 2781-2785.

Katz, Linda M., Kapal Dewan, and Robert L. Bronaugh. "Nanotechnology in cosmetics." *Food and Chemical Toxicology* 85 (2015): 127-137.

Mihranyan, Albert, Natalia Ferraz, and Maria Strømme. "Current status and future prospects of nanotechnology in cosmetics." *Progress in materials science* 57.5 (2012): 875-910.6.

Zhang, Jiangjiang, Lei Mou, and Xingyu Jiang. "Surface chemistry of gold nanoparticles for health-related applications." *Chemical Science* 11.4 (2020): 923-936.

Balfourier, Alice, et al. "Gold-based therapy: From past to present." *Proceedings of the National Academy of Sciences* 117.37 (2020): 22639-22648.

Sibuyi, Nicole Remaliah Samantha, et al. "Multifunctional gold nanoparticles for improved diagnostic and therapeutic applications: a review." *Nanoscale Research Letters* 16.1 (2021): 1-27.

Wang, Qin, and Xun Sun. "Recent advances in nanomedicines for the treatment of rheumatoid arthritis." *Biomaterials science* 5.8 (2017): 1407-1420.

Seku, Kondaiah, et al. "Synthesis of moxifloxacin–Au (III) and Ag (I) metal complexes and their biological activities." *Journal of Analytical Science and Technology* 9.1 (2018): 1-13.

Kus-Liśkiewicz, Małgorzata, Patrick Fickers, and Imen Ben Tahar. "Biocompatibility and cytotoxicity of gold nanoparticles: recent advances in methodologies and regulations." *International Journal of Molecular Sciences* 22.20 (2021): 10952.

Liu, Biwu, and Juewen Liu. "Interface-driven hybrid materials based on DNA-functionalized gold nanoparticles." *Matter* 1.4 (2019): 825-847.

Negahdary, Masoud. "Electrochemical aptasensors based on the gold nanostructures." *Talanta* 216 (2020): 120999.

Zhang, Yang, et al. "Recent advances in gold nanostructures based biosensing and bioimaging." *Coordination Chemistry Reviews* 370 (2018): 1-21.

Karthik, Vivekanandhan, et al. "Nanoarchitectonics is an emerging drug/gene delivery and targeting strategy-a critical review." *Journal of Molecular Structure* 1243 (2021): 130844.

Wang, Song, et al. "Antimicrobial peptide modification enhances the gene delivery and bactericidal efficiency of gold nanoparticles for accelerating diabetic wound

healing." *Biomaterials science* 6.10 (2018): 2757-2772.

Sibuyi, Nicole Remaliah Samantha, et al. "Vascular targeted nanotherapeutic approach for obesity treatment." *International Journal of Nanomedicine* 13 (2018): 7915.

Nijhawans, Priya, Tapan Behl, and Shaveta Bhardwaj. "Angiogenesis in obesity." *Biomedicine & Pharmacotherapy* 126 (2020): 110103.

Dong, Yi, et al. "Fabrication of resveratrol coated gold nanoparticles and investigation of their effect on diabetic retinopathy in streptozotocin induced diabetic rats." *Journal of Photochemistry and Photobiology B: Biology* 195 (2019): 51-57.

Alomari, Ghada, Salehhuddin Hamdan, and Bahaa Al-Trad. "Gold nanoparticles as a promising treatment for diabetes and its complications: Current and future potentials." *Brazilian Journal of Pharmaceutical Sciences* 57 (2021).

Vijayakumar, Sekar, et al. "A novel antimicrobial therapy for the control of Aeromonas hydrophila infection in aquaculture using marine polysaccharide coated gold nanoparticle." *Microbial Pathogenesis* 110 (2017): 140-151.

Khan, Fazlurrahman, et al. "Synthesis and characterization of chitosan oligosaccharide-capped gold nanoparticles as an effective antibiofilm drug against the Pseudomonas aeruginosa PAO1." *Microbial pathogenesis* 135 (2019): 103623.

Albarwary, Safa Anmar, et al. "The Efficiency of AuNPs in Cancer Cell Targeting Compared to Other Nanomedicine Technologies Using Fuzzy PROMETHEE." *Journal of Healthcare Engineering* 2021 (2021).

Haiss, Wolfgang, et al. "Determination of size and concentration of gold nanoparticles from UV− Vis spectra." *Analytical chemistry* 79.11 (2007): 4215-4221.

Feng, Bing, et al. "Near infrared light-actuated gold nanorods with cisplatin–polypeptide wrapping for targeted therapy of triple negative breast cancer." *Nanoscale* 7.36 (2015): 14854-14864.

Lankveld, Daniëlle PK, et al. "Blood clearance and tissue distribution of PEGylated and nonPEGylated gold nanorods after intravenous administration in rats." *Nanomedicine* 6.2 (2011): 339-349.

Khutale, Ganesh V., and Alan Casey. "Synthesis and characterization of a multifunctional golddoxorubicin nanoparticle system for pH triggered intracellular anticancer drug release." *European Journal of Pharmaceutics and Biopharmaceutics* 119 (2017): 372-380.

Zhang, Xuan, Jose G. Teodoro, and Jay L. Nadeau. "Intratumoral gold-doxorubicin is effective in treating melanoma in mice." *Nanomedicine: Nanotechnology, Biology and Medicine* 11.6 (2015): 1365-1375.

Gu, Yan-Juan, et al. "Gold-doxorubicin nanoconjugates for overcoming multidrug resistance." *Nanomedicine: Nanotechnology, Biology and Medicine* 8.2 (2012): 204-211.

Zhang, Xiaojie, et al. "Surface functionalization of pegylated gold nanoparticles with antioxidants suppresses nanoparticle-induced oxidative stress and neurotoxicity." *Chemical Research in Toxicology* 33.5 (2020): 1195-1205.

Barabadi, Hamed, et al. "Emerging antineoplastic gold nanomaterials for cervical cancer therapeutics: a systematic review." *Journal of Cluster Science* 31.6 (2020): 1173-1184.

Hansen, Steffen Foss, and Anders Baun. "European regulation affecting nanomaterials-review of limitations and future recommendations." *Dose-Response* 10.3 (2012): doseresponse.

Dehhaghi, Mona, et al. "A state-of-the-art review on the application of nanomaterials for enhancing biogas production." *Journal of environmental management* 251 (2019): 109597.

Gubala, Vladimir, et al. "Engineered nanomaterials and human health: Part 2. Applications and nanotoxicology (IUPAC Technical Report)." *Pure and Applied Chemistry* 90.8 (2018): 1325-1356.

Kabir, Ehsanul, et al. "Environmental impacts of nanomaterials." *Journal of Environmental Management* 225 (2018): 261-271.

Barman, Jugal, et al. "The role of nanotechnology based wearable electronic textiles in biomedical and healthcare applications." *Materials Today Communications* (2022): 104055.

Pattan, Gurulingappa, and Gautam Kaul. "Health hazards associated with nanomaterials." *Toxicology and industrial health* 30.6 (2014): 499-519.

Papadopoulos, Antonios N., et al. "Nanomaterials and chemical modifications for enhanced key wood properties: A review." *Nanomaterials* 9.4 (2019): 607.

Adeola, Adedapo Oluwasanu, et al. "Scientific applications and prospects of nanomaterials: A multidisciplinary review." *African Journal of Biotechnology* 18.30 (2019): 946-961.

Khan, Waseem S., and Ramazan Asmatulu. "Nanotechnology emerging trends, markets, and concerns." *Nanotechnology safety. Elsevier*, 2013. 1-16.

Weiss, Jochen, Paul Takhistov, and D. Julian McClements. "Functional materials in food nanotechnology." *Journal of food science* 71.9 (2006): R107-R116.

Balaguru, Perumalsamy, and Ken Chong. "Nanotechnology and concrete: research opportunities." *Proceedings of the ACI session on nanotechnology of concrete: recent developments and future perspectives* (2006): 15-28.

Ahmad, Tausif, et al. "A critical review on phytosynthesis of gold nanoparticles: Issues, challenges and future perspectives." *Journal of Cleaner Production* 309 (2021): 127460.

Wang, Cong, et al. "Advanced nanotechnology leading the way to multimodal imaging-guided precision surgical therapy." *Advanced Materials* 31.49 (2019): 1904329.

Zhao, Lirong, et al. "Advanced nanotechnology for hypoxia-associated antitumor therapy." *Nanoscale* 12.5 (2020): 2855-2874.

Ali, Faraat. "Regulatory perspectives of nanomaterials for theranostic application." *Nanotheranostics for Treatment and Diagnosis of Infectious Diseases. Academic Press*, 2022. 373-384.

Nabil, Ghazal, et al. "Nano-engineered delivery systems for cancer imaging and therapy: Recent advances, future direction and patent evaluation." *Drug Discovery Today* 24.2 (2019): 462-491.

Kora, Aruna Jyothi. "Plant and tree gums as renewable feedstocks for the phytosynthesis of nanoparticles: A green chemistry approach." *Green metal nanoparticles: synthesis, characterization and their applications* (2018): 79-

Bahamonde, Javiera, et al. "Gold nanoparticle toxicity in mice and rats: species differences." *Toxicologic pathology* 46.4 (2018): 431-443.

Mironava, Tatsiana, et al. "Gold nanoparticles cellular toxicity and recovery: effect of size, concentration and exposure time." *Nanotoxicology* 4.1 (2010): 120-137.

Carnovale, Catherine, et al. "Identifying trends in gold nanoparticle toxicity and uptake: size, shape, capping ligand, and biological corona." *ACS omega* 4.1 (2019): 242-256.

Yang, Yongjun, et al. "Acute exposure to gold nanoparticles aggravates lipopolysaccharideinduced liver injury by amplifying apoptosis via ROS-mediated macrophagehepatocyte crosstalk." *Journal of nanobiotechnology* 20.1 (2022): 1-21.

Henkart, Pierre A. "Mechanism of lymphocyte-mediated cytotoxicity." *Annual review of immunology* 3.1 (1985): 31-58.

Prasad, Saumya, et al. "Optical and magnetic resonance imaging approaches for investigating the tumour microenvironment: state-of-the-art review and future trends." *Nanotechnology* 32.6 (2020): 062001.

Bácskay, Ildikó, et al. *Role of cytotoxicity experiments in pharmaceutical development*. InTech: London, UK, 2018.

Thovhogi, Ntevheleni, et al. "Targeted delivery using peptide-functionalised gold nanoparticles to white adipose tissues of obese rats." *Journal of Nanoparticle Research* 17.2 (2015): 1-8.

Wusu, Adedoja Dorcas, et al. "Citrate-capped gold nanoparticles with a diameter of 14 nm alter the expression of genes associated with stress response, cytoprotection and lipid metabolism in CaCo-2 cells." *Nanotechnology* 33.10 (2021): 105101.

Icard, Philippe, Laurent Poulain, and Hubert Lincet. "Understanding the central role of citrate in the metabolism of cancer cells." *Biochimica et Biophysica Acta (BBA)-Reviews on Cancer* 1825.1 (2012): 111-116.

Costello, Leslie C., and Renty B. Franklin. "Plasma citrate homeostasis: how it is regulated; and its physiological and clinical implications. An important, but neglected, relationship in medicine." *HSOA journal of human endocrinology* 1.1 (2016).

Bakur, Abdelmoneim, et al. "Synthesis of gold nanoparticles derived from mannosylerythritol lipid and evaluation of their bioactivities." *Amb Express* 9.1 (2019): 1-9.

Oladipo, I. C., et al. "Antidiabetic properties of phytosynthesized gold nanoparticles (AuNPs) from Datura stramonium seed." *IOP Conference Series: Materials Science and Engineering*. Vol. 805. No. 1. IOP Publishing, 2020.

Guo, Ying, et al. "Green synthesis of gold nanoparticles from Fritillaria cirrhosa and its antidiabetic activity on Streptozotocin induced rats." *Arabian Journal of Chemistry* 13.4 (2020): 5096-5106.

Sekar, Velmurugan, et al. "Synthesis of gold nanoparticles (AuNPs) with improved antidiabetic, antioxidant and anti-microbial activity from Physalis minima." *Journal of King Saud University-Science* 34.6 (2022): 102197.

Azzazy, Hassan ME, et al. "Gold nanoparticles in the clinical laboratory: principles of preparation and applications." *Clinical chemistry and laboratory medicine* 50.2 (2012): 193-209.

Modise, Keletso. "The effect of phytonanotherapy on diabetic rats." (2021).Rajput, Vishnu, et al. "Accumulation of nanoparticles in the soil-plant systems and their effects on human health." *Annals of Agricultural Sciences* 65.2 (2020): 137-143.

Pattan, Gurulingappa, and Gautam Kaul. "Health hazards associated with nanomaterials." *Toxicology and industrial health* 30.6 (2014): 499-519.

Lanone, Sophie, and Jorge Boczkowski. "Biomedical applications and potential health risks of nanomaterials: molecular mechanisms." *Current molecular medicine* 6.6 (2006): 651-663.

Zhang, Jiangjiang, Lei Mou, and Xingyu Jiang. "Surface chemistry of gold nanoparticles for health-related applications." *Chemical Science* 11.4 (2020): 923-936.

Ozer A.Y. *Nanomaterials and Nanosystems for Biomedical Applications*. Springer; Dordrecht, The Netherlands: 2007. Applications of light and electron microscopic techniques in liposome research; pp. 145–153.

Kerschbaum, Hubert H., et al. "Trypan blue-adapting a dye used for labelling dead cells to visualize pinocytosis in viable cells." *Cell. Physiol. Biochem* 55 (2021): 171-184.

Yang, Hai-Chun, Shao-Jun Liu, and Agnes B. Fogo. "Kidney regeneration in mammals." *Nephron Experimental Nephrology* 126.2 (2014): 50-53.

Lieber, Charles M. "Nanoscale science and technology: building a big future from small things." *MRS bulletin* 28.7 (2003): 486-491.

Wang, Zhiming M., et al. "Lecture Notes in Nanoscale Science Technology." (2012).

The Nanoscale, "https://introtonanotechnology.weebly.com/the-nanoscale.html".

Djurišić, Aleksandra B., et al. "Toxicity of metal oxide nanoparticles: mechanisms, characterization, and avoiding experimental artefacts." *Small* 11.1 (2015): 26-44.

Sengupta, Jayeeta, et al. "Physiologically important metal nanoparticles and their toxicity." *Journal of Nanoscience and Nanotechnology* 14.1 (2014): 990-1006.

Shahid, Rabia K., et al. "Diabetes and cancer: risk, challenges, management and outcomes." *Cancers* 13.22 (2021): 5735.

Liu, Jinli, et al. "Trends in the incidence of diabetes mellitus: results from the Global Burden of Disease Study 2017 and implications for diabetes mellitus prevention." *BMC public health* 20 (2020): 1-12.

Ling, Suping, et al. "Association of type 2 diabetes with cancer: a meta-analysis with bias analysis for unmeasured confounding in 151 cohorts comprising 32 million people." *Diabetes Care* 43.9 (2020): 2313-2322.

Morviducci, L.; Rota, F.; Rizza, L.; Di Giacinto, P.; Ramponi, S.; Nardone, M.; Tubili, C.; Lenzi, A.; Zuppi, P.; Baldelli, R. Everolimus is a new anti-cancer molecule: Metabolic side effects as lipid disorders and hyperglycemia. *Diabetes Res. Clin. Pract.* 2018, 143, 428–431.

American Diabetes Association. "2. Classification and diagnosis of diabetes: standards of medical care in diabetes—2021." *Diabetes care 44. Supplement*_1 (2021): S15-S33.

Suh, Sunghwan, and Kwang-Won Kim. "Diabetes and cancer: cancer should be screened in routine diabetes assessment." *Diabetes & metabolism journal* 43.6 (2019): 733-743.

Chari, Suresh T., et al. "Probability of pancreatic cancer following diabetes: a population-based study." *Gastroenterology* 129.2 (2005): 504-511.

Sciacca, L., et al. "Clinical and molecular mechanisms favoring cancer initiation and progression in diabetic patients." *Nutrition, Metabolism and Cardiovascular Diseases* 23.9 (2013): 808-815.

Mendonça, Fernando Miguel, et al. "Metabolic syndrome and risk of cancer: which link?" *Metabolism* 64.2 (2015): 182-189.

Abu-Dief, Ahmed M., Mosa Alsehli, and Aziz Awaad. "A higher dose of PEGylated gold nanoparticles reduces the accelerated blood clearance phenomenon effect and induces spleen B lymphocytes in albino mice." *Histochemistry and Cell Biology* 157.6 (2022): 641-656.

Ou, Yu-Chuan, et al. "Diagnosis of immunomarkers in vivo via multiplexed surface enhanced Raman spectroscopy with gold nanostars." *Nanoscale* 10.27 (2018): 13092-13105.

Sztandera, Krzysztof, Michał Gorzkiewicz, and Barbara Klajnert-Maculewicz. "Gold nanoparticles in cancer treatment." *Molecular pharmaceutics* 16.1 (2018): 1-23.

Yu, Yanfang, et al. "Antidiabetic nephropathy effects of synthesized gold nanoparticles through mitigation of oxidative stress." *Arabian Journal of Chemistry* 14.3 (2021): 103007.

Selim, Manar E., Yasmina M. Abd-Elhakim, and Laila Y. Al-Ayadhi. "Pancreatic response to gold nanoparticles includes decrease of oxidative stress and inflammation in autistic diabetic model." *Cellular Physiology and Biochemistry* 35.2 (2015): 586-600.

Kowsalya, Elumalai, et al. "Gold nanoparticles induced apoptosis via oxidative stress and mitochondrial dysfunctions in MCF-7 breast cancer cells." *Applied Organometallic Chemistry* 35.1 (2021): e6071.

Ramalingam, V., et al. "Biogenic gold nanoparticles induce cell cycle arrest through oxidative stress and sensitize mitochondrial membranes in A549 lung cancer cells." *RSC advances* 6.25 (2016): 20598-20608.

Abu-Dief, Ahmed M., M. Salaheldeen, and Tarek El-Dabea. "Recent advances in development of gold nanoparticles for drug delivery systems." *Journal of Modern Nanotechnology* (2021).

Pandey, Rishikesh, et al. "Emerging trends in optical sensing of glycemic markers for diabetes monitoring." *TrAC Trends in Analytical Chemistry* 64 (2015): 100-108.

Arbib, Nissim, et al. "First trimester glycosylated hemoglobin as a predictor of gestational diabetes mellitus." *International Journal of Gynecology & Obstetrics* 145.2 (2019):

Saleh, Jumana. "Glycated hemoglobin and its spinoffs: Cardiovascular disease markers or risk factors?" *World journal of cardiology* 7.8 (2015): 449.

Chen, Xixi, et al. "d-Ribose as a Contributor to Glycated Haemoglobin." *EBioMedicine* 25 (2017): 143-153.

Chen, Lan, et al. "D-Ribosylated Tau forms globular aggregates with high cytotoxicity." *Cellular and molecular life sciences* 66 (2009): 2559-2571.

Wei, Yan, et al. "Rapid glycation with D-ribose induces globular amyloid-like aggregations of BSA with high cytotoxicity to SH-SY5Y cells." *BMC cell biology* 10.1 (2009): 1-15.

Sirsikar et al,"Role of glycated haemoglobin (HbA1c) as a dual marker to predict glyvemic status and dyslipidemiman Type 2 diabetes melittus." *Int.J Res Med Sci*.4.10 (2016): 4524-4529.

Ding, Lin, et al. "Size, shape, and protein corona determine cellular uptake and removal mechanisms of gold nanoparticles." *Small* 14.42 (2018): 1801451.

Kaiafa, Georgia, et al. "Is HbA1c an ideal biomarker of well-controlled diabetes?" *Postgraduate Medical Journal* 97.1148 (2021): 380-383.

Morviducci, L., et al. "Everolimus is a new anti-cancer molecule: Metabolic side effects as lipid disorders and hyperglycemia." *Diabetes Research and Clinical Practice* 143 (2018): 428-431.

Shahid, Rabia K., et al. "Diabetes and cancer: risk, challenges, management and outcomes." *Cancers* 13.22 (2021): 5735.

American Diabetes Association. "2. Classification and diagnosis of diabetes: standards of medical care in diabetes—2021." *Diabetes care 44. Supplement*_1 (2021): S15-S33.

Rosenberg, Amy S. "Effects of protein aggregates: an immunologic perspective." *The AAPS journal* 8 (2006): E501-E507.

Kepchia, Devin, et al. "Diverse proteins aggregate in mild cognitive impairment and Alzheimer's disease brain." *Alzheimer's research & therapy* 12.1 (2020): 1-20.

Goldberg, Ronald B. "Cytokine and cytokine-like inflammation markers, endothelial dysfunction, and imbalanced coagulation in development of diabetes and its complications." *The Journal of Clinical Endocrinology & Metabolism* 94.9 (2009): 3171-3182.

Iberg, Niggi, and R. Flückiger. "Nonenzymatic glycosylation of albumin in vivo. Identification of multiple glycosylated sites." *Journal of Biological Chemistry* 261.29 (1986): 13542-13545.

Guerin-Dubourg, Alexis, et al. "Association between fluorescent advanced glycation end-products and vascular complications in type 2 diabetic patients." *BioMed Research International* 2017 (2017).

Jeffcoate, S. L. "Diabetes control and complications: the role of glycated haemoglobin, 25 years on." *Diabetic Medicine* 21.7 (2004): 657-665.

Cerami, Anthony, and Peter Ulrich. "Pharmaceutical intervention of advanced glycation endproducts." *Ageing Vulnerability: Causes and Interventions: Novartis Foundation Symposium* 235. Vol. 235. Chichester, UK: John Wiley & Sons, Ltd, 2001.

Watt, Matthew J., et al. "The liver as an endocrine organ—linking NAFLD and insulin resistance." *Endocrine reviews* 40.5 (2019): 1367-1393.

Hiller-Sturmhöfel, Susanne, and Andrzej Bartke. "The endocrine system: an overview." *Alcohol health and research world* 22.3 (1998): 153.

Kuppusamy, Palaniselvam, et al. "Biosynthesis of metallic nanoparticles using plant derivatives and their new avenues in pharmacological applications–An updated report." *Saudi Pharmaceutical Journal* 24.4 (2016): 473-484.

Yasmin, Akbar, Kumaraswamy Ramesh, and Shanmugam Rajeshkumar. "Optimization and stabilization of gold nanoparticles by using herbal plant extract with microwave heating." *Nano Convergence* 1.1 (2014): 12.

Baynes, John W. "The role of AGEs in aging: causation or correlation." *Experimental gerontology* 36.9 (2001): 1527-1537.

Moldogazieva, Nurbubu T., et al. "Oxidative stress and advanced lipoxidation and glycation end products (ALEs and AGEs) in aging and age-related diseases." *Oxidative medicine and cellular longevity* 2019 (2019).

Barabadi, Hamed, et al. "Microbial mediated preparation, characterization and optimization of gold nanoparticles." *Brazilian Journal of Microbiology* 45 (2014): 1493-1501.

Sutradhar, Dipankar, and Durlav Hazarika. "A Review of Non-invasive Electromagnetic Blood Glucose Monitoring Techniques." (2022).

Sung, Hyuna, et al. "Global cancer statistics 2020: GLOBOCAN estimates of incidence and mortality worldwide for 36 cancers in 185 countries." *CA: a cancer journal for clinicians* 71.3 (2021): 209-249.

Rodrigo, Ramón, Andrés Miranda, and Leonardo Vergara. "Modulation of endogenous antioxidant system by wine polyphenols in human disease." *Clinica Chimica Acta* 412.5-6 (2011): 410-424.

Lei, Xin Gen, et al. "Paradoxical roles of antioxidant enzymes: basic mechanisms and health implications." *Physiological reviews* 96.1 (2016): 307-364.

Zhang, Xiao-Dong, et al. "Toxicologic effects of gold nanoparticles in vivo by different administration routes." *International journal of nanomedicine* (2010): 771-781.

Ibrahim, Khalid Elfaki, et al. "Histopathology of the liver, kidney, and spleen of mice exposed to gold nanoparticles." *Molecules* 23.8 (2018): 1848.